Universidad de **Valladolid**

Instituto de Oftalmobiología Aplicada (IOBA)

Lente de contacto con sensor nano estructurado para la medida y monitorización de la presión intraocular

Trabajo de investigación presentado por Irene Sánchez Pavón
para optar al grado de Doctor por la Universidad de Valladolid
Dirigido por Raúl Martín Herranz
Valladolid - 2011

Instituto Universitario de Oftalmobiología Aplicada

UNIVERSIDAD de VALLADOLID

AUTORIZACIÓN DEL DIRECTOR DE TESIS

D. RAÚL MARTÍN HERRANZ, con D.N.I. nº 50.447.910-D, Investigador del Instituto Universitario de Oftalmobiología Aplicada de la Universidad de Valladolid (IOBA) y Profesor Contratado Doctor del Departamento de Física Teórica Atómica y Óptica, como Director de la Tesis Doctoral titulada **Lente de contacto con sensor nanoestructurado para la medida y monitorización de la presión intraocular,** presentada por **Dña. Irene Sánchez Pavón,** alumna del Programa de Doctorado Inter Universitario en Ciencias de la Visión, que el IOBA imparte,

AUTORIZA la presentación de la misma, considerando que es **APTA** para su defensa.

Valladolid, 10 de noviembre de 2011

El Director de la Tesis,

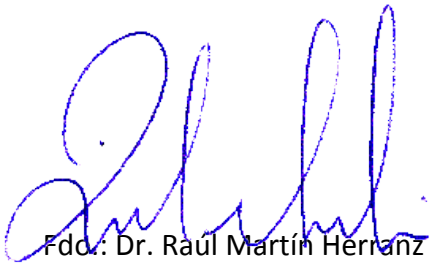

Fdo.: Dr. Raúl Martín Herranz

ILMO. SR. PRESIDENTE DE LA COMISIÓN DE DOCTORADO

Ioba Docencia

La ciencia es respecto al alma
Lo que la luz respecto de los ojos,
Y si las raíces son amargas
Los frutos son muy dulces.

Aristóteles

Felicidad no es hacer lo que uno quiere
Si no querer lo que uno hace

Jean Paul Sartre

Daría todo lo que sé,
Por la mitad de lo que ignoro

René Descartes

Los que no quieren
ser vencidos por la verdad,
Son vencidos por el error

San Agustín

I.- AGRADECIMIENTOS

Agradecer muy en especial a mi familia el haberme ayudado y acompañado en esta larga travesía que ha sido el proyecto de tesis, a Fernando Ussa por su amabilidad y apoyo constante durante este proyecto y a Raúl Martín, director de esta tesis, guía de mi pequeña carrera investigadora desde 2006, por su ayuda, su comprensión, su sabiduría y lo más importante de todo, por ser mi más férreo defensor.

No puedo olvidar a todas las personas que han trabajado en este proyecto tanto del Instituto de Ciencia de los Materiales, del Centro Nacional de Microelectrónica y del Instituto de Oftalmobiología Aplicada, nombrarlos a todos sería imposible, su colaboración y aportación ha sido imprescindible para que esta tesis haya sido posible. También, recordar al personal del matadero Justino Gutiérrez SL (Laguna de Duero, Valladolid, España) por proporcionarnos las muestras necesarias para los experimentales y a la empresa Conóptica SL por entendernos al pedirles “lentes para cerdos” y suministrar y fabricar las lentes de contacto rígidas permeables al gas con el orificio central que han permitido fabricar el prototipo desarrollado en esta tesis.

Por supuesto también es necesario reflejar mi más sincero agradecimiento al CIBER-BBN por creer en el proyecto y a los diferentes organismos que han permitido su financiación, el plan Nacional I+D+i 2008-2011, Iniciativa Ingenio 2010, programa Consolider, acciones CIBER, Instituto de Salud Carlos III con la ayuda del Fondo Europeo de Desarrollo Regional de Fondo, la Generalitat de Catalunya, en el marco del "Programa Operatiu FEDER de Cataluña" a través del contrato VALTEC09-1-0030 y los proyectos SGR2009-516, el Proyecto de la Unión Europea: ONE-P (FP7-NMP-2007 hasta 212.311), la DGI, España, los proyectos CTQ2006-06333/BQUand CTQ2010-19501/BQU.

II.- DIFUSIÓN DE RESULTADOS

Patentes:

- Patente PTC/ES2009/070205 (05/06/09) e internacional WO/2009/147277 A1.
  Nombre: “Lente de contacto sensora, sistema para la monitorización no invasiva de la presión intraocular y método para su medición”.
  Inventores: R. Villa, J Aguiló, N. Ventosa, J. Veciana, C. Rovira, M. Mas-Torrent, JC. Pastor, R. Martín, F. Ussa, E. Lukhina, V. Laukhin.

Publicaciones:

- Sanchez I, Martin R, Ussa F, Fernandez-Bueno I. The parameters of the porcine eyeball. Graefes Arch Clin Exp Ophthalmol. 2011;249:475-82. Review.

- Laukhin V, Sanchez I, Moya A, Laukhina E, Martin R, Ussa F, Rovira C, Guimera A, Villa R, Aguiló J, Pastor JC, Veciana J. Non-invasive intraocular pressure monitoring with a contact lens engineered with a nanostructured polymeric sensing film. Sensors and Actuators A. 2011;170:36- 43.

- Sanchez I, Laukhin V, Moya A, Martin R, Ussa F, Laukhina E, Guimera A, Villa R, Rovira C, Aguiló J, Veciana J, Pastor JC. Prototype of a nano-structured sensing contact lens for noninvasive intraocular pressure monitoring. Invest Ophthalmol Vis Sci. 2011;52:8310-5.

- Moya A, Guimerà A, Sánchez I, Laukin V, Martin R, Ussa F, Laukhina E, Rovira C, Veciana J, Pastor JC, Villa R, Aguiló J. Discrete Portable Measuring Device for Monitoring Noninvasive Intraocular Pressure with a Nano-Structured Sensing Contact Lens Prototype. International Journal of E-Health and Medical Communications, 2(4), 1-19, October-December 2011.

- Sanchez I, Ussa F, Martin R. Measurement of intraocular pressure in a porcine exvivo model eye. Optometry and Vision Science. (En evaluación).

Comunicaciones a congresos:

- Eurosensors XXIII. Comunicación Póster; “Contact lens equipped with flexible transparent pressure gauge for non-invasive intraocular presure measurements”. V Laukin, C Rovira, E Laukina, J Veciana, A Quimera, J Aguiló, R Villa, JC Pastor, F Ussa, I Sánchez, R Martín. 8 a 9 de Septiembre de 2009, Lausane (Swizerland).

- The 20th workshop on micromachinig, micro mechanics and micro systems (MME-2009). Comunicación Póster; “Flexible all-organic strain gauge for monitoring the body’s phisical and mechanical processes”. V Laukin, Pfattner R, Mas-Torrent M, E Laukina, C Rovira, J Veciana, J Aguiló, R Villa, F Ussa, I Sánchez, R Martín, JC Pastor. 20 y 22 de septiembre de 2009, Tolouse (France).

- XXIX Curso de glaucoma. Universidad de Valladolid, IOBA y Hospital Clínico Universitario de Valladolid. Comunicación Oral: “Monitorización continua de la PIO. Proyecto Glauco”. I Sánchez, R Martín, F Ussa, JC Pastor, E Laukhina, V Laukhin, J Veciana, C Rovira, R Villa, J Aquiló, A Guimera, A Moya.

- XXI Congreso de Optometría, Contactología y Óptica Oftálmica, comunicación oral “Monitorización continua de la presión intraocular con lentes de contacto” Sánchez I, Martín R, Ussa F, Pastor JC, Laukhin V, Laukhina E, Veciana J, Villa R, Guimera A, Aguiló J. Celebrado en Madrid del 12 al 14 de marzo de 2010.

- ARVO (Association for Research in Vision and Ophthalmology) 2010. R Martín, I Sánchez, F Ussa, JC Pastor, J Veciana, C Rovira, V Laukhin, E Laukhina, R Villa, J Aguiló. “Noninvasive intraocular pressure monitorization with a sensing contact lens” Fort Lauderdale, Florida, Estados Unidos.

- Pan-American Research Day, Saturday, May 1, 2010. Comunicación Oral: Noninvasive Intraocular Pressure Monitorization With a Sensig Contact Lens. R Martin, I Sánchez, F Ussa, JC Pastor, J Veciana, C Rovira,V Laukhin, E Laukhina, R Villa, J Aguiló.

- XXII Congreso de Optometría, Contactología y Óptica Oftálmica, comunicación poster “Calibración de la medida de la presión intraocular manométrica versus Perkins en un modelo exvivo de ojo porcino” Sánchez I, Martín R, Ussa F. Celebrado en Madrid del 17 al 19 de febrero de 2012.

Premios:

- Premio a la mejor comunicación oral por “monitorización continua de la presión intraocular con lentes de contacto” Sánchez I, Martín R, Ussa F, Pastor JC, Laukhin V, Laukhina E, Veciana J, Villa R, Guimera A, Aguiló J. presentado en XXI Congreso Internacional de Optometría, Contactología y Óptica Oftálmica. Madrid el 12 de marzo 2010.

1.- ÍNDICE

2.- ABREVIATURAS

10X: 10 aumentos.

AM: Antes del meridiano.

ARK: Autorefractometer Keratometer

ASIC: Circuito integrado para aplicaciones específicas

CNM: Centro Nacional de Microelectrónica.

CSIC: Consejo Superior de Investigaciones Científicas.

D: Dioptrías.

DMEM: Dulbecco's Modified Eagle Medium.

DS: Desviación estándar.

G: Gauge

Hg: Mercurio.

IC: Intervalo de confianza.

ICMAB: Instituto de Ciencia de los Materiales de Barcelona.

Kg: Kilogramos.

LC: lente de contacto.

LCRPG: Lente de contacto rígida permeable al gas.

Mm: milímetros

Mm^2: milímetros cuadrados.

Nm: nanómetros.

NY: New York.

ºC: grados Celsius.

OD: Ojo derecho.

Ohm: Ohmios.

p: nivel de significación.

pH: Potencial de hidrógeno.

PIO: Presión intraocular.

Qx: Queratometría.

R^2: Coeficiente de mínimos cuadrados.

UK: United Kingdom.

USA: United States of America.

µl/min: microlitros por minuto.

µm: micrómetros.

Ω/mmHg: Ohmios por milímetro de mercurio.

3.- JUSTIFICACIÓN

La neuropatía óptica glaucomatosa es una patología ocular de etiología neurodegenerativa, irreversible y considerada actualmente como la segunda causa de ceguera mundial.[1] Su prevalencia en España es de un 2,1% en mayores de 45 años oscilando entre el 1% y el 3% según la población estudiada.[2,3] Se estima que el 50% de las personas con neuropatía óptica glaucomatosa no han sido diagnosticadas.[4]

Esta enfermedad se caracteriza por una pérdida de células ganglionares de la retina cuya etiología se relaciona con el aumento y las variaciones de la presión en el interior del globo ocular. Una presión intraocular (PIO) superior a 21 mm Hg mantenida de forma suficientemente prolongada causa un adelgazamiento en la lámina cribosa,[5] zona de encuentro de las células ganglionares de la retina que induce la muerte de estas células nerviosas traduciéndose en

defectos y pérdidas en el campo visual que suelen comenzar con forma arciforme[6] desde el nervio óptico rodeando la mácula y aumentando su tamaño con el tiempo.[2]

Es una patología asintomática y con escasos signos en su comienzo. Su diagnóstico precoz es muy importante dado que las células ganglionares pérdidas no se recuperan, de manera que el defecto provocado en el campo visual es persistente.[7] Para el diagnóstico es importante la monitorización de la forma de la excavación/papila del nervio óptico[8,9] y otros parámetros clínicos, pero el criterio diagnóstico más importante es el valor de la (PIO).

Clásicamente se ha considerado que valores de PIO superiores a 21 mm Hg acompañadas de algún signo clínico indicativo (asimetrías en la relación excavación/papila, etc.) son un indicador suficiente para la sospecha de neuropatía óptica glaucomatosa, aún sin daños en el campo visual.[2] Aunque actualmente hay estudios que revelan que el 30% de las neuropatías ópticas glaucomatosas son normotensionales, es decir, se produce una pérdida de fibras nerviosas y daño en el campo visual a pesar de tener valores de PIO menores a 21 mm Hg.[10]

La pérdida en el campo visual puede deberse a que la PIO no tiene un valor constante a lo largo del día, sino que se ve afectada por el ritmo circadiano, alcanzando su valor máximo al amanecer y su valor mínimo a media tarde. Se estima que la variación diaria en un sujeto normal es de 5 mm Hg. Sin embargo, los pacientes con glaucoma pueden mostrar una variación diaria de

hasta 10 mm Hg.[11] Estas variaciones de la PIO podrían explicar las neuropatías ópticas glaucomatosas normotensionales y la progresión de la patología en algunos pacientes que muestran un valor de PIO dentro de los parámetros normales durante las exploraciones clínicas mantenido gracias al tratamiento farmacológico pautado.

Por tanto, la implicación del valor de la PIO en la patogénesis del glaucoma es muy relevante, sin embargo, su medida clínica es controvertida. Actualmente, el “gold standar” para la medida de la PIO es la tonometría de aplanación de tipo Goldman.

Esta medida se basa en la ley de Imbert Fick que establece que la PIO es igual al cociente entre el peso que ejerce el tonómetro y el área aplanada, suponiendo que el ojo se comporta como una membrana infinitamente delgada, seca, elástica y esférica. Los conos que se utilizan para la medida de la PIO tienen un diámetro plano de 7 mm y en el momento de la medida se provoca una aplanamiento corneal con un diámetro de 3,06 mm, que corresponde al punto en el que se iguala la presión ejercida con el tonómetro con la presión en el interior del globo ocular.[12] Los tonómetros de aplanación como los de tipo Goldman y otros están calibrados para un espesor corneal de 550 µm y la medida requiere un factor de corrección si el espesor corneal se aleja de este valor.[13] Además solo ofrecen una medida puntual de la PIO. De ahí que históricamente la monitorización continua de la PIO haya sigo objeto de investigación hasta la actualidad.[14]

Ha habido numerosos intentos de monitorización continua de la PIO, pero solo un dispositivo ha logrado integrarse en la práctica clínica. Los fracasos se debieron principalmente a problemas técnicos y/o falta de estabilidad a largo plazo.[15-19]

El primer intento fue por parte de Maurice[15] en 1958 con un tonómetro de indentación tipo Schiötz sujeto a la cabeza que registraba las medidas de la PIO. Posteriormente en 1974 Greene & Gilman,[16] publicaron el primer sistema de monitorización de la PIO de forma no invasiva usando una lente de contacto. Este sistema fue probado en conejos y se basada en unas galgas metálicas que debían quedar colocadas en el limbo esclerocorneal y que detectaban los cambios en la PIO por los cambios en el ángulo iridocorneal.

En 1980 Wolbarsht,[17] diseñó un transductor de presión en forma de banda que era capaz de registrar las medidas de PIO. Esta banda fue implantada en gatos, colocándose alrededor del globo ocular, entre el recto superior y la esclera. En 1982, Flower[18] experimentó con monos adultos (*M. Rhesus)*. En 1992, Svedbergh[19] diseñó una lente intraocular con la capacidad de medir la PIO. En la actualidad existen investigadores encaminados a conseguirlo.[20-21] Leonardi[20] junto con la empresa Sensimed, ha desarrollado un dispositivo comercial de lente de contacto sensora que ya está disponible en el mercado europeo, y en proceso de evaluación por la FDA en Estados Unidos.

Hasta el momento, el único método fiable al alcance de cualquier profesional para determinar si existen o no aumentos en la PIO en cualquier momento del

día es practicar una curva tensional de 24 horas que requiere el ingreso hospitalario del paciente.[22] La implantación clínica de un dispositivo capaz de medir y monitorizar los valores de PIO sería muy importante ya que se estima[23] que la monitorización de la PIO durante 24 horas podría cambiar el manejo clínico de un alto porcentaje de los pacientes con glaucoma.

Los sensores capaces de monitorizar la PIO de forma no invasiva incorporados en lentes de contacto se basan en el principio de que un cambio en PIO de 1 mm Hg varía la curvatura corneal en 3 μm para un radio típico de 7,80 mm.[14,24]

El Instituto de Ciencia de los Materiales de Barcelona (ICMAB-CSIC) ha desarrollado un sensor mediante una película flexible de policarbonato piezorresistivo con moléculas metálicas adheridas de β -$(ET)_2I_3$ que muestra una gran sensibilidad ante pequeños cambios de presión.[25-27] Esta película electro-conductora puede detectar la resistencia a la tensión con una sensibilidad extremadamente alta de manera que la película es capaz de detectar una tensión relativa de $\approx 10^3$ %.[28] Por lo que se obtiene una lámina policristalina de un superconductor molecular de β-$(ET)_2I_3$.[24,25]

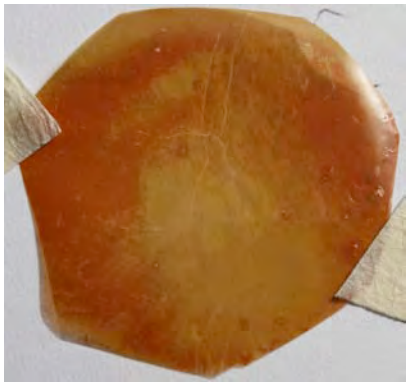

Figura 1. Lámina flexible de polímero sensor fabricado por el Instituto de Ciencias de los Materiales de Barcelona (CSIC).

El presente trabajo, pretende probar una nueva aplicabilidad de este sensor para la monitorización de la PIO de forma continua y no invasiva. En referencia a las propiedades mencionadas de la película encapsulada como una membrana en una LC puede ser aplicada como un sensor de presión de alta sensibilidad que pueda cumplir los requisitos para la medida no invasiva de la PIO.

4.- HIPÓTESIS

Es posible determinar cambios en la presión intraocular con una lente de contacto que incorpore un nanosensor estructurado que permita abrir la posibilidad de su futuro uso clínico para la monitorización y determinación de la presión intraocular en humanos.

5.- OBJETIVOS

1. Elección del modelo experimental adecuado para la calibración de la lente de contacto sensora.
2. Mejorar el conocimiento anatómico de los parámetros oculares del ojo porcino, especialmente a nivel corneal, así como la influencia en este estudio de las diferencias con el ojo humano.
3. Puesta a punto de un modelo experimental exvivo de ojo porcino que permita verificar la capacidad del sensor para detectar cambios en la PIO.
4. Calibración de la lente de contacto sensora.
    I. Sin control térmico (modelo exvivo).
    II. Controlando las variaciones térmicas (modelo exvivo).
    III. Influencia del parpadeo y los movimientos oculares (prueba de concepto invivo).

5. Diseño de un sistema de telemetría inalámbrico para el suministro de energía al dispositivo y la recogida de datos.
6. Determinación de la biocompatibilidad del material sensor.

6.- MATERIAL Y MÉTODO

6.1 Fabricación de la lente de contacto sensora

Se fabricaron de forma manual cinco prototipos de lente de contacto rígida permeable al gas (LCRPG) por parte de la empresa Conóptica SL, a partir del diseño que se realizó acorde a los parámetros que se le facilitaron de la córnea porcina. Se eligió un diseño de LCRPG con geometría inversa ya que para realizar las medidas es muy importante la proximidad entre el ápex corneal y el sensor. El radio más plano fue de 12 mm y el más curvado de 8,8 mm con un diámetro de 12,50 mm. A cada lente se le practicó un orificio de 3,0 mm de diámetro en el centro con objeto de permitir la colocación del sensor nanoestructurado (figura 2). El sensor se adaptó en el ICMAB - CSIC de forma manual incorporando también los cables para las conexiones del sensor con el sistema de registro para almacenar las medidas de las variaciones de la PIO.

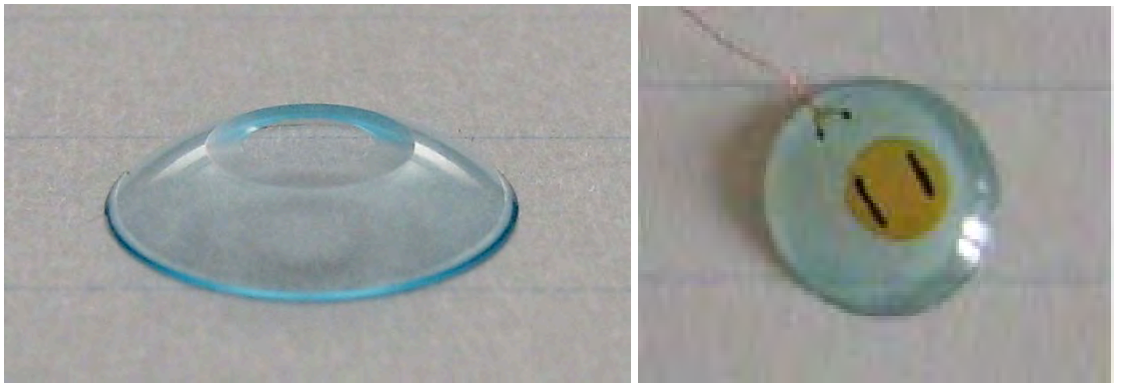

Figura 2. A la izquierda, LCRPG semiterminada con el orificio de 3,0 mm en su zona central. A la derecha, el prototipo de lente de contacto sensora con el sensor y cables de conexión incorporados.

6.2. Elección del modelo experimental

Se realizó una búsqueda bibliográfica en PubMed para determinar los modelos animales más utilizados en estudios de valoración de la PIO en glaucoma, de todos ellos se eligió el cerdo porque es muy utilizado al ser razonablemente parecido al globo ocular humano. Dada la diversidad y dispersión de la información sobre la anatomía del ojo porcino se realizó una extensa revisión de las características del globo ocular porcino que se completó con un estudio experimental en 5 ojos porcinos que permitió completar la información en la bibliografía y realizar el diseño de la lente de contacto sensora.

Para todos los experimentos realizados durante este trabajo se emplearon ojos de cerdo enucleados del matadero local. Los animales fueron cerdos blancos domésticos de entre 6 y 8 meses, no albinos, de entre 120 y 150 kg. Los ojos se obtenían entorno a las 8:30 AM justo después del sacrificio del animal. Las medidas se realizaron entre las 9:00 AM y las 12:00 AM. El exceso de tejido que rodea el globo ocular se retiró con unas pinzas *"moorfields conjuctival"* y unas tijeras *"wescott tenotomy wide hadle"* (John weiss international, Milton

Keynes, UK) para facilitar las medidas experimentales. Los ojos se mantuvieron en medio de cultivo DMEM (Dulbecco's Modified Eagle Medium) suplementado con una mezcla de antibiótico y antimicótico (Gibco, UK) desde su extracción hasta el momento de las medidas experimentales en el laboratorio.

Dado que la enucleación no se practicó por un cirujano experto se desecharon los globos oculares que presentasen signos de haber sufrido algún traumatismo durante la enucleación como pérdida de la forma del globo ocular, signos de desprendimiento de retina o luxación del cristalino que se comprobó mediante oftalmoscopía directa, previamente a la realización de las medidas experimentales.

6.3 Estudio anatómico del modelo experimental

La revisión bibliográfica dejaba algunos aspectos sin determinar como la queratometría corneal del ojo porcino que es de gran importancia para la adaptación de lentes de contacto especialmente las de tipo RPG. Por lo que se realizó un estudio anatómico en cinco ojos para completar la información no recogida en la literatura.

La curvatura corneal del ojo porcino se midió con el queratómetro manual (OM-4 Topcon) y con el autorrefractometro-queratómetro portátil (ARK-30 Nidek, Fremont, California).[30] El espesor corneal se midió mediante paquimetría ultrasónica con el paquímetro (Corneo-Gage Sonogage Inc., Cleveland, Ohio; calibrado por el fabricante). Además, se realizó un estudio topográfico de la superficie corneal con el topógrafo ORBSCAN II (Bausch & Lomb, Rochester,

NY, versión 3.12) determinando el espesor central y periférico, la curvatura, el poder refractivo y el diámetro corneal (distancia blanco-blanco). El diámetro antero-posterior se midió con un calibre (Centigraff SA, Barcelona, España, precisión 0,05 mm).

6.4. Puesta a punto del modelo experimental exvivo de ojo porcino

Para comprobar el punto en el que la presión manométrica del globo ocular se mantiene más estable, se optó por comparar las medidas canulando los ojos tanto en cámara anterior como en cámara vítrea.

Se tomaron 46 medidas de 6 ojos que se canularon dos milímetros por delante del limbo esclerocorneal de forma paralela al iris, con cuidado de no rozar el iris o el endotelio corneal, con una palomilla de 23G. Por otro lado, se tomaron 49 medidas de 5 ojos que se canularon en cámara vítrea a 3,5 milímetros del limbo esclerocorneal con una cánula de 20G usada habitualmente en la cirugía de vitrectomía.

Para monitorizar los cambios en la PIO inducidos en el ojo exvivo se diseñó un dispositivo experimental de manera que el globo ocular se conectó a un transductor de bajas presiones WIKA CPC 2000 (WIKA Alexander Wiegand GmbH & Co, Klingenberg, Alemania) que emite aire por un conducto que se comunicaba con una botella de cristal de Ringer lactato, la presión en la botella de cristal hace fluir el líquido por otro conducto que llega hasta la cánula en el globo ocular. Teniendo en cuenta que la altura del nivel del suero ha de ser la misma que el punto de canulación del ojo, la presión en el globo ocular será la

que se programe en el transductor de bajas presiones, ya que todo el circuito tendrá una presión homogénea evitando la diferencia de alturas. El circuito de aire que sale del transductor hacia la botella de cristal debe permanecer libre de líquido, y en el circuito de líquido que sale de la botella de cristal hacia el globo ocular también hay que evitar las burbujas de aire. Los aumentos de presión que se realizaron con el transductor fueron escalonados y cuando la presión en el transductor se estabilizaba, se realizaba a medición la PIO mediante tonometría de aplanación Perkins. En la figura 3 se muestra el esquema del dispositivo experimental.

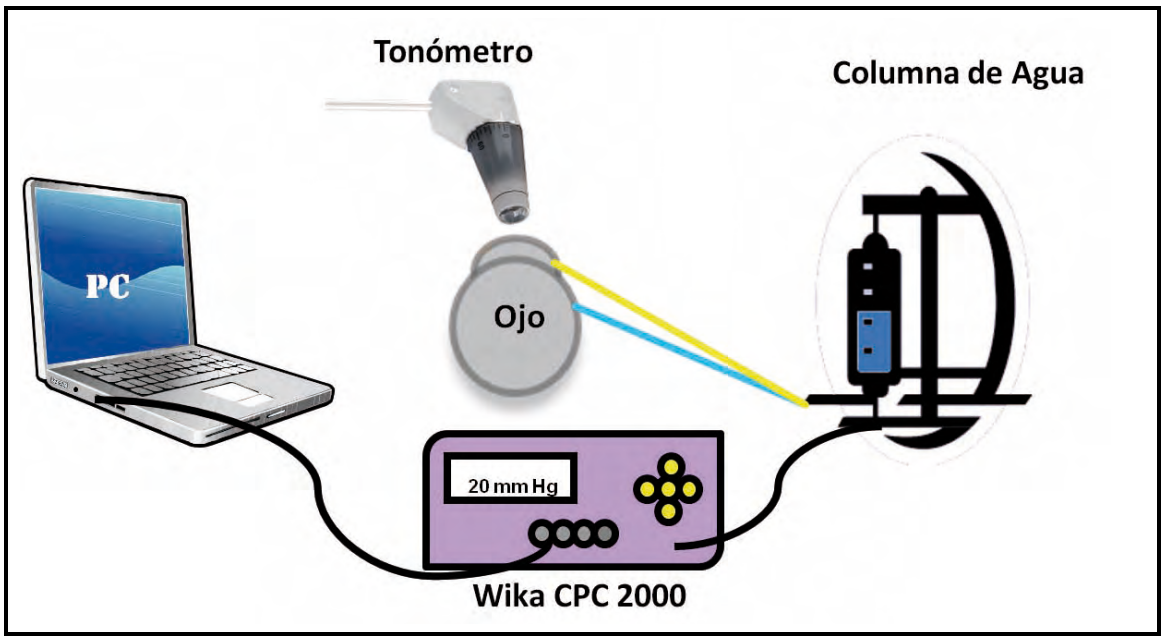

Figura 3. Representación esquemática del diseño experimental para calcular la relación entre la presión en el interior del globo ocular y la medida de la PIO con el tonómetro Perkins.

6.5. Diseño experimental de calibración de la lente de contacto sensora sin control térmico

Se utilizaron 30 ojos para calibrar la lente de contacto sensora con un diseño experimental semejante al empleado para determinar la zona de canulación. El globo ocular una vez canulado se conectó, a través de una columna de agua, al

transductor de bajas presiones WIKA CPC 2000 que registró las medidas cada cinco segundos. Sobre el ojo se colocó el prototipo de lente de contacto sensora de manera que la LC quedara centrada en la córnea con una adaptación plana que permitiera la posición idónea del sensor en el ápex corneal, así el sensor detectaba las mínimas deformaciones corneales que se producen con las variaciones de la presión en el interior del globo ocular. La lente sensora se conectó mediante unos finos hilos de cobre a un multímetro (Agilent 34410A, Agilent Technologies, USA) que registraba cada dos segundos los cambios en la resistencia eléctrica detectados por el sensor con las deformaciones corneales provocadas por los cambios de PIO. Ambos registros, las variaciones de presión del transductor y las variaciones de resistencia eléctrica detectadas por el sensor, se almacenaron en el mismo ordenador. El dispositivo experimental se muestra en la figura 4.

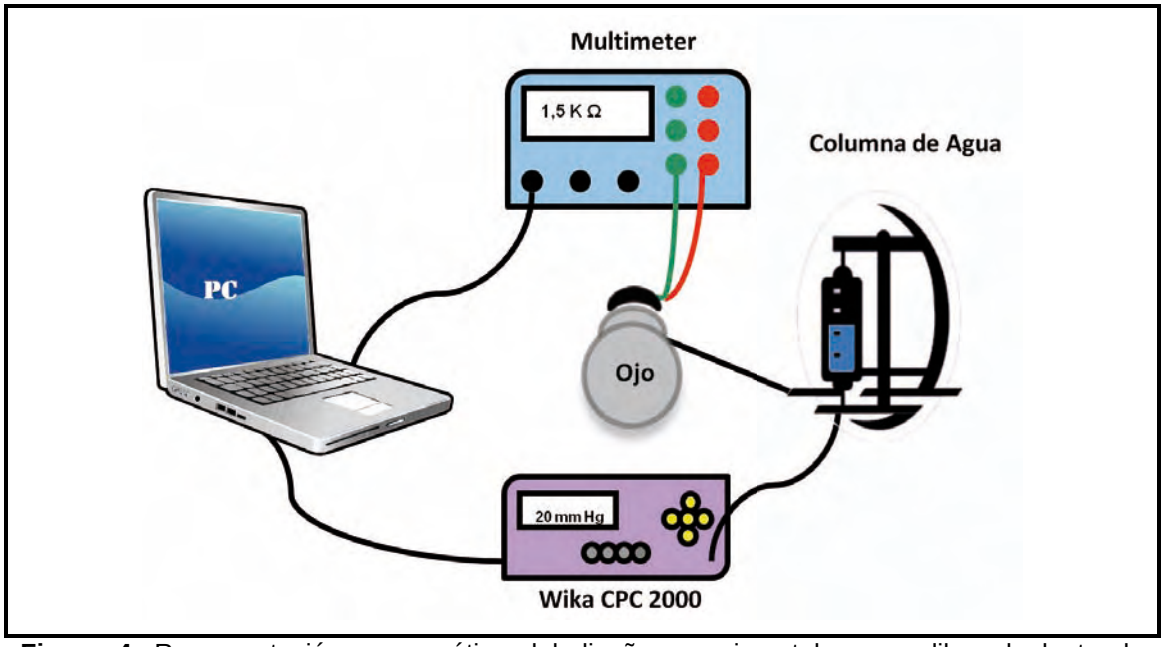

Figura 4. Representación esquemática del diseño experimental para calibrar la lente de contacto sensora**.**

6.6. Diseño experimental de calibración de la lente de contacto sensora con control de temperatura

El polímero sensor es sensible a la deformación pero también es sensible a las variaciones térmicas. En el primer experimental el sistema de recogida de datos era sencillo y no realizaba el ajuste a cero de la variación térmica, durante su realización se procuró mantener la temperatura de la sala de medida entre 20º y 22º C, Pero en la señal obtenida se observaban incongruencias con las variaciones de presión ejercidas con el transductor, de lo que se planteó la necesidad de tener en cuenta el posible efecto de variaciones térmicas en las medidas realizadas.

En el nuevo experimental el Centro Nacional de Microelectrónica (CNM-CSIC) diseñó un multímetro (dispositivo discreto) de menor tamaño y que se comunicaba con el ordenador vía bluetooth, además poseía batería y memoria interna para almacenar 24 horas de medidas continuas y posteriormente transferirlas al ordenador. En esta nueva variación el multímetro se conecta a dos sensores y mediante un circuito integrado de aplicación específica (puente de Wheatshtone) se consigue anular el efecto de la temperatura en la medición. La primera lente se colocó en el globo ocular, y mientras que la segunda lente permanecía junto al globo ocular conectándose al multímetro de manera que se utiliza como referencia para detectar los cambios debidos a la temperatura y poder eliminar así su influencia en la medida de las variaciones de presión intraocular. El globo ocular, las dos lentes y el multímetro se colocaron dentro de una caja de poliestireno expandido (comúnmente conocido como poliespam) que permaneció cerrada durante la realización de las

medidas para que la temperatura fuera lo más estable posible en su interior. El dispositivo experimental se muestra en la figura 5.

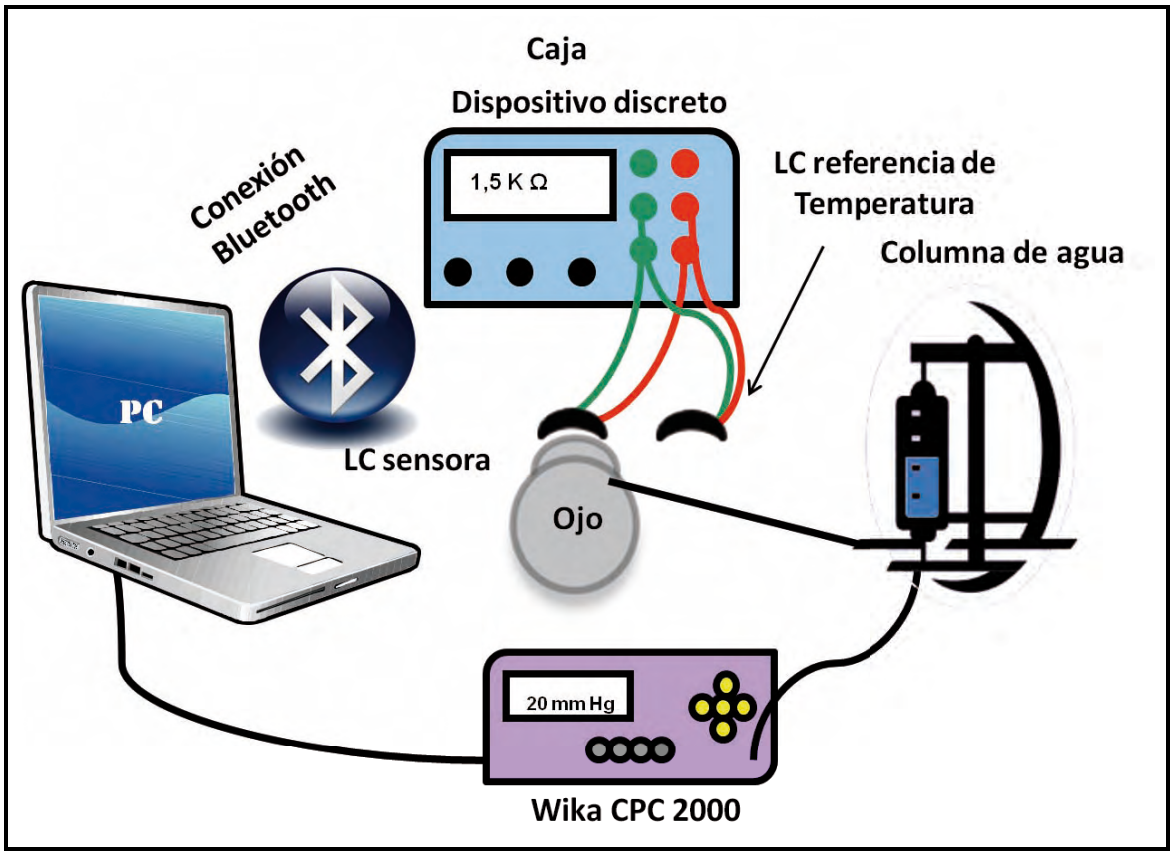

Figura 5. Representación esquemática del dispositivo experimental. El globo ocular, ambas lentes de contacto y el dispositivo discreto permanecerían dentro de la caja de polispam con único orificio que conecta con la columna de agua.

6.7. Procedimiento experimental invivo (prueba de concepto)

Se diseñó una lente de contacto sensora para adaptar en el globo ocular de un voluntario del equipo investigador. La lente de contacto se fabricó a partir de los datos de la topografía corneal ORBSCAN II (Bausch & Lomb, Rochester, NY, versión 3.12). La prueba tuvo una duración de dos horas y durante este periodo se registró la influencia del parpadeo, movimientos oculares en las medidas del sensor. La superficie ocular del voluntario fue anestesiada con una gota de oxibuprocaína clorhidrato y clorhidrato de tetracaína (Colircusi de Alcon, Cusi

S.A, Barcelona, España). También se adaptó una lente de contacto terapéutica (Purevision® Bausch & Lomb, USA) para proteger la córnea de posibles erosiones epiteliales, es decir se empleó un sistema de piggyback. La lente de contacto sensora se conectó al dispositivo discreto para tener un registro continuo de las variaciones de resistencia captadas por el sensor causadas por el parpadeo, los movimientos oculares y variación de la PIO durante una maniobra de Valsalva o la aplicación de una ligera presión sobre el globo ocular. Como el dispositivo se conectaba al ordenador vía Bluetooth el voluntario tenía libertad de movimientos.

El sujeto fue tratado de acuerdo con la declaración de Helsinki.

Figura 6. A la izquierda, voluntario con la lente de contacto sensora en el OD. A la derecha, imagen de la lente sensora tomada con lámpara de hendidura.

6.8. Biocompatibilidad del polímero sensor

Dado que el polímero sensor no tenía ninguna aplicación sanitaria previa, se consideró oportuno realizar un estudio de biocompatibilidad para asegurar la seguridad de su uso en aplicaciones biomédicas. Por su composición química mayoritariamente orgánica era un buen candidato para este uso, pero era necesario comparar su biocompatibilidad con la banda de silicona biocompatible que se utiliza en algunas de las cirugías de retina. En la figura 7 se puede observar ambos materiales.

Figura 7. A la izquierda, las porciones del polímero sensor. A la derecha, porciones de silicona que se insertaron bajo la piel de los cobayos.

Se tomaron 6 cobayos machos adultos (Dunkin Hartley) a los que se anestesió con ketamina (Imalgene 1000®, Merial; Barcelona, España. Solución inyectable en frasco de 10 ml), xilacina (Rompun®, Bayer; Leverkusen, Alemania. Solución inyectable en frasco de 25 ml) y atropina (Atropina Braun, B. Braun; Barcelona, España. Solución Inyectable en ampollas de 1 mg/1 ml) de forma intraperitoneal, subcutánea en la zona de la incisión e intramuscular por no ser suficiente con las dos primeras.

Se afeitó y desinfectó la zona. Se les practicó una incisión de un centímetro en la zona interescapular de la piel y bajo ella se colocó en el costado derecho del animal un pedazo de banda de silicona (control) y en el costado izquierdo un pedazo del mismo tamaño de material sensor (muestra). Una vez acabado el procedimiento se suturó la herida (figura 8).

Figura 8. Presentación de los cobayos anestesiados posteriormente a la intervención.

A los 20 días se sacrificaron los animales y se tomaron biopsias del tejido adyacente a la banda de silicona y al polímero sensor en los seis animales para su posterior estudio anatomopatológico.

7.- RESULTADOS

En primer lugar se presentan los resultados obtenidos de revisar las características anatómicas del globo ocular porcino para comprobar su adecuación como modelo experimental para este estudio. En segundo lugar se presentan las pruebas realizadas para la puesta a punto del modelo experimental. En tercer lugar se muestran los resultados de los experimentales realizados para la calibración de la lente de contacto sensora incluyendo la prueba de concepto en un ojo humano. En cuarto lugar el diseño del sistema de telemetría inalámbrico para la recogida de los datos por último los resultados de biocompatibilidad del polímero sensor.

7.1. Características anatómicas del modelo experimental de ojo porcino exvivo

Se han completado las medidas anatómicas del globo ocular porcino recogidas en la literatura mediante la medida del diámetro de iris visible, diámetro anteroposterior, paquimetría ultrasónica y topográfica, queratometría manual y automática junto con su astigmatismo corneal, que se muestran en la tabla 1.

Parámetro medido	**Media ± DS**	**IC 95%**
Ø Horizontal visible iris	14.31±0.25 mm	(14.03−14.59) mm
Ø Vertical visible iris	12±0.0 mm	−
Ø Anteroposterior	23.9±0.08 mm	(23.01−29.99) mm
Paquimetría ultrasonic	877.6±13.58 µm	(865.70−889.50) µm
Paquimetría topográfica	906.2±15.30 µm	(892.78−919.61) µm
Qx automática R1	41.19±1.76 D	(40.53−41.86) D
Qx automática R2	38.83±2.89 D	(37.76−39.89) D
Astigmatismo corneal [a]	2.36±1.70 D	(1.72−3.00) D
Qx manual R1	41.05±0.54 D	(40.57−41.52) D
Qx manual R2	39.30±1.15 D	(38.29−40.31) D
Astigmatismo corneal [b]	1.75±1.31 D	(0.60−2.90) D

Tabla 1. Parámetros oculares obtenidos por medidas experimentales (n=5). La segunda columna muestra la media con su desviación estándar (DS) y la tercera columna el intervalo de confianza al 95% (IC 95%). Ø=diametro; Qx=Queratometría; R1=Meridiano corneal más curvado; R2=Meridiano corneal más plano.

[a]Astigmatismo corneal tomado como la diferencia de los meridianos corneales obtenidos con queratometría automática ARK-30.

[b]Astigmatismo corneal tomado como la diferencia de los meridianos corneales obtenidos con queratometría manual.

En la tabla 2 se comparan los datos corneales del globo ocular porcino con el globo ocular humano. Se toma el valor de paquimetría ultrasónica exvivo dado que el modelo animal que se utilizará será exvivo.

Parámetro medido	**Ojo de Cerdo**	**Ojo Humano**
Ø Horizontal visible iris	14.31 mm	11.7 mm
Ø Vertical visible iris	12 mm	10.6 mm
Ø Anteroposterior	23.9 mm	24 mm
Paquimetría ultrasónica	877.6 µm	520 µm
Radio corneal medio	8.45 mm	7.80 mm

Tabla 2. Comparación de los parámetros medios del globo ocular humano según la literatura con las medias obtenidas del globo ocular porcino.

7.2. Puesta a punto del modelo experimental exvivo de ojo porcino

Existe una gran diferencia entre la presión manométrica y la PIO medida con tonometría de aplanación Perkins en el caso del modelo experimental de ojo porcino. Esta diferencia de presiones se atribuye a la diferencia de espesor corneal entre el globo ocular humano y el globo ocular porcino y que al ser un modelo exvivo es necesario recuperar el tono del globo ocular porcino, que una vez enucleado sufre ptisis. Por lo que para medir en un rango de PIO Perkins de entre 5 mm Hg y 45 mm Hg se establece un rango de trabajo de presión manómetrica de entre 20 mm Hg y 70 mm Hg.

Respecto a la diferencia en la tonometría de aplanación Perkins según el lugar de infusión, no se han encontrado diferencias estadísticamente significativas (ANOVA p=0,500) entre la presión inducida canulando en cámara anterior o en

cámara vítrea. Tampoco se han encontrado diferencias entre los incrementos de presión inducidos por el transductor de bajas presión comparados con la medida de la PIO Perkins (ANOVA p=0,138) canulando en cámara anterior o vítrea. Se realizó un análisis de comparación múltiple con corrección de Bonferroni encontrando un nivel de significación cercano a uno (p>0,939), de manera que no hay diferencias en las medidas entre ojos (comparación por pares).

Canulación en la cámara anterior

La presión inducida por el transductor está linealmente relacionada con la medida Perkins (R^2=0,940, p<0,001) obteniendo una ecuación que relaciona la presión del transductor con la PIO medida con tonómetro Perkins:

$$\text{Perkins} = -7{,}749 + 0{,}763\text{Transductor}$$

como se muestra en la figura 9.

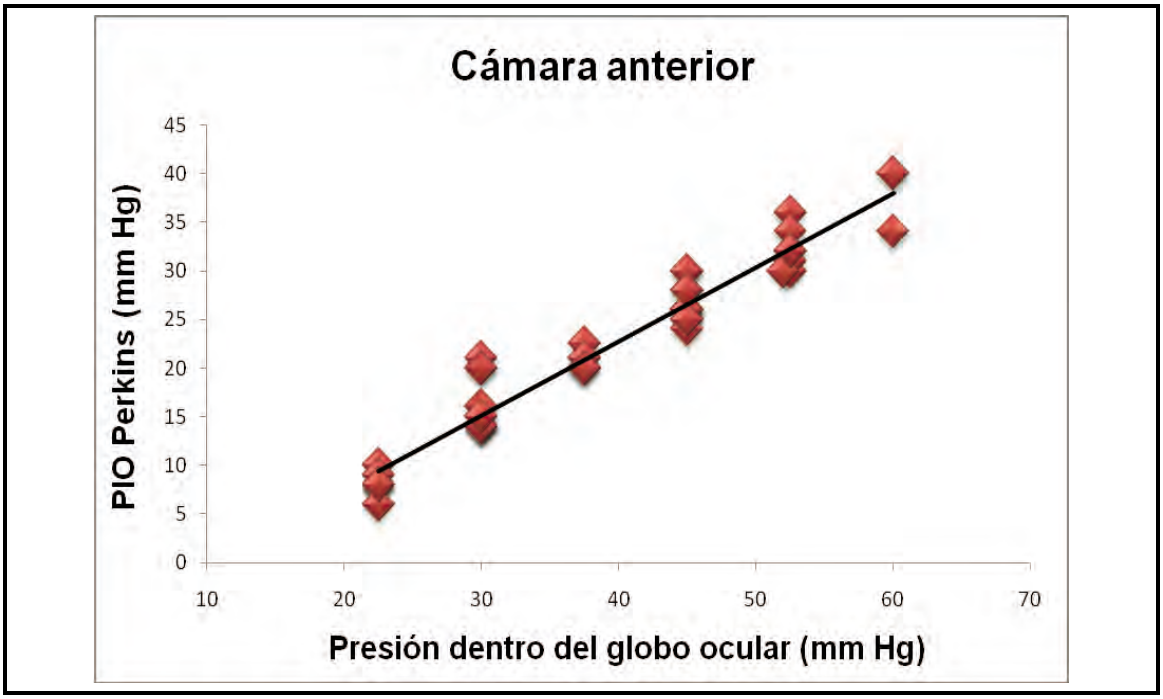

Figura 9. Representación gráfica de la ecuación que relación la presión generada en el interior del ojo mediante la infusión de líquido y la PIO tomada por tonometría Perkins, para ojos canulados en cámara anterior.

Canulación en la cámara vítrea

La presión inducida por el transductor está linealmente relacionada con la medida Perkins (R^2=0,885, p<0,001) obteniendo una ecuación que relaciona la presión del transductor con la PIO medida con tonómetro Perkins:

Perkins = -7,476 +0,730Transductor

como se muestra en la figura 10.

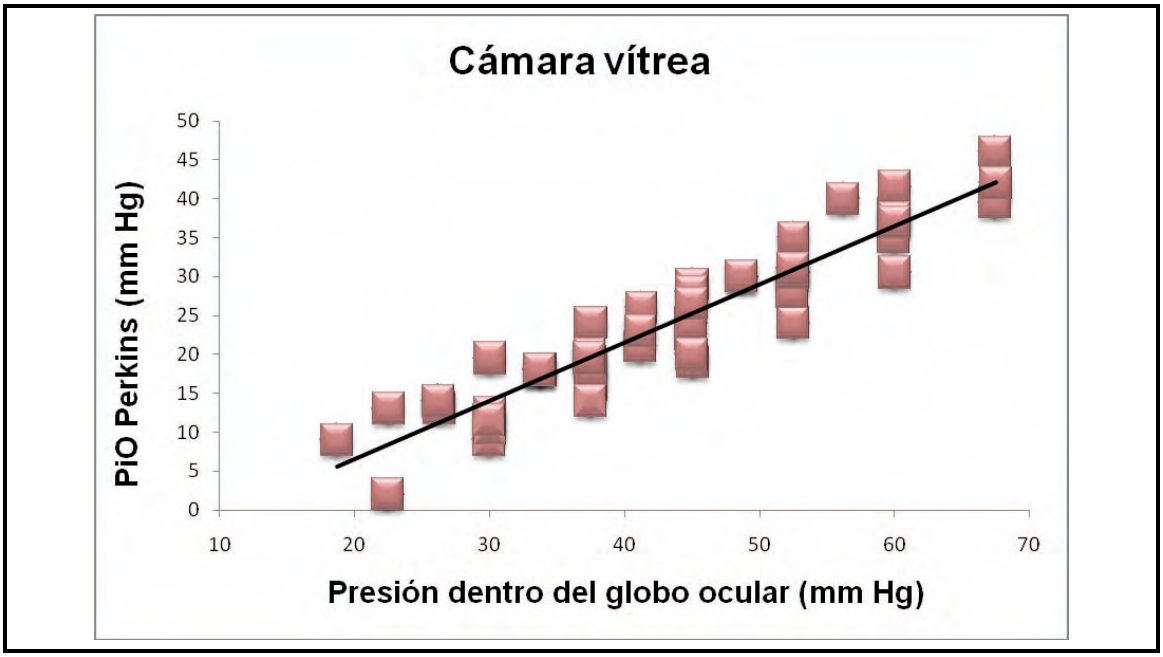

Figura 10. Representación gráfica de la ecuación que relación la presión generada en el interior del ojo mediante la infusión de líquido y la PIO tomada por tonometría Perkins, para ojos canulados en cámara vítrea.

Análisis por ojos

La presión inducida por el transductor está linealmente relacionada con la medida de la PIO Perkins obteniendo una ecuación para cada ojo, que las relaciona mediante un modelo regresión lineal con p≤0,001 para todos los ojos. En la tabla 3 se representan las ecuaciones correspondientes para cada ojo tanto canulando en cámara anterior como en cámara vítrea con su correspondiente coeficiente de correlación por ajuste de mínimos cuadrados (R^2).

Ojo	Ecuación	R^2
Cámara vítrea		
# 1	P = -4,607 + 0,689 T	0,954
# 2	P = -5,497 + 0,762 T	0,949
# 3	P = -12,568 + 0,760 T	0,938
# 4	P = -14,701 + 0,899 T	0,960
# 5	P = -15,151 + 0,863 T	0,966
# 6	P = -5,545 + 0,678 T	0,993
Cámara anterior		
# 7	P = -10,750 + 0,842 T	0,963
# 8	P = -4,845 + 0,744 T	0,897
# 9	P = -7,076 + 0,731 T	0,897
# 10	P = -9,286 + 0,800 T	0,988
# 11	P = -9,714 + 0,800 T	0,988

Tabla 3. Ecuación que relaciona la presión en el interior del globo ocular con la PIO Perkins, con su correspondiente coeficiente de mínimos cuadrados, para cada ojo medido. Del 1 al 5 canulando en cámara vítrea y del 6 al 11 en cámara anterior P = Perkins; T = Transductor.

7.3. Calibración de la LC sensora sin control térmico

Se realizaron medidas válidas en 30 ojos porcinos. Al observar su representación gráfica se aprecia que la resistencia variaba adecuadamente con los cambios de presión inducidos en el globo ocular, pero estas medidas no eran repetibles ni reproducibles, por lo que realizó un estudio pormenorizado de los cinco ojos porcinos con mejor respuesta en variaciones de resistencia.

Se realizó un análisis de los incrementos y disminuciones de la resistencia en estos cincos ojos, cuya representación gráfica se muestra a continuación (figura 11). Se observa un acuerdo en la pendiente pero con resultados muy dispares en el eje de ordenadas. Al realizar un ajuste de mínimos cuadrados se obtuvo un valor R^2=0,51 inferior de los que se esperaba para este polímero. De estas medidas se deduce que el control de la temperatura es necesario para la calibración de la lente de contacto sensora.

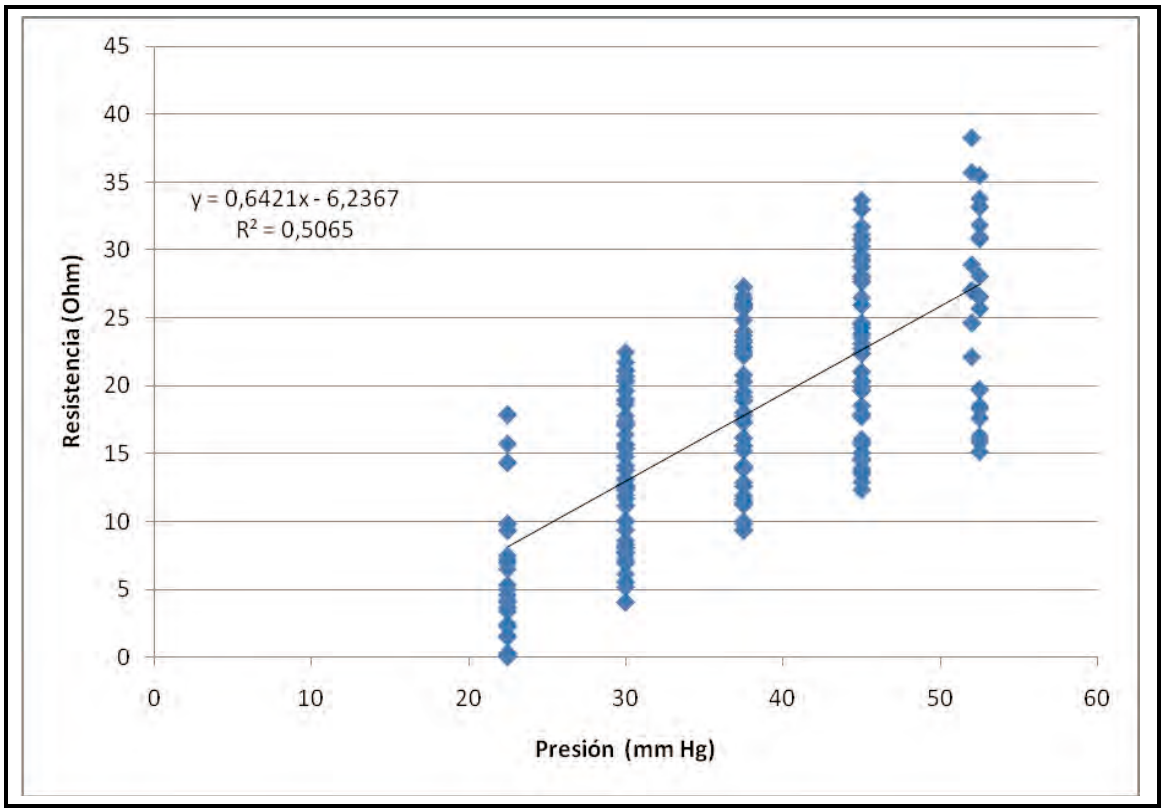

Figura 11. Representación gráfica de los incrementos y disminuciones de la resistencia de las cinco mejores medidas en el modelo de ojo porcino exvivo.

7.4. Calibración de la LC sensora controlando la temperatura

En este experimental se emplearon dos lentes de contacto conectadas al mismo multímetro, una sobre el ojo porcino, que se ve influenciada por los cambios de PIO y otra al lado del globo ocular que permitía controlar el efecto

de los cambios de temperatura. Con este diseño experimental se tomaron varias medidas. La representación gráfica de una de ellas se muestra en la figura 12.

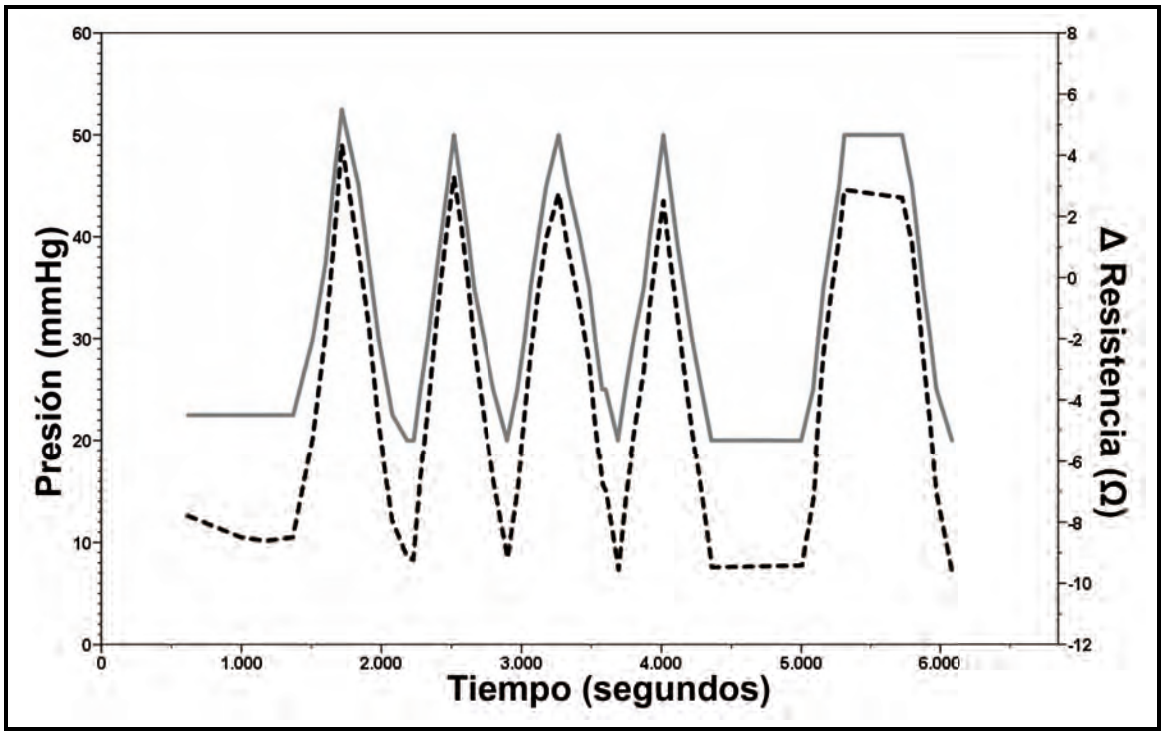

Figura 12. Representación gráfica de las variaciones de PIO y las medidas obtenidas de la lente de contacto sensora a lo largo del tiempo. Cambios de presión (mm Hg transductor Wika) se representan con la línea gris sólida y las variaciones de la resistencia eléctrica (Ohm) medidas por el sensor se representan con la línea discontinua negra. Ambos cambios de presión y resistencia (incrementos y disminuciones) muestran una tendencia similar y cuando la presión es constante la resistencia también.

Analizando los incrementos y disminuciones de la gráfica de la figura 12, es decir, la representación gráfica de los cinco ascensos y de los cinco descensos se obtiene una recta definida y un coeficiente R^2=0,99 que se muestra en la figura 13. La LC sensora tiene buena sensibilidad (0,4 Ω / mm Hg) para su uso en la monitorización no invasiva de la presión intraocular.

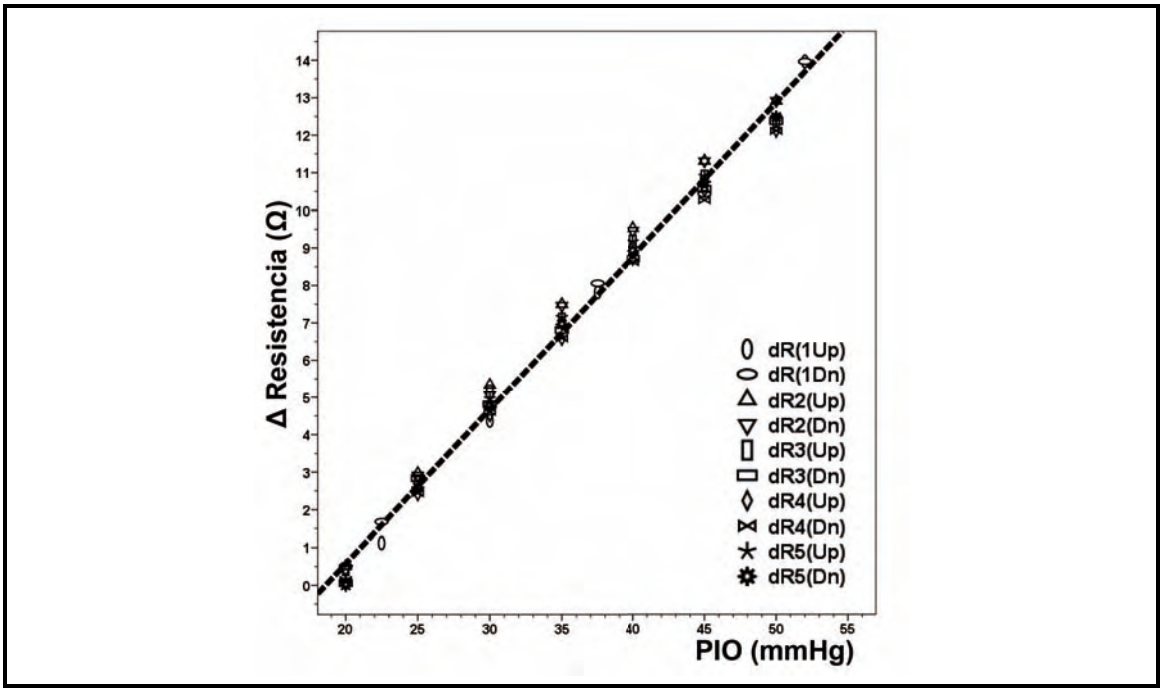

Figura 13. Calibración de la lente de contacto sensora teniendo en cuenta las variaciones térmicas. Los datos se tomaron de las cinco subidas y bajadas mostradas en la Figura 12. Se muestra una alta correlación entre los cambios en la PIO y los cambios en la Resistencia eléctrica (r^2=0.99), con una sensibilidad de 0,4 Ω/mmHg. (PIO=-7.6+0.41Ω).

7.5. Influencia de los movimientos oculares, parpadeo, etc.

En la figura 14 se muestran los resultados de la prueba de concepto en un sujeto vivo, en la figura se muestra como influyen en la señal los parpadeos, movimientos oculares, presión sobre el ojo y maniobra de Valsalva.

Todas estas causas de variaciones de presión muestran perturbaciones bruscas y cortas de la señal que el sistema de telemetría ha de filtrar para mostrar únicamente las variaciones de PIO que se correspondan con el ritmo circadiano, o la eficacia de los tratamientos que pretenden de disminuir la PIO.

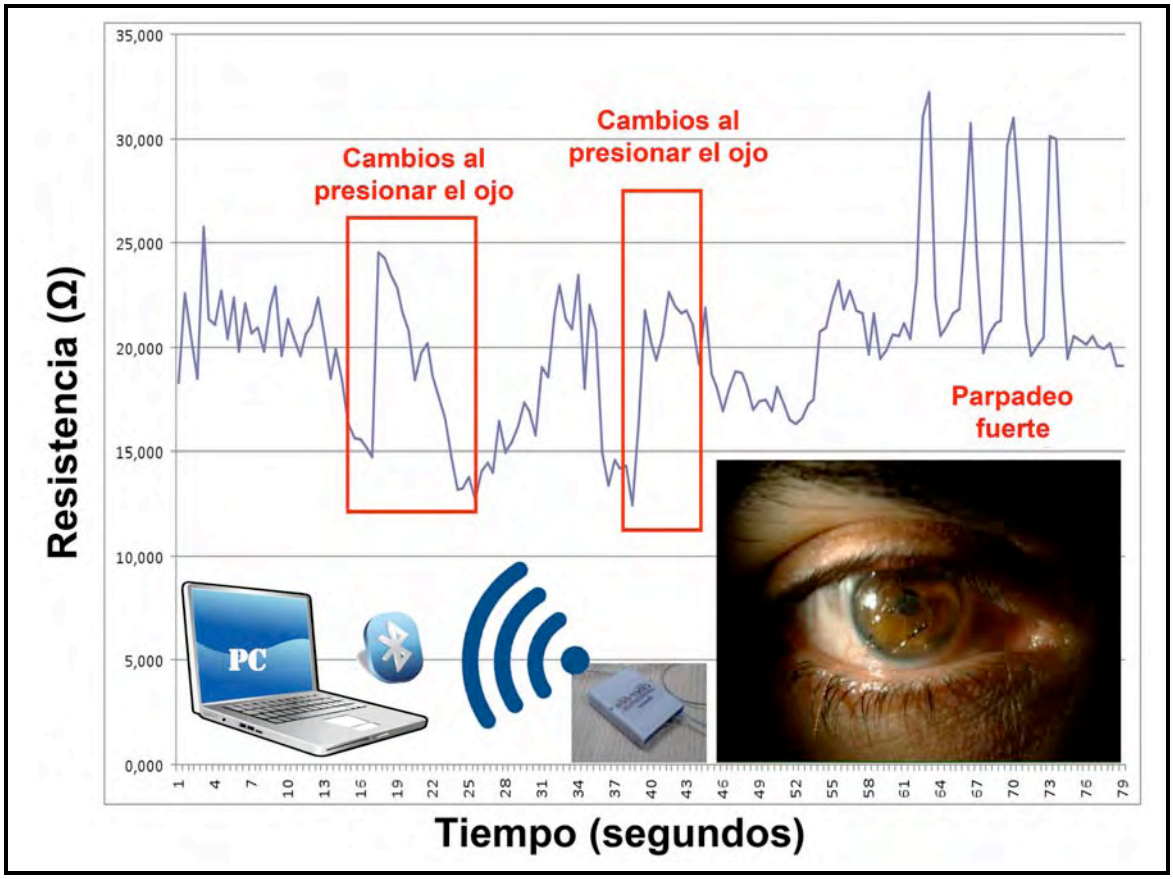

Figure 14. Diseño experimental y resultados del experimento in-vivo. Los cambios de resistencia están marcados con la línea gris. Representan cambios en la PIO por presionar el ojo, y fuertes parpadeos. Debajo, una fotografía de la LC-sensora en el ojo y el sistema de Bluetooth que registra los datos y los transmite al ordenador.

7.6. Medidas electrónicas de la lente sensora

En el desarrollo de un sistema para la monitorización de la PIO, es necesario un sistema electrónico de medida, registro y envío de los datos que esté encapsulado en la LC para evitar la incomodad que supondrían los cables entre la lente de contacto sensora y el sistema de almacenamiento para los pacientes. En un sensor ideal los datos medidos deben ser transmitidos al sistema de almacenamiento de forma inalámbrica.

Para desarrollar un sistema integrado de medición electrónico ASIC, se ha diseñado y probado un dispositivo discreto para el acondicionamiento y

digitalización de los datos (figura 15). El propósito de este dispositivo es establecer las características de la membrana y estudiar la viabilidad de los circuitos para desarrollar con éxito el ASIC.[52] Al mismo tiempo, también tiene que ser usado para estudiar los efectos en la señal de la película lagrimal, del parpadeo, de los movimientos oculares, de los cambios de temperatura, etc. para determinar si pueden ser filtrados por software o hardware en posteriores fases de investigación en la continuación de este proyecto.

Figura 15. Dispositivo discreto diseñado para la recogida, almacenaje y transmisión de los datos medidos por la lente sensora.

7.7. Biocompatibilidad del polímero sensor

Las biopsias de los tejidos circundantes al polímero sensor y a la banda de silicona insertadas bajo la piel de los cobayos se estudiaron anatomopatologicamente para identificar la reacción inflamatoria provocada por cada uno de los polímeros (banda de silicona y sensor) y poder determinar el grado de biocompatibilidad de sensor comparando la reacción inflamatoria provocada por cada polímero.

Se encontró una menor reacción inflamatoria en el tejido que rodeaba al polímero sensor que en el tejido que rodeaba la banda de silicona (figura 16) en todas las muestras, concluyendo que el polímero sensor es más biocompatible que la banda de silicona que se utiliza en cirugía ocular.

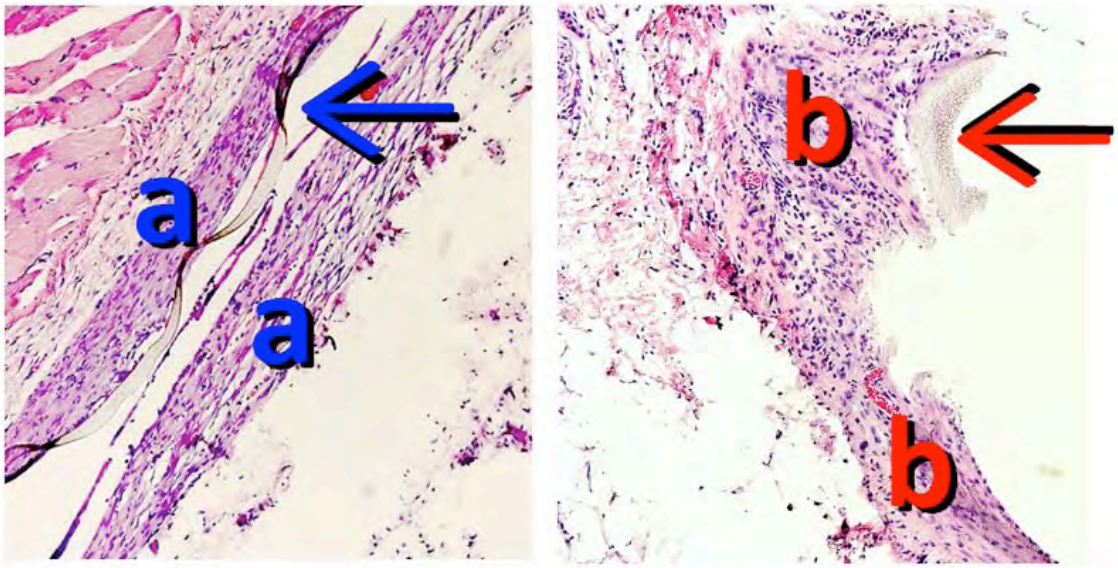

Figura 16. Tinción de Hematoxilina-Eosina de los tejidos adyacentes al polímero sensor y a la banda de silicona.

A la izquierda, el polímero sensor (flecha azul) rodeado de una capsula de tejido fibroso (a) con linfocitos ocasionales.

A la derecha, la banda de silicona (flecha roja) rodeada de una capsula fibrosa y un moderado infiltrado inflamatorio compuesto de linfocitos, con presencia de leucocitos polimorfonucleares ocasionales (b). (magnificación original 10X).

8.- DISCUSIÓN

8.1. Limitaciones del estudio

Este prototipo abre una línea de investigación prometedora en la que todavía queda un largo camino por recorrer, con resultados preliminares muy alentadores que animan a continuar investigando para conseguir un prototipo de lente de contacto sensora que permita su uso clínico de forma segura, sin molestias a los pacientes y con medidas precisas de la PIO y sus variaciones.

Aunque es necesario destacar que los resultados de esta tesis han sido obtenidos en globos oculares porcinos enucleados y, por tanto es necesario contrastar esta información con medidas bien en modelos animales vivos o bien en humanos (en ensayos clínicos controlados).

Uno de los problemas del modelo experimental fue el cálculo del rango de trabajo, el transductor de bajas presiones necesita insuflar una presión más alta de lo esperado para empezar a medir la PIO con tonómetro de Perkins en el rango de “valores clínicos” entre 5 y 45 mm Hg. Esto es debido a que el ojo enucleado se encuentra en ptisis, por la falta de producción de humor acuoso, el vaciado de los vasos y por la falta del flujo uveal coroideo, que es de gran importancia para mantener la presión basal del globo ocular. Por estas razones, fue necesario aumentar la presión dentro del globo ocular para recuperar su tono natural y a partir de ese valor realizar los cambios en la PIO.

Otra limitación del estudio se debe al diseño de los tonómetros empleados para la medida de la PIO, ya que el tonómetro de Perkins se basa en la ley de Imbert-Fick, que establece la PIO es la relación entre el peso del tonómetro y del área aplanada, suponiendo que el ojo se comporta como una membrana infinitamente delgada, seca, elástica y esférica. El cono-prisma tiene un diámetro de 7,0 mm, y en el proceso de medida, la zona de la córnea aplanada ha de tener un diámetro de 3,06 mm en el momento en el que se igualen la presión ejercida con el tonómetro y la PIO[12] suponiendo un espesor corneal de 550 micras y un radio corneal de 7,80 mm que están muy alejados de los parámetros de la córnea porcina que tiene una queratometría más plana con un radio medio de 8,45 mm. Además es más gruesa, con un espesor de 877,6 µm muy superior al empleado en la calibración del tonómetro Perkins.

Por esta razón, cuando el tonómetro Perkins aplane un diámetro mayor de 3,06 mm realizará una fuerza mayor que afectará al valor de PIO medido. Este error

será similar para todas las medidas, ya que los ojos empleados en los estudios experimentales de esta tesis tienen un espesor y un radio corneal similar. Por esta razón, el error de la medida de la PIO de Perkins probablemente tenga una repercusión limitada en las conclusiones de esta tesis. Además, se ha encontrado la equivalencia entre la presión dentro del globo ocular porcino y la PIO medida por tonometría de aplanación Perkins que podría ser útil en los modelos exvivo de globo ocular porcino, si bien se necesita más investigación para validar esta equivalencia en un modelo porcino invivo de hipertensión ocular.

Otra limitación importante tiene que ver con el diseño del dispositivo de telemetría. Dado el pequeño área útil de la LC para incorporar el sistema de telemetría sería necesario un diseño muy reducido y que además debe cumplir dos funciones; generar la energía para que todo el dispositivo funcione (que requiere un sistema de transmisión de energía inalámbrico, que a su vez implica el diseño de un dispositivo electrónico de bajo consumo), y ser capaz de realizar la recopilación y transmisión de los datos correspondiente a las medidas de la PIO. Esto sólo puede lograrse mediante el desarrollo de un circuito integrado de aplicación específica (ASIC)[31] cuyo coste no puede abordarse en la actual fase de desarrollo del prototipo del sensor desarrollado en esta tesis doctoral.

El dispositivo discreto empleado en los estudios experimentales en esta tesis se ha conectado mediante cables a la LC sensora, lo que permitió su uso durante pocas horas para realizar una prueba de concepto del sensor.

Lamentablemente el prototipo actual no es lo suficientemente confortable para su uso durante un tiempo más prolongado. Por este motivo, es necesario desarrollar un sistema inalámbrico que permita a los pacientes realizar sus actividades normales mientras se registran las variaciones de PIO a lo largo del día.

8.2. Selección del modelo experimental

Se han recogido todos los hallazgos en la literatura de la anatomía del globo ocular porcino tanto de las estructuras extraoculares (músculos extraoculares y párpados) como de las estructuras intraoculares [esclera, córnea (se han completado con un estudio experimental), cristalino, el drenaje uveoescleral y la estructura retiniana] así como de su respuesta inflamatoria.

8.2.1. Estructuras extraoculares

Motilidad ocular extrínseca

Los seis músculos extraoculares del ojo porcino son muy similares a los del globo ocular humano; además existe un séptimo músculo extraocular que rodea el nervio óptico y los vasos sanguíneos llamado músculo retractor bulbi. Este músculo introduce el globo ocular en la órbita.[32]

Párpado

El ojo porcino posee membrana nictitante, es decir, el tercer párpado accesorio que puede ocasionar ciertas molestias en cirugías oculares en las que el animal sea anestesiado.[33] El tercer párpado está situado en el canto medial del ojo, su función es la protección mecánica de la córnea, esparcir la película

lagrimal y la defensa inmunológica local mediante la secreción procedente de los nódulos linfáticos. Parte de la película lagrimal se genera en la glándula superficial del tercer párpado.[34] El movimiento del tercer párpado es pasivo y depende de la acción del músculo retractor bulbi, la retracción del globo ocular implica la protusión del tercer párpado hacia el ángulo temporal.[34] La glándula profunda del tercer párpado también se llama Glándula Herderian.[34] Su estructura es lobular y está situada dentro de la periórbita en la parte medial de la pared orbitaria. Su secreción tiene función lubricante de la superficie ocular y además de propiedades antibacterianas e inmunológicas.[35]

8.2.2. Estructuras intraoculares

Drenaje uveoescleral

El ángulo iridocorneal porcino es una medida muy heterogénea intra-especie como muestra el trabajo de Bartholomew.[36] El drenaje uveoescleral fue medido en el trabajo de Wagner JA, para evaluar el drenaje coroideo manteniendo constante la PIO en 10 mm Hg, obteniendo una media de 2,8 ± 0,9 µl/min . Después de bloquear el conducto convencional de drenaje, este disminuye hasta una media de 1,1 ± 0,5 µl/min. Bloqueando las venas vorticosas no existe cambio en el drenaje uveoescleral que se mantiene en 1,2 ± 0,8 µl/min.[37]

Esclera

La esclera porcina está cargada negativamente con un pH de 7,4.[38] El espolón escleral está especialmente marcado en algunos puntos. Existen variaciones en la profundidad del sulco escleral (sulcus) dependiendo del punto de la circunferencia del limbo en el que se observe.[39] Existe una escasa inervación

en esta área.[40] El espesor de la pared escleral se estima en un rango entre (830 - 1250 µm)[38-41] y la parte anterior está fuertemente pigmentada.[42] El contenido de agua es del 69,5% ± 1.18%.[41] Histológicamente la esclera porcina es muy similar a la esclera humana aunque el colágeno parece más desorganizado que el de la esclera humana.[41]

Córnea

El diámetro horizontal es de 14,23 mm y el diámetro vertical es de 12,09 mm.[36] La paquimetría ultrasónica en modelos exvivo es de 1013 ± 10 µm[43] y en modelos in vivo es de 666 µm (con un rango de 534 µm a 797 µm) ,[44] la diferencia se puede asociar a la hidratación de los tejidos postmortem. En el modelo exvivo el epitelio corneal tiene un espesor de 80 µm, que varía unas 25 µm de unas zonas a otras. El espesor del estroma es de 900 µm y la membrana de Descemet junto con el endotelio tiene un espesor de 30 µm aproximadamente. La cornea porcina carece de capa de Bowman.[43] El estroma tiene gran cantidad de colágeno tipo I[43] y su orientación es principalmente circunferencial.[45] La membrana de Descemet se extiende por debajo del origen de la córnea y se inserta estrechamente en los ligamentos.[39] El contenido de agua de la cornea porcina es del 71,93 ± 0,47% y su transparencia es del 54,77 ± 0,47%.[46]

Cristalino

El cristalino porcino se compone de tres tipos de proteínas cristalinas que pueden ser solubles o insolubles, solubles son α, β y γ cristalinas. Las α cristalinas forman el 35% del exterior del cristalino y forman el 22% del interior

del cristalino (núcleo). Las β cristalinas forman el 45% del exterior del cristalino y el 35% del núcleo. Las γ cristalinas solubles se encuentran en menor proporción que las α cristalinas y β cristalinas, presentando una mayor concentración en el núcleo del cristalino. El aumento de las γ cristalinas puede contribuir al gradiente del índice de refracción. Las proteínas insolubles están en una proporción mayor en la corteza que en el núcleo y su proporción aumenta constantemente hasta alcanzar la concentración máxima del 25%.[47]

El poder refractivo del cristalino es del 49,9 ± 1,5 D y su índice refractivo es de 1,4686 con una aberración esférica de -3,6 ± 2,0 D. Su radio anterior y posterior es de 7,08 ± 0,35 mm y 5,08 ± 0,14 mm respectivamente. El espesor del cristalino es del 7,4 ± 0,1 mm.[48] La cámara anterior tiene una profundidad alrededor de 3,5 mm.[49]

Retina

En la retina porcina, se mantiene la estructura de las 10 capas que se encuentran en la retina humana dado que el desarrollo embrionario es semejante en ambas especies.[50] Existe un área central deprimida, rica en conos, que es comparable con la mácula humana.[32,50,51] Su forma es de banda horizontal, se localiza sobre la cabeza del nervio óptico[42] y recibe el nombre de *"foveal streak"*.[52] La densidad de conos en ese área es de 15000 a 40000 células/mm^2. [42]

La proporción entre conos y bastones es similar a la de la retina humana y la densidad paramacular de conos también.[32] Estos datos se pueden obtener por

electrorretinografía. El reflejo del fondo de ojo es desde anaranjado a gris pálido con células epiteliales pigmentadas. Al igual que el ojo humano, el ojo porcino también carece de tapetum.[33] La circulación sanguínea de la retina es holoangiótica.[32].

8.2.3. Respuesta inflamatoria

Respuesta inflamatoria

La respuesta inflamatoria postoperatoria del globo ocular porcino es mayor que la del globo ocular humano y en ocasiones durante las cirugías de polo posterior puede producirse una hemorragia coroidea difusa que en muchos casos es irreparable.[32] El flujo sanguíneo coroideo con la arteria retiniana bloqueada es de 500 µl/min.[51]

Las diferencias más importantes entre el globo ocular porcino y el humano se pueden resumir en la pigmentación de la esclera, [42] la falta de membrana de Bowman,[43] la diferencia del espesor corneal,[43,44] un séptimo músculo extraocular, el retractor bulbi que retrae el globo ocular hacia el interior de la órbita,[45] la presencia de la membrana nictitante,[32] la aparición de reacciones inflamatorias mayores postcirugía,[32,53] la forma y espesor del cristalino.[48,54]

Dado que no existían trabajos anteriores que describieran las características de la córnea porcina, en particular los radios cornéales que son sencillos del medir por topografía corneal o queratometría automática se completaron los hallazgos bibliográficos con un estudio anatómico experimental. El diámetro corneal del ojo porcino es mayor,[44] con radios corneales más planos[55] que la

córnea humana con un astigmatismo corneal también mayor. Estas diferencias topográficas junto con la diferencia de espesor corneal sugieren que el globo ocular porcino puede no ser un buen modelo animal para la cirugía refractiva, implantes de lentes intraoculares u otras condiciones, si bien, estas diferencias anatómicas pueden tener una menor importancia en su uso como modelo de hipertensión en glaucoma o estudios de patología o función retiniana.

A la luz de los resultados de la revisión y puesta a punto del modelo experimental exvivo, el ojo porcino ha demostrado ser fiable para las necesidades de este estudio, es decir, para representar variaciones mínimas de PIO y en consecuencia verificar la capacidad de la LC sensora para detectar cambios en la PIO. El polímero sensor ya había demostrado ser fiable en la medida de deformaciones[28] pero no se había comprobado la posibilidad de que el polímero se incorporara en una LC y que fuese capaz de captar las variación en la curvatura corneal generada por la variación de la PIO. Por este motivo era necesario comprobar experimentalmente esta capacidad del sensor antes de proponerlo como método de monitorización de la PIO.

8.3. Puesta a punto del modelo experimental

El ojo de cerdo es un modelo animal de glaucoma muy utilizado ya que su tamaño es semejante al del globo ocular humano. Muchos trabajos lo utilizan como modelo de hipertensión ocular invivo y exvivo. Existen distintos métodos para generar modelos de hipertensión ocular en modelos invivo,[56,57] se puede cauterizar las venas epiesclerales,[56,58] o bloquear el ángulo iridocorneal para

impedir el flujo del humor acuoso por la malla trabecular.[59] En modelos exvivo[60-62] se suele inyectar fluidos en el interior globo ocular.

Estos modelos animales se emplean para estudios de farmacocinética y farmacodinámica probando nuevos tratamientos para la disminución de la presión intraocular,[63-65] tratamientos láser con función semejante a la iridotomía,[66] monitorizar la pérdida de las células ganglionares[53,54] o las lesiones en la lámina cribosa.[59,60]

Dentro de los modelos exvivo de hipertensión ocular por inyección de líquido no parece estar claro cuál es el método correcto para la infusión del líquido. Hay estudios en los que se opta por canular en cámara anterior,[67,68] otros en cámara vítrea[69] y algunos realizan la infusión a través del nervio óptico,[70] sin embargo no existen trabajos que comparen los cambios en la PIO dependiendo de la zona ocular en la que se realice la infusión. Además es necesario destacar que habitualmente en experimentación animal no se utiliza la tonometría Goldman para la medida de la PIO ya que es un dispositivo que requiere el uso de una lámpara de hendidura. Alternativamente, se utilizan otras técnicas como tonometría de aplanación Perkins u otro tipo de tonómetros como el Tonopen.[71,72] Sin embargo, este último tonómetro no ha demostrado una gran precisión en la medida de la PIO frente a otros tonómetros especialmente en valores de presión superior a 20 mm Hg. Por este motivo, se decidió emplear el tonómetro Perkins en esta tesis.

Se ha encontrado una relación directa entre la presión insuflada en el interior del globo ocular y la medida desde el exterior, que podría ser descrita matemáticamente por la ecuación de una recta, independientemente del punto de la canulación. Este resultado indica que el globo ocular porcino cumple razonablemente con la ley de Hooke para los cuerpos elásticos, de acuerdo con hallazgos anteriores.[73] Sin embargo, no hubo diferencias estadísticamente significativas en la presión medida por tonometría de aplanación Perkins entre las zonas de canulación (cámara anterior y posterior) por las que se llevó a cabo la infusión de líquido para variar la PIO.

8.4. Calibración lente de contacto sensora

El resultado de la calibración de la lente de contacto sensora ha resultado razonablemente satisfactorio, cuando se anula el factor de la temperatura, obteniendo una medida repetible y reproducible de los cambios de PIO inducidos. El problema de la medida recogida por el sensor es que el valor registrado está indirectamente relacionado con la PIO, de manera que el sensor ofrece variaciones de resistencia eléctrica que deben ser convertidas en variaciones de PIO, es decir, no se trata de una medida directa del valor de la PIO. Sin embargo, sí que se ha demostrado que los incrementos son constantes como muestra la figura 13 con una precisión de 0,4 Ohmios por cada milímetro de mercurio que varía la PIO.

Sin embargo, para conocer el valor de PIO en cada medida sería necesario una medida del valor basal de PIO por ejemplo mediante tonometría de aplanación Goldmann (considerada como el gold estándar para la medida de la PIO) y a

partir de este valor basal calcular el valor de PIO. Esta calibración se tendría que realizar con cada paciente, para poder tener una estimación del valor máximo de PIO alcanzada en un sujeto que portase la lente sensora para monitorizar su PIO.

Estos problemas de medida indirecta y calibración son comunes a otros sensores de PIO en lente de contacto como por ejemplo la lente comercializada por Sensimed,[14,20] que también realiza una medida indirecta de las variaciones de PIO, pero en este caso su medida es en voltios.

8.5. Implicaciones Clínicas

La monitorización continua de la PIO puede ser de suma importancia en pacientes sospechosos de padecer glaucoma; por ejemplo, en pacientes que en la consulta presentan una PIO normal pero el patrón de pérdida de campo visual y la cabeza del nervio óptico sugieren un diagnóstico de glaucoma normotensional. La monitorización de la PIO también podría utilizarse para ajustar el tratamiento de los pacientes diagnosticados de glaucoma.[23] Hasta el momento, el único método fiable para conocer las variaciones de PIO durante todo el día es la realización de una curva tensional durante 24 horas, para lo cual es necesario el ingreso hospitalario del paciente.[22]

Este estudio propone un nuevo método para la monitorización continua de la PIO, mediante una LC sensora, validando este principio en un modelo exvivo de ojo porcino y realizando una prueba de concepto en un ojo humano que muestra las perturbaciones generadas en la señal por los movimientos oculares

y el parpadeo que deben ser filtrados para mostrar sólo los cambios debidos a las variaciones de la PIO. A priori, estas señales son fácilmente reconocibles, y es de esperar que puedan identificarse como una perturbación en la señal fuerte y corta permitiendo su filtrado, si bien, este proceso debe ser validado en posteriores trabajos de investigación.

9-. CONCLUSIONES

Se ha revisado y completado los datos sobre la anatomía del globo ocular porcino que permite considerarlo un modelo experimental exvivo adecuado para el estudio de los cambios de la PIO.

Además se ha verificado la correlación entre la PIO medida por tonometría de aplanación Perkins y la presión intraocular inducida por canulación en cámara anterior o posterior con un transductor de bajas presiones.

Se ha determinado una ecuación que correlaciona la presión manométrica con la PIO Perkins, que permite su uso en estudios que utilicen el ojo porcino como modelo animal exvivo de hipertensión en glaucoma, facilitando la interpretación de las medidas manométricas.

Se ha determinado la sensibilidad del sensor nanoestructurado para identificar y medir cambios en la PIO en un modelo exvivo de ojo porcino. Los resultados de experimentales con la LC sensora muestran que este prototipo presenta una sensibilidad adecuada para la monitorización continua de la PIO, y que podría ser muy útil para el diagnóstico y tratamiento del glaucoma.

Se ha realizado una prueba de concepto en humanos con el prototipo de lente de contacto sensora con resultados satisfactorios. En el futuro, el desarrollo del este dispositivo en una lente sensora hidrofílica permitiría que fuera mínimamente invasiva permitiendo la monitorización continua de la PIO de forma precisa durante largos periodos de tiempo mientras el paciente pueda realizar sus tareas habituales, sin interferir en su visión.

Se ha diseñado un sistema de telemetría inalámbrico capaz de generar la energía necesaria para que el dispositivo funcione, y rentabilizar al máximo la sensibilidad del sensor nanoestructurado con el desarrollo de un circuito integrado de aplicación específica (ASIC).

Se ha comprobado la biocompatibilidad del sensor. La tinción con hematoxilina-eosina del tejido de los cobayos ha demostrado la biocompatibilidad del sensor nanoestructurado con unos niveles de respuesta inmunitaria mínimos.

10.- BIBLIOGRAFÍA

1. Resnikoff S, Pascolini D, Etya'ale D, Kocur I, Pararajasegaram R, Pokharel GP, Mariotti SP. Global data on visual impairment in the year 2002. Bull World Health Organ. 2004;82:844-851.
2. Sung VC, Koppens JM, Vernon SA, Pawson P, Rubinstein M, King AJ, Tattersall CL. Longitudinal glaucoma screening for siblings of patients with primary open angle glaucoma: the Nottingham Family Glaucoma Screening Study. Br J Ophthalmol. 2006;90:59-63.
3. Raychaudhuri A, Lahiri SK, Bandyopadhyay M, Foster PJ, Reeves BC, Johnson GJ. A population based survey of the prevalence and types of glaucoma in rural West Bengal: the West Bengal Glaucoma Study. Br J Ophthalmol. 2005;89:1559-1564.
4. Sharts-Hopko NC, Glynn-Milley C. Primary open-angle glaucoma. Am J Nurs. 2009;109:40-47.

5. Ren R, Wang N, Li B, Li L, Gao F, Xu X, Jonas JB. Lamina cribrosa and peripapillary sclera histomorphometry in normal and advanced glaucomatous Chinese eyes with various axial length. Invest Ophthalmol Vis Sci. 2009;50:2175-2184.
6. Goldbaum MH, Jang GJ, Bowd C, Hao J, Zangwill LM, Liebmann J, Girkin C, Jung TP, Weinreb RN, Sample PA. Patterns of glaucomatous visual field loss in sita fields automatically identified using independent component analysis. Trans Am Ophthalmol Soc. 2009;107:136-144.
7. Harwerth RS, Vilupuru AS, Rangaswamy NV, Smith EL 3rd. The relationship between nerve fiber layer and perimetry measurements. Invest Ophthalmol Vis Sci. 2007;48:763-773.
8. Li S, Wang X, Li S, Wu G, Wang N. Evaluation of optic nerve head and retinal nerve fiber layer in early and advance glaucoma using frequency-domain optical coherence tomography. Graefes Arch Clin Exp Ophthalmol. 2010;248:429-434.
9. Shin IH, Kang SY, Hong S, Kim SK, Seong GJ, Tak MK, Kim CY. Comparison of OCT and HRT findings among normal, normal tension glaucoma, and high tension glaucoma. Korean J Ophthalmol. 2008;22:236-241.
10. Shuba LM. Diurnal fluctuation and concordance of IOP in glaucoma suspects and normal tension glaucoma patients. J Glaucoma 2007;16:307-312.
11. Wilensky JT. The role of diurnal pressure measurements in the management of open angle glaucoma. Curr Opin Ophthalmol. 2004;15:90-92.

12. Ma J. Cone prism: principles of optical design and linear measurement of the applanation diameter or area of the cornea. Appl Opt. 1999;38:2086-2091.
13. Shimmyo M, Ross AJ, Moy A, Mostafavi R. Intraocular pressure, Goldmann applanation tension, corneal thickness, and corneal curvature in Caucasians, Asians, Hispanics, and African Americans. Am J Ophthalmol. 2003;136:603-613.
14. Leonardi M, Leuenberger P, Bertrand D, Bertsch A, Renaud P. First steps toward noninvasive intraocular pressure monitoring with a sensing contact lens. Invest Ophthalmol Vis Sci. 2004;45:3113-3117.
15. Maurice DM. A recording tonometer. Br J Ophthalmol. 1958;42:321-335.
16. Greene ME, Gilman BG. Intraocular pressure measurement with instrumented contact lenses. Invest Ophthalmol. 1974;13:299-302.
17. Wolbarsht ML, Wortman J, Schwartz B, Cook D. A scleral buckle pressure gauge for continuous monitoring of intraocular pressure. Int Ophthalmol. 1980;3:11-17.
18. Flower RW, Maumenee AE, Michelson EA. Long-term continuous monitoring of intraocular pressure in conscious primates. Ophthalmic Res. 1982;14:98-106.
19. Svedbergh B, Bäcklund Y, Hök B, Rosengren L. The IOP-IOL. A probe into the eye. Acta Ophthalmol (Copenh). 1992;70:266-268.
20. Leonardi M, Pitchon EM, Bertsch A, Renaud P, Mermoud A. Wireless contact lens sensor for intraocular pressure monitoring: assessment on enucleated pig eyes. Acta Ophthalmol. 2009;87:433-437.

21. Hediger A, Kniestedt C, Zweifel S, Knecht P, Funk J, Kanngiesser H. Continuous intraocular pressure measurement: First results with a pressure-sensitive contact lens. Ophthalmologe. 2009;106:1111-1115.
22. Konstas AG, Mylopoulos N, Karabatsas CH, et al. Diurnal intraocular pressure reduction with latanoprost 0.005% compared to timolol maleate 0.5% as monotherapy in subjects with exfoliation glaucoma. Eye. 2004;18:893-899.
23. Hughes E, Spry P, Diamond J. 24-Hour monitoring of intraocular pressure in glaucoma management: a retrospective review. J Glaucoma. 2003;12:232-236.
24. Lam AK, Douthwaite WA. The effect of an artificially elevated intraocular pressure on the central corneal curvature. Ophthalmic Physiol Opt. 1997;17:18-24.
25. Laukhina E, Ulanski J, Khomenko A, et al. Systematic Study of the $(ET)_2I_3$ Reticulate Doped Polycarbonate Films: Structure, ESR, Transport Properties and Superconductivity. J. *Phys. I France*. 1997;7:1665-1675.
26. Ulanski J, Kryszewski M. The Encyclopedia of Advanced Materials, (Eds.: D. Bloor, R. J. Brook, M. C. Fleming, S. Mahajan, R. W. Cahn), Pergamon, Oxford; 1994:2301-2304.
27. Laukhina E, Tkacheva V, Chuev I, et al. New Flexible Low-Density Metallic Materials Containing the (BEDT-TTF)2(IxBr1-x)3 Molecular Metals as Active Components Phys. Chem. B. 2001;105:11089-11097.
28. Laukhina E, Pfattner R, Ferreras LR, et al. Ultrasensitive piezoresistive all-organic flexible thin films. Adv Mater. 2010;22:977-981.

29. Laukhina E., Rovira C., Ulanskii J., Organic metals as active components in surface conducting semi-transparent films. Synth. Met. 2001;121:1407-1408.
30. Pesudovs K. Autorefraction as an outcome measure of laser in situ keratomileusis. J Cataract Refract Surg. 2004;30:1921-1928.
31. Durà R, Mathieu F, Nicu L, Pérez-Murano F, Serra-Graells F. A 0.3mW/Ch 1.25V Piezo-Resistance Digital ROIC for Liquid Dispensing MEMS, IEEE Transactions on Circuits and Systems-I, 2009;56:957-965.
32. Bertschinger DR, Beknazar E, Simonutti M, Safran AB, Sahel JA, Rosolen SG, Picaud S, Salzmann J. A review of in vivo animal studies in retinal prosthesis research. Graefes Arch Clin Exp Ophthalmol. 2008;246:1505-1517.
33. Ng YF, Chan HH, Chu PH, To CH, Gilger BC, Petters RM, Wong F. Multifocal electroretinogram in rhodopsin P347L transgenic pigs. Invest. Ophthalmol. Vis Sci. 2008;49:2208-2215.
34. Klećkowska-Nawrot J, Dziegiel P. Morphology of the third eyelid and superficial gland of the third eyelid on pig fetuses. Anat Histol Embryol. 2007;36:428-432.
35. Klećkowska-Nawrot J, Dziegiel P. Morphology of deep gland of the third eyelid in pig foetuses. Anat Histol Embryol. 2008;37:36-40.
36. Bartholomew LR, Pang DX, Sam DA, Cavender JC. Ultrasound biomicroscopy of globes from young adult pigs. Am J Vet Res. 1997;58:942-948.

37. Wagner JA, Edwards A, Schuman JS. Characterization of uveoscleral outflow in enucleated porcine eyes perfused under constant pressure. Invest Ophthalmol Vis Sci. 2004;45:3203-3206.

38. Nicoli S, Ferrari G, Quarta M, Macaluso C, Santi P. In vitro transscleral iontophoresis of high molecular weight neutral compounds. Eur J Pharm Sci. 2009;36:486-492.

39. McMenamin PG, Steptoe RJ. Normal anatomy of the aqueous humour outflow system in the domestic pig eye. J Anat. 1991;178:65-77.

40. May CA, Skorski LM, Lütjen-Drecoll E. Innervation of the porcine ciliary muscle and outflow region. J Anat. 2005;206:231-236.

41. Nicoli S, Ferrari G, Quarta M, Macaluso C, Govoni P, Dallatana D, Santi P. Porcine sclera as a model of human sclera for in vitro transport experiments: histology, SEM, and comparative permeability. Mol Vis. 2009;15:259-266.

42. Voss Kyhn M, Kiilgaard JF, Lopez AG, Scherfig E, Prause JU, la Cour M. The multifocal electroretinogram (mfERG) in the pig. Acta Ophthalmol Scand. 2007;85:438-444.

43. Jay L, Brocas A, Singh K, Kieffer JC, Brunette I, Ozaki T. Determination of porcine corneal layers with high spatial resolution by simultaneous second and third harmonic generation microscopy. Opt Express. 2008;16:16284-16293.

44. Faber C, Scherfig E, Prause JU, Søresen KE. Corneal thickness in pigs measured by ultrasound pachymetry in vivo. Scan J Lab Anim Sci. 2008;35:39-43.

45. Elsheikh A, Alhasso D. Mechanical anisotropy of porcine cornea and correlation with stromal microstructure. Exp Eye Res. 2009;88:1084-1091.

46. Xu YG, Xu YS, Huang C, Feng Y, Li Y, Wang W. Development of a rabbit corneal equivalent using an acellular corneal matrix of a porcine substrate. Mol Vis. 2008;14: 2180-2189.

47. Keenan J, Orr DF, Pierscionek BK. Patterns of crystallin distribution in porcine eye lenses. Mol Vis. 2008;14:1245-1253.

48. Wong KH, Koopmans SA, Terwee T, Kooijman AC. Changes in spherical aberration after lens refilling with a silicone oil. Invest Ophthalmol Vis Sci. 2007;48:1261-1267.

49. Chong C, Suzuki T, Totsuka K, Morosawa A, Sakai T. Large coherence length swept source for axial length measurement of the eye. Appl Opt. 2009;48:144-150.

50. Gu P, Harwood LJ, Zhang X, Wylie M, Curry WJ, Cogliati T. Isolation of retinal progenitor and stem cells from the porcine eye. Mol Vis. 2007;13:1045-1057.

51. Pandav S, Morgan WH, Townsend R, Cringle SJ, Yu DY. Inability of a Confocal Scanning Laser Doppler Flowmeter to Measure Choroidal Blood Flow in the Pig Eye. Open Ophthalmol J. 2008;2:146-152.

52. Kiilgaard JF, Prause JU, Prause M, Scherfig E, Nissen MH, la Cour M. Subretinal posterior pole injury induces selective proliferation of RPE cells in the periphery in in vivo studies in pigs. Invest Ophthalmol Vis Sci. 2007;48:355-360.

53. Warfvinge K, Kiilgaard JF, Klassen H, Zamiri P, Scherfig E, Streilein W, Prause JU, Young MJ. Retinal progenitor cell xenografts to the pig retina: immunological reactions. Cell Transplant. 2006;15:603-612.
54. Nishi O, Nishi K, Nishi Y, Chang S. Capsular bag refilling using a new accommodating intraocular lens. J Cataract Refract Surg. 2008;34:302-309.
55. Newell FW. Oftalmología Fundamentos y Conceptos. Séptima ed. Mosby, España. 2008.
56. Ruiz-Ederra J, García M, Martín F, Urcola H, Hernández M, Araiz J, Durán J, Vecino E. Comparison of three methods of inducing chronic elevation of intraocular pressure in the pig (experimental glaucoma). Arch Soc Esp Oftalmol. 2005;80:571-579.
57. Balaratnasingam C, Morgan WH, Bass L, Matich G, Cringle SJ, Yu DY. Axonal transport and cytoskeletal changes in the laminar regions after elevated intraocular pressure. Invest Ophthalmol Vis Sci. 2007;48:3632-3644.
58. Suarez T, Vecino E. Expression of endothelial leukocyte adhesion molecule 1 in the aqueous outflow pathway of porcine eyes with induced glaucoma. Mol Vis. 2006;12:1467-1472.
59. Rosolen SG, Rigaudière F, Le Gargasson JF. A new model of induced ocular hyperpressure using the minipig. J Fr Ophtalmol. 2003;26:259-267.
60. Thornton IL, Dupps WJ, Roy AS, Krueger RR. Biomechanical effects of intraocular pressure elevation on optic nerve/lamina cribrosa before and

after peripapillary scleral collagen cross-linking. Invest Ophthalmol Vis Sci. 2009;50:1227-1233.

61. Zhang M, Rao PV. Blebbistatin, A novel inhibitor of myosin II ATPase activity, increases aqueous humor outflow facility in perfused enucleated porcine eyes. Invest Ophthalmol Vis Sci. 2005;46:4130-4138.
62. Morgan WH, Cringle SJ, Kang MH, Pandav S, Balaratnasingam C, Ezekial D, Yu DY. Optimizing the calibration and interpretation of dynamic ocular force measurements. Graefes Arch Clin Exp Ophthalmol. 2010;248:401-4077.
63. Hasegawa Y, Nishimura J, Niiro N, Hirano K, Ishibashi T, Kanaide H. Prostaglandin F2alpha, but not latanoprost, increases the Ca2+ sensitivity of the pig iris sphincter muscle. Invest Ophthalmol Vis Sci. 2006;47:4865-4871.
64. Hosseini M, Rose AY, Song K, Bohan C, Alexander JP, Kelley MJ, Acott TS. IL-1 and TNF induction of matrix metalloproteinase-3 by c-Jun N-terminal kinase in trabecular meshwork. Invest Ophthalmol Vis Sci. 2006;47:1469-1476.
65. Song J, Deng PF, Stinnett SS, Epstein DL, Rao PV. Effects of cholesterol-lowering statins on the aqueous humor outflow pathway. Invest Ophthalmol Vis Sci. 2005;46:2424-2432.
66. Liu Y, Nakamura H, Witt TE, Edward DP, Gordon RJ. Femtosecond laser photodisruption of porcine anterior chamber angle: an ex vivo study. Ophthalmic Surg Lasers Imaging. 2008;39:485-490.

67. Vaajanen A, Vapaatalo H, Oksala O. A modified in vitro method for aqueous humor outflow studies in enucleated porcine eyes. J Ocul Pharmacol Ther. 2007;23:124-131.

68. Shaarawy T, Wu R, Mermoud A, Flammer J, Haefliger IO. Influence of non-penetrating glaucoma surgery on aqueous outflow facility in isolated porcine eyes. Br J Ophthalmol. 2004;88:950-952.

69. Hallberg P, Lindén C, Bäcklund T, Eklund A. Symmetric sensor for applanation resonance tomometry of the eye. Med Biol Eng Comput. 2006;44:54-60.

70. Von Freyberg A, Sorg M, Fuhrmann M, Kreiner CF, Pfannkuche J, Klink T, Hensler D, Grehn F, Goch G. Acoustic tonometry: feasibility study of a new principle of intraocular pressure measurement. J Glaucoma. 2009;18:316-320.

71. Kalesnykas G, Uusitalo H. Comparison of simultaneous readings of intraocular pressure in rabbits using Perkins handheld, Tono-Pen XL, and TonoVet tonometers. Graefes Arch Clin Exp Ophthalmol. 2007;245:761-762.

72. Andrada Márquez MT, Fesser Oroz I, Antón López A. Comparative study of two portable tonometers: Tono-Pen XL and Perkins. Arch Soc Esp Oftalmol. 2003;78:189-96.

73. Maquet Dussart JA. La rigidez ocular. Estudio clínico experimental. Tesis Doctoral. Universidad de Valladolid, facultad de Medicina. 1985.

11.- ANEXO I

PATENTE

LENTE DE CONTACTO SENSORA, SISTEMA PARA LA MONITORIZACIÓN NO INVASIVA DE LA PRESIÓN INTRAOCULAR Y MÉTODO PARA SU MEDICIÓN WO/2009/147277

Europäisches Patentamt
European Patent Office
Office européen des brevets

European Patent Office
Postbus 5818
2280 HV RIJSWIJK
NETHERLANDS
Tel. +31 (0)70 340-2040
Fax +31 (0)70 340-3016

MARTIN HERRANZ, Raul
Universidad De Valladolid
C/ Plaza de Santa Cruz 8
E-47002 Valladolid
ESPAGNE

For any questions about this communication:
Tel.:+31 (0)70 340 45 00

Date
31.01.11

Reference	Application No./Patent No.
	09757656.5 - 1265 PCT/ES2009070205

Applicant/Proprietor
Consejo Superior De Investigaciones Científicas, e t al

Notification of the data mentioned in Rule 19(3) EPC

In the above-identified patent application you are designated as inventor/co-inventor.
Pursuant to Rule 19(3) EPC the following data are notified herewith:

DATE OF FILING	: 05.06.09
PRIORITY	: ES/06.06.08/ ESA 200801722
TITLE	: SENSOR CONTACT LENS, SYSTEM FOR THE NON-INVASIVE MONITORING OF INTRAOCULAR PRESSURE AND METHOD FOR MEASURING SAME
DESIGNATED STATES	: AT BE BG CH CY CZ DE DK EE ES FI FR GB GR HR HU IE IS IT LI LT LU LV MC MK MT NL NO PL PT RO SE SI SK TR

Receiving Section

Europäisches Patentamt • European Patent Office • Office européen des brevets

(12) SOLICITUD INTERNACIONAL PUBLICADA EN VIRTUD DEL TRATADO DE COOPERACIÓNEN MATERIA DE PATENTES (PCT)

(19) Organización Mundial de la Propiedad Intelectual
Oficina internacional

(43) Fecha de publicación internacional
10 de diciembre de 2009 (10.12.2009)

PCT

(10) Número de Publicación Internacional
WO 2009/147277 A1

(51) Clasificación Internacional de Patentes:
A61B 3/16 (2006.01)

(21) Número de la solicitud internacional:
PCT/ES2009/070205

(22) Fecha de presentación internacional:
5 de junio de 2009 (05.06.2009)

(25) Idioma de presentación: español

(26) Idioma de publicación: español

(30) Datos relativos a la prioridad:
P200801722 6 de junio de 2008 (06.06.2008) ES

(71) Solicitantes *(para todos los Estados designados salvo US)*: **CONSEJO SUPERIOR DE INVESTIGACIONES CIENTÍFICAS** [ES/ES]; C/ Serrano, 117, E-28006 Madrid (ES). **UNIVERSIDAD DE VALLADOLID** [ES/ES]; C/ Plaza de Santa Cruz, 8, E-47002 Valladolid (ES). **INSTITUCIÓ CATALANA DE RECERCA I ESTUDIS** [ES/ES]; Passeig Lluis Companys, 23, E-08010 Barcelona (ES). **UNIVERSIDAD AUTÓNOMA DE BARCELONA** [ES/ES]; Campus de Bellaterra, s/n, E-08193 Cerdanyola del Valles (Barcelona) (ES). **CIBER-BBN** [ES/ES]; C/ Maria de Luna, 11, E-50018 Zaragoza (ES).

(72) Inventores; e

(75) Inventores/Solicitantes *(para US solamente)*: **VECIANA, Jaume** [ES/ES]; Instituto De Ciencia De Materiales De Barcelona (ICMAB), Campus Universidad Autónoma, E-08193 Bellaterra (Barcelona) (ES). **ROVIRA, Concepció** [ES/ES]; Instituto De Ciencia De Materiales De Barcelona (ICMAB), Campus Universidad Autónoma, E-08193 Bellaterra (Barcelona) (ES). **MAS-TORRENT, Marta** [ES/ES]; Instituto De Ciencia De Materiales De Barcelona (ICMAB), Campus Universidad Autónoma, E-08193 Bellaterra (Barcelona) (ES). **VILLA SANZ, Rosa** [ES/ES]; Instituto De Microelectrónica De Barcelona (IMB-CNM), Campus Universidad Autónoma, E-08193 Bellaterra (Barcelona) (ES). **AGUILÓ LLOBET, Jordi** [ES/ES]; Universidad Autónoma De Barcelona, Campus de Bellaterra, s/n, E-08193 Cerdanyola del Valles (Barcelona) (ES). **PASTOR, José Carlos** [ES/ES]; Universidad De Valladolid, C/ Plaza de Santa Cruz, 8, E-47002 Valladolid (ES). **USSA, Fernando** [ES/ES]; Universidad De Valladolid, C/ Plaza de Santa Cruz, 8, E-47002 Valladolid (ES). **LAUKHINA, Elena** [RU/ES]; CIBER-BBN, C/ Maria de Luna, 11, E-50018 Zaragoza (ES). **LAUKHIN, Vladimir** [RU/ES]; Institució Catalana De Recerca I Estudis Avançats, Passeig Lluis Companys, 23, E-08010 Barcelona (ES).

[Continúa en la página siguiente]

(54) **Title**: SENSOR CONTACT LENS, SYSTEM FOR THE NON-INVASIVE MONITORING OF INTRAOCULAR PRESSURE AND METHOD FOR MEASURING SAME

(54) **Título**: LENTE DE CONTACTO SENSORA, SISTEMA PARA LA MONITORIZACIÓN NO INVASIVA DE LA PRESIÓN INTRAOCULAR Y MÉTODO PARA SU MEDIDA

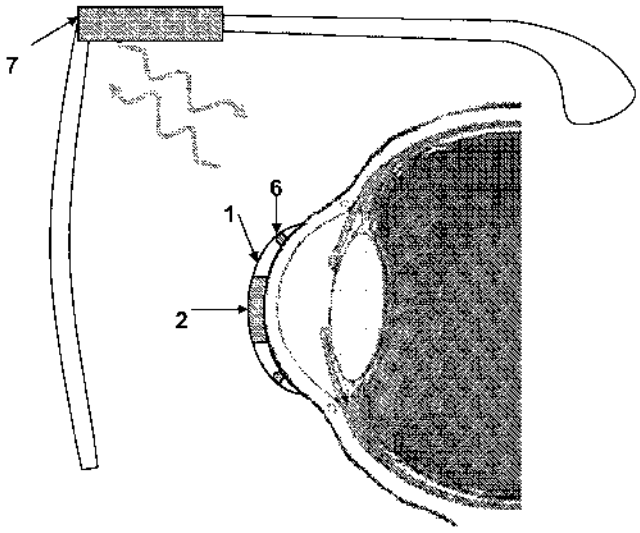

FIG. 4

(57) **Abstract:** The invention is characterised in that it includes a truncated contact lens (1) having a truncation plane parallel to the base of the contact lens and a centrally disposed polymer nanocomposite material (2) joined to the perimeter of the truncated zone, said material being sensitive to pressure changes, biocompatible and transparent and including contact electrodes (3). The invention is also characterised in that it includes means for transmitting intraocular pressure measurement data to an external system. The invention also relates to an intraocular pressure measurement method using said lens, consisting of: i) positioning the sensor contact lens on an eye in order to determine the intraocular pressure thereof; ii) supplying a direct current between the external electrodes; iii) measuring ΔV between the internal electrodes; and iv) identifying if the value obtained is outside the linear response expressed as changes in resistivity of the polymer nanocomposite material. The invention further relates to a telemetry system including said lens.

(57) **Resumen:**

[Continúa en la página siguiente]

WO 2009/147277 A1

(74) **Mandatario: PONS ARIÑO, Ángel**; Glorieta de Rubén Darío, 4, E-28010 Madrid (ES).

(81) **Estados designados** *(a menos que se indique otra cosa, para toda clase de protección nacional admisible)*: AE, AG, AL, AM, AO, AT, AU, AZ, BA, BB, BG, BH, BR, BW, BY, BZ, CA, CH, CL, CN, CO, CR, CU, CZ, DE, DK, DM, DO, DZ, EC, EE, EG, ES, FI, GB, GD, GE, GH, GM, GT, HN, HR, HU, ID, IL, IN, IS, JP, KE, KG, KM, KN, KP, KR, KZ, LA, LC, LK, LR, LS, LT, LU, LY, MA, MD, ME, MG, MK, MN, MW, MX, MY, MZ, NA, NG, NI, NO, NZ, OM, PG, PH, PL, PT, RO, RS, RU, SC, SD, SE, SG, SK, SL, SM, ST, SV, SY, TJ, TM, TN, TR, TT, TZ, UA, UG, US, UZ, VC, VN, ZA, ZM, ZW.

(84) **Estados designados** *(a menos que se indique otra cosa, para toda clase de protección regional admisible)*: ARIPO (BW, GH, GM, KE, LS, MW, MZ, NA, SD, SL, SZ, TZ, UG, ZM, ZW), euroasiática (AM, AZ, BY, KG, KZ, MD, RU, TJ, TM), europea (AT, BE, BG, CH, CY, CZ, DE, DK, EE, ES, FI, FR, GB, GR, HR, HU, IE, IS, IT, LT, LU, LV, MC, MK, MT, NL, NO, PL, PT, RO, SE, SI, SK, TR), OAPI (BF, BJ, CF, CG, CI, CM, GA, GN, GQ, GW, ML, MR, NE, SN, TD, TG).

Publicada:

— *con informe de búsqueda internacional (Art. 21(3))*

— *antes de la expiración del plazo para modificar las reivindicaciones y para ser republicada si se reciben modificaciones (Regla 48.2(h))*

La invención se caracteriza porque comprende una lente de contacto truncada (1), cuyo plano de truncamiento es paralelo a la base de dicha lente de contacto, y un material nanocompuesto polimérico (2) dispuesto centradamente y unido al perímetro de la zona truncada, siendo dicho material sensible a los cambios de presión, biocompatible y transparente e incluyendo electrodos de contacto (3), y por el hecho de que además comprende medios de transmisión de datos de medida de la PIO a un sistema externo. La invención también se refiere a un método de medición de la PIO utilizando dicha lente que comprende: i) colocar dicha lente de contacto sensora en un ojo a determinar su presión intraocular; ii) suministrar un valor de corriente continua entre electrodos externos; iii) medir ΔV entre electrodos internos; e iv) identificar si el valor obtenido está fuera de la respuesta lineal, expresada en cambios de resistividad, del material nanocompuesto polimérico. La invención también se refiere a un sistema de telemetría que comprende dicha lente.

(19) Europäisches Patentamt
European Patent Office
Office européen des brevets

(11) EP 2 305 100 A1

(12) EUROPEAN PATENT APPLICATION

published in accordance with Art. 153(4) EPC

(43) Date of publication:
06.04.2011 Bulletin 2011/14

(21) Application number: **09757656.5**

(22) Date of filing: **05.06.2009**

(51) Int Cl.:
A61B 3/16 *(2006.01)*

(86) International application number:
PCT/ES2009/070205

(87) International publication number:
WO 2009/147277 (10.12.2009 Gazette 2009/50)

(84) Designated Contracting States:
AT BE BG CH CY CZ DE DK EE ES FI FR GB GR HR HU IE IS IT LI LT LU LV MC MK MT NL NO PL PT RO SE SI SK TR
Designated Extension States:
AL BA RS

(30) Priority: **06.06.2008 ES 200801722**

(71) Applicants:
- **Consejo Superior De Investigaciones Científicas**
  28006 Madrid (ES)
- **Universidad De Valladolid**
  47002 Valladolid (ES)
- **Institució Catalana De Recerca I Estudis**
  08010 Barcelona (ES)
- **Universitat Autònoma De Barcelona**
  08193 Cardanyola del Valles, Barcelona (ES)
- **Ciber-BBN**
  50018 Zaragoza (ES)

(72) Inventors:
- **VECIANA, Jaume**
  E-08193 Bellaterra (Barcelona) (ES)
- **ROVIRA, Concepció**
  E-08193 Bellaterra (Barcelona) (ES)
- **MAS-TORRENT, Marta**
  E-08193 Bellaterra (Barcelona) (ES)
- **VILLA SANZ, Rosa**
  E-08193 Bellaterra (Barcelona) (ES)
- **AGUILÓ LLOBET, Jordi**
  E-08193 Cerdanyola del Valles (Barcelona) (ES)
- **PASTOR, José Carlos**
  E-47002 Valladolid (ES)
- **USSA, Fernando**
  E-47002 Valladolid (ES)
- **LAUKHINA, Elena**
  E-50018 Zaragoza (ES)
- **LAUKHIN, Vladimir**
  E-08010 Barcelona (ES)
- **MARTIN HERRANZ, Raul**
  E-47002 Valladolid (ES)
- **GUIMERA, Anton**
  E-28006 Madrid (ES)

(74) Representative: **Pons Ariño, Angel**
Glorieta Ruben Dario 4
28010 Madrid (ES)

(54) SENSOR CONTACT LENS, SYSTEM FOR THE NON-INVASIVE MONITORING OF INTRAOCULAR PRESSURE AND METHOD FOR MEASURING SAME

(57) The invention is **characterised in that** it includes a truncated contact lens (1) having a truncation plane parallel to the base of the contact lens and a centrally disposed polymer nanocomposite material (2) joined to the perimeter of the truncated zone, said material being sensitive to pressure changes, biocompatible and transparent and including contact electrodes (3). The invention is also **characterised in that** it includes means for transmitting intraocular pressure measurement data to an external system. The invention also relates to an intraocular pressure measurement method using said lens, consisting of: i) positioning the sensor contact lens on an eye in order to determine the intraocular pressure thereof; ii) supplying a direct current between the external electrodes; iii) measuring ?V between the internal electrodes; and iv) identifying if the value obtained is outside the linear response expressed as changes in resistivity of the polymer nanocomposite material. The invention further relates to a telemetry system including said lens.

FIG 4

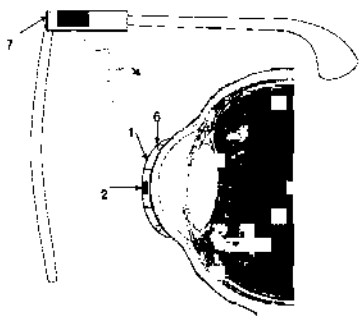

EP 2 305 100 A1

Description

FIELD OF THE INVENTION

[0001] The present invention relates to a sensor contact lens for the monitoring of intraocular pressure (IOP) using a non-invasive technique and a method for measuring intraocular pressure using such sensor contact lens.

[0002] In particular, the invention relates to a sensor contact lens comprising in the central area a transparent polymeric nanocomposite material which continuously and noninvasively takes direct measurements of intraocular pressure.

[0003] The invention also relates to a telemetry system for monitoring intraocular pressure comprising said sensor contact lens.

BACKGROUND OF THE INVENTION

[0004] Glaucoma is an eye condition due to an increase in intraocular pressure (IOP). This increase results in a slow irreversible damage to the optic nerve which is very difficult to detect in early stages and is also difficult to control because of the numerous fluctuations in IOP throughout the day. Therefore, glaucoma is the second leading cause of visual impairment or blindness in the industrial sector.

[0005] The diagnosis and control is performed by measuring the IOP and the most common measurement method used is the Goldmann applanation tonometry.

[0006] Thus, patents U.S. 6,994,672 and U.S. 7,169,106, both of the same owner and inventor, disclose devices for measuring intraocular pressure of the eye based on the above technique. They involve a specific measurements or measurements with a certain amount of time between them and, therefore, noncontinuous. In the specific case of U.S. Patent 7,169,106 it discloses a contact lens with a sensor adhered to a part of its inner surface. Said sensor comprises a surface in contact with a portion of the eye surface. The contact surface includes an outer region and an inner region manufactured as an impedance element so that the impedance varies as the inner region changes shape due to the pressure from an outer applanator on its surface modifying said shape and, therefore, varying the impedance.

[0007] Furthermore, patent application WO/2003/001991 has developed sensor lenses based on micro-fabricated strain gauge on a polyimide substrate inserted in the outer area of a silicone lens. The IOP measuring system comprises a contact lens, made of silicone for instance, and an active strain gauge attached to said contact lens and is **characterized in that** the active tension gauge is a circular arc and is located on the outside area and around the C centre of the contact lens.

[0008] Said contact lens correlates the spherical distortion of the eye to IOP changes and, therefore, IOP is measured indirectly and in terms of curvature changes of the cornea of the human eye of approximately 3μm, within a typical radius of 7.8 mm. In addition, this measurement system and its accuracy depend on the eye movements, blinking and lens movements. This implies signal filtering to remove noise, and factors such as corneal thickness and rigidity or astigmatism, among others, which also affect the measurement accuracy and are more difficult to control.

[0009] It is noteworthy that the material used in said international patent application is polyimide-silicone, a hydrophobic material that causes problems with the liquid surface of the eye.

[0010] Thus, the systems disclosed to date measure only the changes in IOP and do not involve a direct measurement sensor that could be considered an absolute pressure sensor.

[0011] Therefore, the prior art has not yet disclosed a device such as a sensor contact lens non-invasively taking direct and continuous IOP measurements which also overcomes the drawbacks of the techniques disclosed to date.

BRIEF DESCRIPTION OF THE INVENTION

[0012] In a first aspect the present invention relates to a non-invasive sensor contact lens, for directly and continuously monitoring intraocular pressure (IOP) comprising a polymeric nanocomposite material being sensitive to changes in pressure, biocompatible and transparent.

[0013] In a second aspect, the invention relates to a method for measuring intraocular pressure (IOP) using the sensor contact lens according to the first aspect of the invention.

[0014] The invention also relates in a third aspect to a telemetry system for monitoring intraocular pressure comprising said sensor contact lens.

FIGURES

[0015]

Figure 1 shows a sensor contact lens according to the invention for continuously and non-invasively monitoring the intraocular pressure comprising a truncated contact lens 1, whose truncation plane is parallel to the base of such contact lens, and a centrally disposed polymeric nanocomposite material (2) attached to the perimeter of the truncated area. Said material includes contact electrodes 3 and said truncated contact lens 1, means for transmitting 4 IOP measurement data to an external system (not shown). In said embodiment the means of transmission are wires.

Figure 2 shows an embodiment of the telemetry system of the invention wherein the means of transmission by telemetry include an integrated circuit 5 and an antenna 6. Said figure 2 schematically shows the configuration of a sensor contact lens according to

the first aspect of the invention wherein the organic nanocomposite material 2 is connected to an integrated circuit 5 which, via an antenna 6, sends the data to a receiving unit (RU) 7. This unit can be located on a support such as, for example, glasses as shown in Figure 4 below. In addition this unit (RU) provides power to the integrated circuit and via radio frequency (RF) or wires can send the information stored in a PC or PDA (personal device assistant) type data processing unit 8. This unit allows the handling, storage and visualization of data.

Figure 3 shows the response of an embodiment of the ocular sensor lens according to the first aspect of the invention during a variation in the intraocular pressure (IOP) in terms of resistivity changes with a polymeric nanocomposite material of $(BET\text{-}TTF)_2 IxBr_3\text{-}x$ on a polycarbonate base support.

Figure 4 shows an embodiment of the sensor contact lens of the invention placed on the eyeball and the operation diagram of the system with telemetry elements incorporated in an eyeglass frame, where the references have the meanings given above.

DETAILED DESCRIPTION OF THE INVENTION

[0016] The first aspect of the invention provides a sensor contact lens, of polymethylmethacrylate for instance, to monitor intraocular pressure (IOP), **characterized in that** it comprises a truncated contact lens (1), whose truncation plane is parallel to the base of said contact lens, and a polymeric nanocomposite material (2) centrally disposed and attached to the perimeter of the truncated area, said material being sensitive to pressure changes, biocompatible and transparent, and including contact electrodes (3), and in that it also comprises means for transmitting IOP measurement data to an external system.

[0017] The means for transmitting IOP measurement data comprise either wires 4 or an integrated circuit 5 and an antenna 6, wherein said antenna 6 can be located in the truncated lens 1 or as a bonding element with the polymer nanocomposite material 2. Said antenna can be made of platinum, gold or a polymeric nanocomposite material.

[0018] On the other hand, the contact electrodes 3 comprise two external electrodes to supply continuous power to the polymeric nanocomposite material and two internal electrodes to measure the differential voltage thereof.

[0019] The polymeric nanocomposite material 2 has been obtained from a polymer matrix (base substrate) covered with a layer of organic conductive material intimately linked to the polymer matrix. The conductive layer is formed by a mesh/grid of crystals of a molecular conductor based on a charge-transfer salt.

[0020] Advantageously, the use of said polymeric nanocomposite material enables a linear response between changes in intraocular pressure (IOP) in terms of resistivity changes.

[0021] Said polymeric nanocomposite material is sensitive to changes in pressure, is biocompatible and transparent and, in particular, is obtained from:

i) a layer of conductive organic material consisting of at least one salt or conductive complex comprising a molecule A and a dopant D, said molecule A being an organic molecule or macromolecule, being an electron donor or acceptor capable of forming a salt or a conductive complex, but which without being doped has no conductivity, and said dopant D being an electron acceptor or donor compound capable of forming a salt or conductive complex with the molecule or macromolecule A; and

ii) a base substrate or polymer matrix, in intimate contact with the layer of organic material i), wherein said base substrate is inert to the layer of organic material i).

[0022] Such a molecule or macromolecule A will be selected from between a derivative of acene, of coronene, of tetrathiafulvalene or of tetracyanoquinodimethane, preferably bis (ethylenthio) tetrathiafulvalene (BET-TTF) or bis (ethylenedithio) tetrathiafulvalene (BEDT-TTF). Said dopant D is a halogen species, advantageously being a species selected from iodine, bromine or iodine bromide.

[0023] Preferably, said salt is selected from between $(BET\text{-}TTF)_2I_3$, $(BET\text{-}TTF)_2Br{\cdot}3H_2O$, $(BET\text{-}TTF)_2IxBr_3\text{-}x$, and $(BET\text{-}TTF)_2IxBr_3\text{-}x$, where BET-TTF is bis (ethylenthio) tetrathiafulvalene and BEDT-TTF is bis (ethylenedithio) tetrathiafulvalene, preferably being $(BET\text{-}TTF)_2Br{\cdot}3H_2O$, and said base substrate which is inert to the conductive layer of organic material is selected from a non-conductive organic polymer, preferably a thermoplastic polymer or elastomer, more preferably, polycarbonate, polyamide, polymethylmethacrylate, polyethylene or polypropylene.

[0024] For pressure sensor applications the substrate having a high resistance to loads mechanically applied in cycles and that difficult to break through load application will be preferred. Also for this application it will be preferable to have an organic layer sensitive to changes in pressure, distortion or stress consisting of a high-piezoresistive material with a low heat resistance coefficient, preferably being $(BET\text{-}TTF)_2Br{\cdot}3H_2O$ as an organic layer.

[0025] For a better understanding of the obtaining of polymeric nanocomposite material 2, the content of Spanish patent application P200602887 is included.

[0026] Advantageously, the sensor contact lens according to the first aspect of the invention can take non-invasive direct pressure values over extended periods of time. In addition, the polymeric nanocomposite material 2 used avoids the disadvantages of prior art relating to the cornea thickness.

[0027] Also advantageously, said polymeric nanocom-

posite material 2 not only acts as a pressure sensor but its composition allows the integrated telemetry circuitry to be designed on its surface in order to extract the signals and thus provide a sensor contact lens that is easy to use and allow IOP monitoring in the most physiological manner possible.

[0028] So, by means of a thermo printing technique electronic circuits can be designed directly on the surface of polymeric nanocomposite material 2. For a better understanding of the thermo-chemical printing technique the contents of the international patent application W02007/014975 is incorporated by way of reference.

[0029] It is noteworthy that according to the sensor contact lens according to the invention, it provides a direct measurement system of intraocular pressure of the human or animal eye overcoming the drawbacks of the techniques disclosed so far.

[0030] In particular, according to the first aspect of the invention, the intraocular pressure is transferred directly to the deformation of the entire polymeric nanocomposite material thus changing its resistance and, therefore, directly measuring the intraocular pressure changes. The polymeric nanocomposite material 2 is much more sensitive to changes in pressure and therefore more deformable than the truncated contact lens 1 which surrounds it due to its Young's modulus. In addition, said polymeric nanocomposite material is totally organic and therefore, better for disposal.

[0031] The sensor contact lens according to the first aspect of the invention shows a linear response and high sensitivity to pressure in the pressure range required for measuring the intraocular pressure of the eye between 10 and 21 mmHg.

[0032] In a second aspect, the invention relates to a method for measuring intraocular pressure (IOP) using the sensor contact lens according to the first aspect of the invention. Said method comprises the following steps:

i) placing said sensor contact lens on an eye to determine its intraocular pressure;
ii) providing a direct current value between the external contact electrodes;
iii) measuring the differential voltage ΔV between the internal contact electrodes ;
iv) identifying whether the value obtained is outside the linear response, expressed in resistivity changes, between the resistance dependence and the pressure of said polymeric nanocomposite material.

[0033] In a preferred embodiment of the invention, the polymer nanocomposite material 2 of said lens is a molecular conductor of $(BET)_2IxBr_3$-x on a polycarbonate base substrate that gives the linear response defined in Figure 3 below.

[0034] Direct current values between the external contact electrodes are typically between 10 and 100 μA.

[0035] The identification of whether the value obtained in step iv) is beyond the linear response of the polymeric nanocomposite materials defined in accordance with the present invention is carried out by telemetry transmission to a receiver unit (RU) 7 that is sent to a PC or PDA (*personal device assistant*) 8 via radiofrequency (RF) or wires.

[0036] According to the second aspect of the invention, step iv) of the method of measuring intraocular pressure is an essential step to determine the existence of the disease known as glaucoma, such step taking place outside the human or animal body.

[0037] The invention also relates in a third aspect to a telemetry system comprising said sensor contact lens. This system is **characterized in that** it comprises a sensor contact lens according to any of claims 1 to 8, a receiving unit (7) for receiving data which, via radio frequency (RF) or wires, sends information to a PC or PDA type data processing unit (8) for the handling, storage and visualization of data.

EMBODIMENT OF THE INVENTION

[0038] The following example embodiment describes the system for the non-invasive monitoring of intraocular pressure (IOP) object of the invention and methodology of use in humans or animals.

[0039] The aim of the implementation of the system for the non-invasive IOP monitoring object of the invention is to allow continuous monitoring, for 24 hours for example, to assess the pressure changes that occur throughout the day and can be very marked depending on the hour (circadian rate) or due to medication effects. These fluctuations are difficult or impossible to detect with specific measurements. This sensor monitoring object of the invention is very accurate and physiologically distinct from other systems previously known. Humans targeted by this system are mainly people susceptible to glaucoma where the fluctuations can be very important.

DESCRIPTION OF THE MEASURING SYSTEM OF THE PIO

[0040] This example uses the IOP monitoring system object of the invention comprising the following configuration:

[0041] A sensor contact lens for non-invasively measuring IOP, consisting of the sensor contact lens model with wires according to Figure 1. A standard ocular lens cut parallel to the base of the lens, leaving a perimeter of 6 mm in diameter where the transparent organic polymer nanocomposite material is attached and presenting four gold electrodes of 0.3 mm in diameter and 1 mm apart. Said electrodes are connected to the measuring system through wires.

[0042] A four-wire device for measuring the strength of the sensor material has been used (e.g., Agilent 34970A multimeter source meters, Keithley 2400 source meters, Keithley 2601 source meters). Current (DC) is

injected, between 10 and 100μA,- between the two external electrodes (I + and I-) and the voltage difference between the internal electrodes (V + and V-) is measured.

[0043] The values obtained show resistance variations (Ω) with respect to changes in pressure (mmHg). These values will relate to the pressure values according to a resistance-pressure correlation table shown in Figure 3 for a polymer nanocomposite material in a molecular conductor of $(BET\text{-}TTF)_2IxBr_3\text{-}x$ on a polycarbonate base substrate.

DESCRIPTION OF THE METHODOLOGY

Calibration:

[0044] Prior to its placement in the eye the IOP will be measured using standard equipment: Goldmann applanation tonometer, and will be taken as the reference value since the system monitors the relative pressure values.

Handling and measurements:

[0045] The sensor contact lens will then be placed as if it were a normal ocular lens. This example uses the wire model and therefore care must be taken to route the wires to the outer edge of the eye so the lid can open and close without any interference.

[0046] The wire will be connected from the polymeric nanocomposite material 2 to the meter. Data will be recorded for 24 hours. The data are relayed to a PC for storage, filtration and analysis.

Values calculation:

[0047] Finally, data is displayed on a 24-hour graph calibrated with the initial absolute value recorded.

[0048] Normal values of IOP fluctuate throughout the day due to the circadian rhythm. IOP values are between 10 and 21 mmHg. Peaks or increased elevations beyond baseline values will involve therapeutic changes for the patient to avoid injury to the optic nerve.

[0049] During monitoring, patient's vision remains normal because the sensor lens is transparent.

[0050] In the model which incorporates the telemetry (see Figure 2) a human can continue with his or her everyday life and the IOP measure will reflect even better the normal physiological conditions the of person whose IOP is measured.

Claims

1. sensor contact lens for the non-invasive monitoring of intraocular pressure (IOP), **characterized in that** it comprises a truncated contact lens (1), which truncation plane is parallel to the base of said contact lens, and a polymeric nanocomposite material (2) centrally arranged and attached to the perimeter of the truncated area, said material being responsive to pressure changes, biocompatible and transparent, and including contact electrodes (3), and **in that** it also comprises means of transmitting IOP measurement data to an external system.

2. Sensor contact lens according to claim 1, wherein said polymeric nanocomposite material is obtained from:

   i) a layer of organic material made up of at least one salt or conductive complex comprising a molecule A and a dopant D, said molecule A being to an organic molecule or macromolecule, being an electron donor or acceptor capable of forming a salt or conductive complex, but having no conductivity without being doped, and said dopant D being an electron acceptor or donor compound capable of forming a salt or conductive complex with the molecule or macromolecule A; and
   ii) a base substrate or polymer matrix, in intimate contact with said layer of organic material i), wherein said base substrate is inert to said layer of organic material i).

3. Sensor contact lens according to claim 1 or 2, wherein said polymeric nanocomposite material (2) is based on (BET-TTF)2IxBr3-x on a polycarbonate polymeric matrix.

4. Sensor contact lens according to claim 1, wherein said truncated contact lens (1) is made of polymethylmethacrylate.

5. Sensor contact lens according to claim 1, wherein said means of transmitting IOP measurement data comprise either wires (4) or an integrated circuit (5) and an antenna (6).

6. Sensor contact lens according to claims 1 and 5, wherein said antenna (6) is located in the truncated contact lens (1).

7. Sensor contact lens according to claim 6, wherein said antenna (6) is made of platinum, gold or said polymeric nanocomposite material.

8. Sensor contact lens according to claim 1, wherein said contact electrodes (3) are two external electrodes for supplying direct current and two internal electrodes for measuring the differential voltage.

9. Method for measuring intraocular pressure (IOP) using a sensor contact lens according to any of claims 1 to 8 comprising the following steps:

   i) placing said sensor contact lens in the eye to

determine its intraocular pressure;
ii) supplying a direct current value between the external contact electrodes;
iii) measuring the differential voltage ΔV between the internal contact electrodes;
iv) identifying whether the value obtained is outside the linear response, expressed in changes of resistivity, between the dependence of the resistance and the pressure of said polymeric nanocomposite material.

10. Method for measuring intraocular pressure (IOP) according to claim 9, wherein, said polymeric nanocomposite material being based on a molecular conductor of $(BET\text{-}TTF)_2IxBr_3\text{-}x$ on a polycarbonate base substrate, the linear response defined in Figure 3 is obtained.

11. System for monitoring intraocular pressure, **characterized in that** it comprises a sensor contact lens according to any of claims 1 to 8, a data receiving unit (7) which sends information to a PC or PDA (8) type data processing unit via radio frequency (RF) or wires for data handling, storage and visualization.

FIG 1

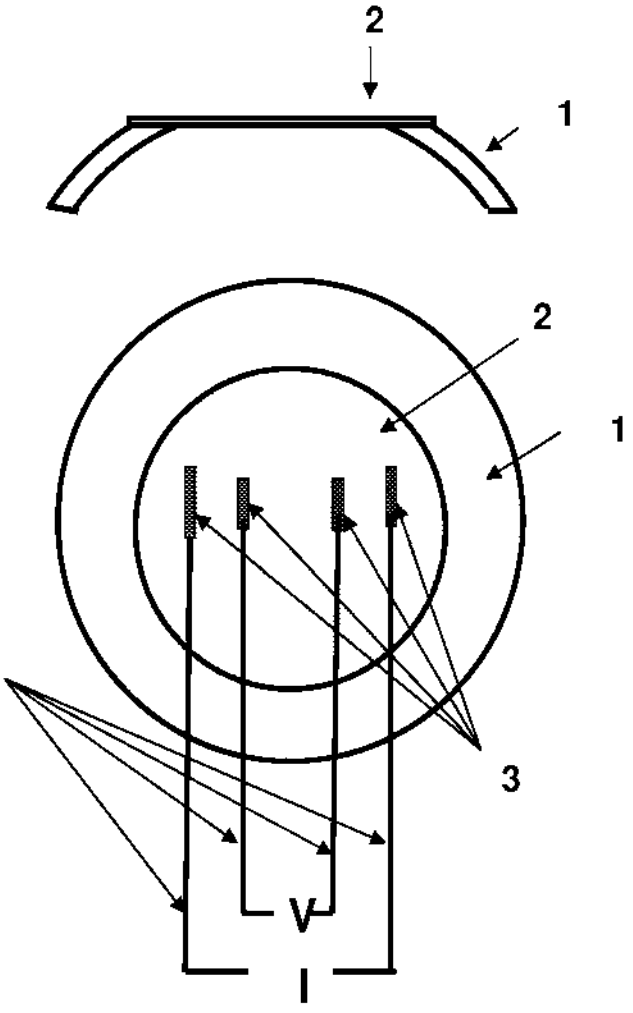

FIG 2

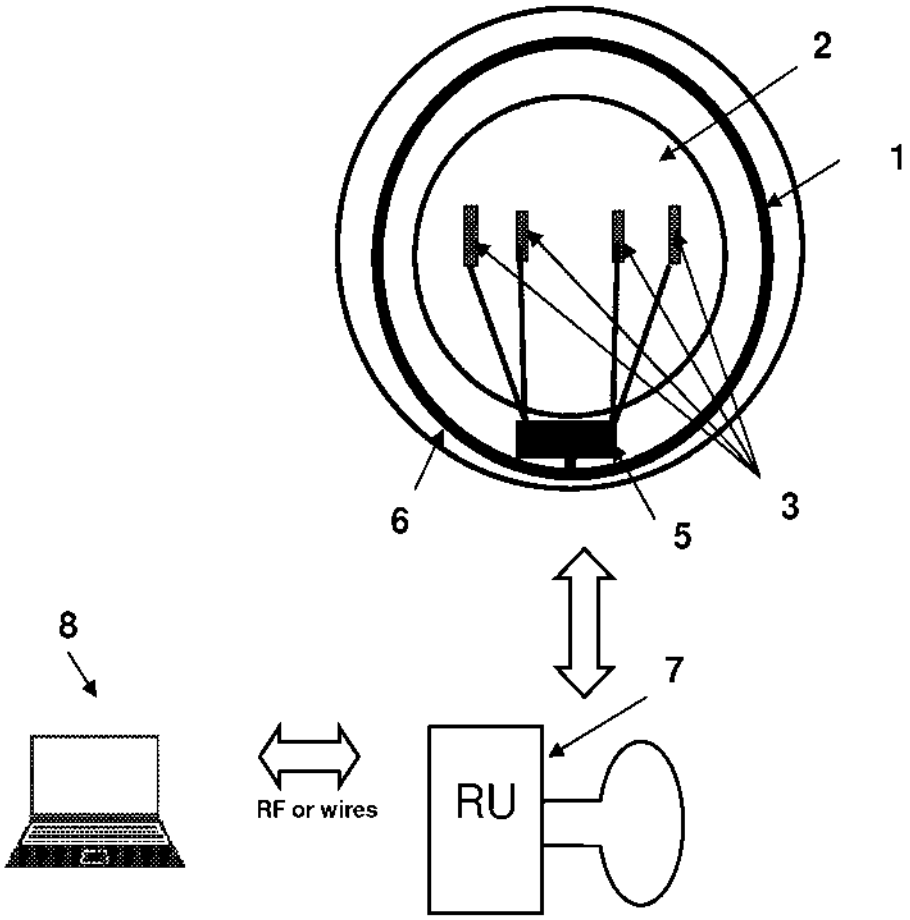

FIG 3

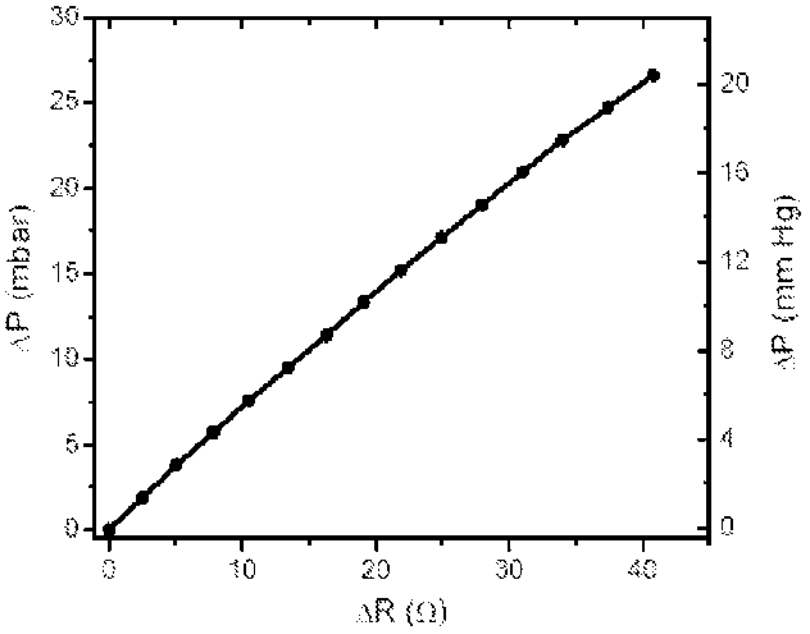

FIG 4

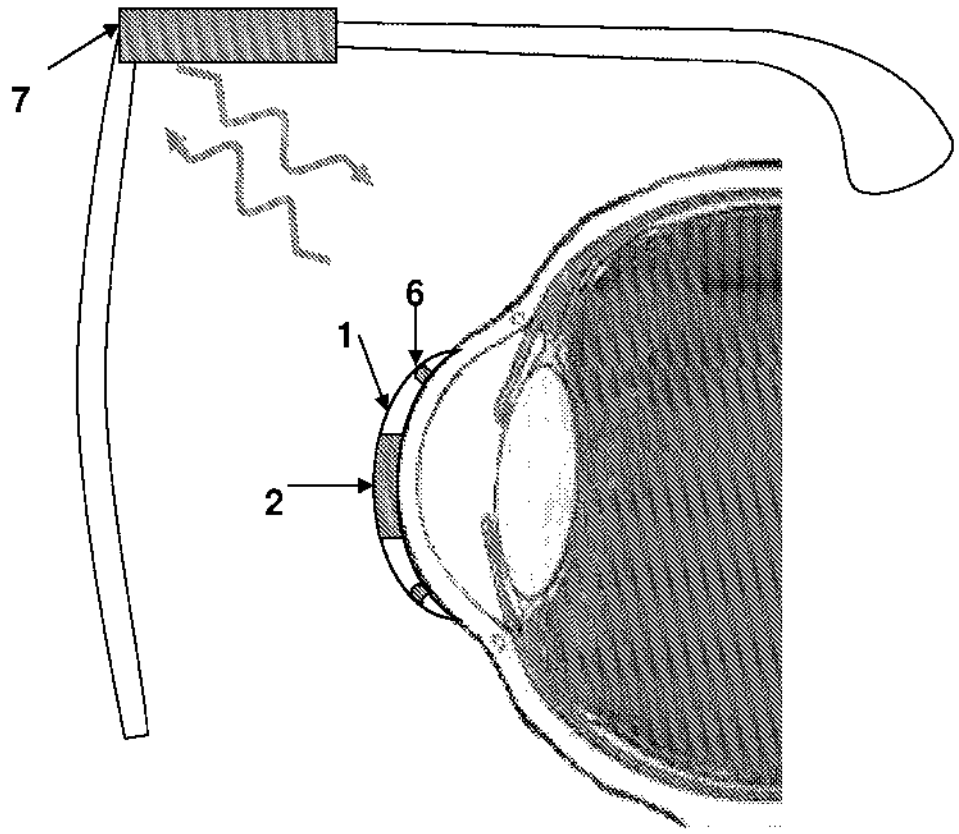

INTERNATIONAL SEARCH REPORT

International application No.
PCT/ES 2009/070205

A. CLASSIFICATION OF SUBJECT MATTER

A61B 3/16 (2006.01)
According to International Patent Classification (IPC) or to both national classification and IPC

B. FIELDS SEARCHED

Minimum documentation searched (classification system followed by classification symbols)
A61B3, G02C7

Documentation searched other than minimum documentation to the extent that such documents are included in the fields searched

Electronic data base consulted during the international search (name of data base and, where practicable, search terms used)

INVENES,EPODOC,WPI,INSPEC,BIOSIS,MEDLINE,NPL.

C. DOCUMENTS CONSIDERED TO BE RELEVANT

Category*	Citation of document, with indication, where appropriate, of the relevant passages	Relevant to claim No.
A	WO 03088867 A1 (THE CLEVELAND CLINIC FOUNDATION) 30.10.2003, the whole document.	1 - 11
A	US 20070123767 A1 (MONTEGRANDE et al) 31.05.2007, the whole document.	1 - 11
A	US 6579235 B1 (ABITA et al.) 17.06.2003, the whole document.	1 - 11
A	DE 102004061543 A1 (MESOTEC GMBH) 29.06.2006, the whole document.	1,9,11
A	Dekker Peter W. "Principles of contact lens tonometry", International Ophthalmology, 1998-1999, vol. 22, nº 2, pages 105-111	1, 9

☒ Further documents are listed in the continuation of Box C. ☒ See patent family annex.

* Special categories of cited documents:
"A" document defining the general state of the art which is not considered to be of particular relevance.
"E" earlier document but published on or after the international filing date
"L" document which may throw doubts on priority claim(s) or which is cited to establish the publication date of another citation or other special reason (as specified)
"O" document referring to an oral disclosure use, exhibition, or other means
"P" document published prior to the international filing date but later than the priority date claimed
"T" later document published after the international filing date or priority date and not in conflict with the application but cited to understand the principle or theory underlying the invention
"X" document of particular relevance; the claimed invention cannot be considered novel or cannot be considered to involve an inventive step when the document is taken alone
"Y" document of particular relevance; the claimed invention cannot be considered to involve an inventive step when the document is combined with one or more other documents, such combination being obvious to a person skilled in the art
"&" document member of the same patent family

Date of the actual completion of the international search	Date of mailing of the international search report
02.November.2009 (02.11.2009)	**(06/11/2009)**
Name and mailing address of the ISA/ O.E.P.M. Paseo de la Castellana, 75 28071 Madrid, España. Facsimile No. 34 91 3495304	Authorized officer A. Cardenas Villar Telephone No. +34 91 349 53 93

Form PCT/ISA/210 (second sheet) (July 2008)

INTERNATIONAL SEARCH REPORT

International application No.
PCT/ES 2009/070205

C (continuation). DOCUMENTS CONSIDERED TO BE RELEVANT

Category*	Citation of documents, with indication, where appropriate, of the relevant passages	Relevant to claim No.
A	Base of datos MEDLINE/NLM, AN NLM16853126, Laukhina E. et al. "Harnessing IC1 reduction processes for synthesis of different BEDT-TTF-based molecular conductors", abstract, The journal of physical chemistry, 8.9.2005	3, 10
A	Base of datos MEDLINE/NLM, AN NLM16596615, Laukhina E. et al. "Linked crystallites in the conducting topmost layer of polymer bilayer films controlled by temperature: from micro- to nanocrystallites", abstract, Chemphyschem, 10.04.2006	3, 10

Form PCT/ISA/210 (continuation of second sheet) (July 2008)

INTERNATIONAL SEARCH REPORT

Information on patent family members

International application No
PCT/ES 2009/070205

Patent document cited in the search report	Publication date	Patent family member(s)	Publication date
WO 03088867 A	30.10.2003	US 2002193674 A	19.12.2002
		US 6749568 B	15.06.2004
		CA 2482359 A	30.10.2003
		AU 2003223685 A	03.11.2003
		US 2004207808 A	21.10.2004
		US 7169106 B	30.01.2007
		EP 1496821 A	19.01.2005
		EP 20030719882	22.04.2003
		US 2007129623 A	07.06.2007
US 2007123767 A	31.05.2007	US 2003225318 A	04.12.2003
		WO 03102632 A	11.12.2003
		AU 2003273544 A	19.12.2003
		US 2005159660 A	21.07.2005
			21.07.2005
			21.07.2005
US 6579235 B	17.06.2003	NONE	----------
DE 102004061543 A	29.06.2006	NONE	----------

Form PCT/ISA/210 (patent family annex) (July 2008)

REFERENCES CITED IN THE DESCRIPTION

This list of references cited by the applicant is for the reader's convenience only. It does not form part of the European patent document. Even though great care has been taken in compiling the references, errors or omissions cannot be excluded and the EPO disclaims all liability in this regard.

Patent documents cited in the description

- US 6994672 B **[0006]**
- US 7169106 B **[0006]**
- WO 2003001991 A **[0007]**
- ES P200602887 **[0025]**
- WO 2007014975 A **[0028]**

12.- ANEXO II

AUTORIZACIONES DE LOS COAUTORES

Según la Normativa de la Universidad de Valladolid se debe adjuntar por escrito la conformidad de los coautores de las publicaciones a la presentación de los trabajos como para de la tesis y su renuncia a que formen parte de otra tesis doctoral.

ACEPTACIÓN DE LOS COAUTORES

D/Dña Fernando Ussa Herrera, con DNI nº 71316906R como coautor de las publicaciones

Sánchez I, Martín R, Ussa F, Fernandez-Bueno I. The parameters of the porcine eyeball. Graefes Arch Clin Exp Ophthalmol 2011 249: 475-482.

Laukhin V, Sánchez I, Moya A, Laukhina E, Martin R, Ussa F, Rovira C, Guimera A, Villa R, Aguiló J, Pastor JC, Veciana J. Non-invasive intraocular pressure monitoring with a contact lens engineered with a nanostructured polymeric sensing film. Sensors and Actuators A 170 (2011) 36– 43.

Sánchez I, Laukhin V, Moya A, Martin R, Ussa F, Laukhina E, Guimera A, Villa R, Rovira C, Aguiló J, Veciana J, Pastor JC. Prototype of a nano-structured sensing contact lens for noninvasive intraocular pressure monitoring. Invest Ophthalmol Vis Sci Oct 21;52(11):8310-5.

Moya A, Guimerà A, Sánchez I, Laukin V, Martin R, Ussa F, Laukhina E, Rovira C, Veciana J, Pastor JC, Villa R, Aguiló J. Discrete portable measuring device for monitoring noninvasive intraocular pressure with a nano-structured sensing contact lens prototype. International Journal of E-Health and Medical Communications. 2011 2011; 2: 1-19.

Sánchez I, Martín R, Ussa F. Measurement of intraocular pressure in a porcine ex vivo model eye. Journal of Glaucoma (Enviado)

doy mi consentimiento para que éstas formen parte de la Tesis Doctoral en la modalidad de "compendio de publicaciones" presentada en la Universidad de Valladolid por D/Dña Irene Sánchez Pavón, y titulada "*Lente de contacto con sensor nanoestructurado para la medida y monitorización de la presión intraocular*", asimismo renuncio a la presentación de las publicaciones como parte de otra tesis doctoral.

Fecha y firma

DNI: 71316906R

Valladolid, 19 diciembre de 2011.

ACEPTACIÓN DE LOS COAUTORES

D/Dña Raúl Martín Herranz, con DNI nº 50.447.910-D como coautor de las publicaciones

Sánchez I, Martín R, Ussa F, Fernandez-Bueno I. The parameters of the porcine eyeball. Graefes Arch Clin Exp Ophthalmol 2011 249: 475-482.

Laukhin V, Sánchez I, Moya A, Laukhina E, Martin R, Ussa F, Rovira C, Guimera A, Villa R, Aguiló J, Pastor JC, Veciana J. Non-invasive intraocular pressure monitoring with a contact lens engineered with a nanostructured polymeric sensing film. Sensors and Actuators A 170 (2011) 36– 43.

Sánchez I, Laukhin V, Moya A, Martin R, Ussa F, Laukhina E, Guimera A, Villa R, Rovira C, Aguiló J, Veciana J, Pastor JC. Prototype of a nano-structured sensing contact lens for noninvasive intraocular pressure monitoring. Invest Ophthalmol Vis Sci Oct 21;52(11):8310-5.

Moya A, Guimerà A, Sánchez I, Laukin V, Martin R, Ussa F, Laukhina E, Rovira C, Veciana J, Pastor JC, Villa R, Aguiló J. Discrete portable measuring device for monitoring noninvasive intraocular pressure with a nano-structured sensing contact lens prototype. International Journal of E-Health and Medical Communications. 2011 2011; 2: 1-19.

Sánchez I, Martín R, Ussa F. Measurement of intraocular pressure in a porcine ex vivo model eye. Journal of Glaucoma (Enviado)

doy mi consentimiento para que éstas formen parte de la Tesis Doctoral en la modalidad de “compendio de publicaciones” presentada en la Universidad de Valladolid por D/Dña Irene Sánchez Pavón, y titulada “*Lente de contacto con sensor nanoestructurado para la medida y monitorización de la presión intraocular”*, asimismo renuncio a la presentación de las publicaciones como parte de otra tesis doctoral.

Fecha y firma

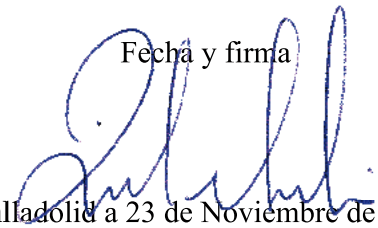

Valladolid a 23 de Noviembre de 2011

ACEPTACIÓN DE LOS COAUTORES

D/Dña José Carlos Pastor Jimeno, con DNI/Pasaporte nº..1577134 como coautor de las publicaciones

Laukhin V, Sánchez I, Moya A, Laukhina E, Martin R, Ussa F, Rovira C, Guimera A, Villa R, Aguiló J, Pastor JC, Veciana J. Non-invasive intraocular pressure monitoring with a contact lens engineered with a nanostructured polymeric sensing film. Sensors and Actuators A 170 (2011) 36– 43.

Sánchez I, Laukhin V, Moya A, Martin R, Ussa F, Laukhina E, Guimera A, Villa R, Rovira C, Aguiló J, Veciana J, Pastor JC. Prototype of a nano-structured sensing contact lens for noninvasive intraocular pressure monitoring. Invest Ophthalmol Vis Sci (Aceptado).

Moya A, Guimerà A, Sánchez I, Laukin V, Martin R, Ussa F, Laukhina E, Rovira C, Veciana J, Pastor JC, Villa R, Aguiló J. Discrete portable measuring device for monitoring noninvasive intraocular pressure with a nano-structured sensing contact lens prototype. International Journal of E-Health and Medical Communications. 2011 (Aceptado).

doy mi consentimiento para que éstas formen parte de la Tesis Doctoral en la modalidad de "compendio de publicaciones" presentada en la Universidad de Valladolid por D/Dña Irene Sánchez Pavón, y titulada "*Lente de contacto con sensor nanoestructurado para la medida y monitorización de la presión intraocular*", asimismo renuncio a la presentación de las publicaciones como parte de otra tesis doctoral.

Fecha y firma

26.9.2011

ACEPTACIÓN DE LOS COAUTORES

D/Dña Iván Fernández Bueno, con DNI/Pasaporte nº 09438653M como coautor de las publicaciones

Sánchez I, Martín R, Ussa F, Fernandez-Bueno I. The parameters of the porcine eyeball. Graefes Arch Clin Exp Ophthalmol 2011 249: 475-482.

doy mi consentimiento para que éstas formen parte de la Tesis Doctoral en la modalidad de "compendio de publicaciones" presentada en la Universidad de Valladolid por D/Dña Irene Sánchez Pavón, y titulada "*Lente de contacto con sensor nanoestructurado para la medida y monitorización de la presión intraocular*", asimismo renuncio a la presentación de las publicaciones como parte de otra tesis doctoral.

Valladolid, 15 de septiembre de 2011

Fdo.: Iván Fernández Bueno

ACEPTACIÓN DE LOS COAUTORES

D/Dña Ana Moya Lara, con DNI/Pasaporte nº 47153741S como coautor de las publicaciones

Laukhin V, Sánchez I, Moya A, Laukhina E, Martin R, Ussa F, Rovira C, Guimera A, Villa R, Aguiló J, Pastor JC, Veciana J. Non-invasive intraocular pressure monitoring with a contact lens engineered with a nanostructured polymeric sensing film. Sensors and Actuators A 170 (2011) 36– 43.

Sánchez I, Laukhin V, Moya A, Martin R, Ussa F, Laukhina E, Guimera A, Villa R, Rovira C, Aguiló J, Veciana J, Pastor JC. Prototype of a nano-structured sensing contact lens for noninvasive intraocular pressure monitoring. Invest Ophthalmol Vis Sci (Aceptado).

Moya A, Guimerà A, Sánchez I, Laukin V, Martin R, Ussa F, Laukhina E, Rovira C, Veciana J, Pastor JC, Villa R, Aguiló J. Discrete portable measuring device for monitoring noninvasive intraocular pressure with a nano-structured sensing contact lens prototype. International Journal of E-Health and Medical Communications. 2011 (Aceptado).

doy mi consentimiento para que éstas formen parte de la Tesis Doctoral en la modalidad de "compendio de publicaciones" presentada en la Universidad de Valladolid por D/Dña Irene Sánchez Pavón, y titulada "*Lente de contacto con sensor nanoestructurado para la medida y monitorización de la presión intraocular*", asimismo renuncio a la presentación de las publicaciones como parte de otra tesis doctoral.

Fecha y firma

16/09/2011

CO-AUTHOR PERMISSION

Mr/Ms Vladimir Laukhin, ID/Passport nº X2026817-B as co-author of the articles

Laukhin V, Sánchez I, Moya A, Laukhina E, Martin R, Ussa F, Rovira C, Guimera A, Villa R, Aguiló J, Pastor JC, Veciana J. Non-invasive intraocular pressure monitoring with a contact lens engineered with a nanostructured polymeric sensing film. Sensors and Actuators A 170 (2011) 36– 43.

Sánchez I, Laukhin V, Moya A, Martin R, Ussa F, Laukhina E, Guimera A, Villa R, Rovira C, Aguiló J, Veciana J, Pastor JC. Prototype of a nano-structured sensing contact lens for noninvasive intraocular pressure monitoring. Invest Ophthalmol Vis Sci (Aceptado).

Moya A, Guimerà A, Sánchez I, Laukin V, Martin R, Ussa F, Laukhina E, Rovira C, Veciana J, Pastor JC, Villa R, Aguiló J. Discrete portable measuring device for monitoring noninvasive intraocular pressure with a nano-structured sensing contact lens prototype. International Journal of E-Health and Medical Communications. 2011 (Aceptado).

I give my full consent for its/their use as part of the PhD Thesis elaborated as "compendium of publications" presented at the University of Valladolid by Mr/Ms Irene Sánchez Pavón, Entitled "*Lente de contacto con sensor nanoestructurado para la medida y monitorización de la presión intraocular*", renouncing as well to present them as part of any other PhD thesis.

Date and signature

07/10/2011

ACEPTACIÓN DE LOS COAUTORES

D/Dña Antón Guimerà Brunet, con DNI/Pasaporte nº 77114102R como coautor de las publicaciones

Laukhin V, Sánchez I, Moya A, Laukhina E, Martin R, Ussa F, Rovira C, Guimera A, Villa R, Aguiló J, Pastor JC, Veciana J. Non-invasive intraocular pressure monitoring with a contact lens engineered with a nanostructured polymeric sensing film. Sensors and Actuators A 170 (2011) 36– 43.

Sánchez I, Laukhin V, Moya A, Martin R, Ussa F, Laukhina E, Guimera A, Villa R, Rovira C, Aguiló J, Veciana J, Pastor JC. Prototype of a nano-structured sensing contact lens for noninvasive intraocular pressure monitoring. Invest Ophthalmol Vis Sci (Aceptado).

Moya A, Guimerà A, Sánchez I, Laukin V, Martin R, Ussa F, Laukhina E, Rovira C, Veciana J, Pastor JC, Villa R, Aguiló J. Discrete portable measuring device for monitoring noninvasive intraocular pressure with a nano-structured sensing contact lens prototype. International Journal of E-Health and Medical Communications. 2011 (Aceptado).

doy mi consentimiento para que éstas formen parte de la Tesis Doctoral en la modalidad de "compendio de publicaciones" presentada en la Universidad de Valladolid por D/Dña Irene Sánchez Pavón, y titulada "*Lente de contacto con sensor nanoestructurado para la medida y monitorización de la presión intraocular*", asimismo renuncio a la presentación de las publicaciones como parte de otra tesis doctoral.

Fecha y firma

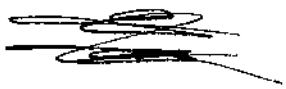

22-09-2011

CO-AUTHOR PERMISSION

Dr. Elena Laukhina, ID/Passport nº X 2379884-M, as co-author of the articles

Laukhin V, Sánchez I, Moya A, Laukhina E, Martin R, Ussa F, Rovira C, Guimera A, Villa R, Aguiló J, Pastor JC, Veciana J. Non-invasive intraocular pressure monitoring with a contact lens engineered with a nanostructured polymeric sensing film. Sensors and Actuators A 170 (2011) 36– 43.

Sánchez I, Laukhin V, Moya A, Martin R, Ussa F, Laukhina E, Guimera A, Villa R, Rovira C, Aguiló J, Veciana J, Pastor JC. Prototype of a nano-structured sensing contact lens for noninvasive intraocular pressure monitoring. Invest Ophthalmol Vis Sci (Aceptado).

Moya A, Guimerà A, Sánchez I, Laukin V, Martin R, Ussa F, Laukhina E, Rovira C, Veciana J, Pastor JC, Villa R, Aguiló J. Discrete portable measuring device for monitoring noninvasive intraocular pressure with a nano-structured sensing contact lens prototype. International Journal of E-Health and Medical Communications. 2011 (Aceptado).

I give my full consent for their use as part of the PhD Thesis elaborated as "compendium of publications" presented at the University of Valladolid by
Ms. Irene Sánchez Pavón, Entitled "*Lente de contacto con sensor nanoestructurado para la medida y monitorización de la presión intraocular*", renouncing as well to present them as part of any other PhD thesis.

Date and signature

19.09.2011,

ACEPTACIÓN DE LOS COAUTORES

D/Dña Rosa Villa Sanz, con DNI/Pasaporte nº 18004945Q como coautor de las publicaciones

Laukhin V, Sánchez I, Moya A, Laukhina E, Martin R, Ussa F, Rovira C, Guimera A, Villa R, Aguiló J, Pastor JC, Veciana J. Non-invasive intraocular pressure monitoring with a contact lens engineered with a nanostructured polymeric sensing film. Sensors and Actuators A 170 (2011) 36– 43.

Sánchez I, Laukhin V, Moya A, Martin R, Ussa F, Laukhina E, Guimera A, Villa R, Rovira C, Aguiló J, Veciana J, Pastor JC. Prototype of a nano-structured sensing contact lens for noninvasive intraocular pressure monitoring. Invest Ophthalmol Vis Sci (Aceptado).

Moya A, Guimerà A, Sánchez I, Laukin V, Martin R, Ussa F, Laukhina E, Rovira C, Veciana J, Pastor JC, Villa R, Aguiló J. Discrete portable measuring device for monitoring noninvasive intraocular pressure with a nano-structured sensing contact lens prototype. International Journal of E-Health and Medical Communications. 2011 (Aceptado).

doy mi consentimiento para que éstas formen parte de la Tesis Doctoral en la modalidad de "compendio de publicaciones" presentada en la Universidad de Valladolid por D/Dña Irene Sánchez Pavón, y titulada "*Lente de contacto con sensor nanoestructurado para la medida y monitorización de la presión intraocular*", asimismo renuncio a la presentación de las publicaciones como parte de otra tesis doctoral.

Fecha y firma

ACEPTACIÓN DE LOS COAUTORES

D/Dña Jaume Veciana Miró, con DNI/Pasaporte nº 46104447G como coautor de las publicaciones

Laukhin V, Sánchez I, Moya A, Laukhina E, Martin R, Ussa F, Rovira C, Guimera A, Villa R, Aguiló J, Pastor JC, Veciana J. Non-invasive intraocular pressure monitoring with a contact lens engineered with a nanostructured polymeric sensing film. Sensors and Actuators A 170 (2011) 36– 43.

Sánchez I, Laukhin V, Moya A, Martin R, Ussa F, Laukhina E, Guimera A, Villa R, Rovira C, Aguiló J, Veciana J, Pastor JC. Prototype of a nano-structured sensing contact lens for noninvasive intraocular pressure monitoring. Invest Ophthalmol Vis Sci (Aceptado).

Moya A, Guimerà A, Sánchez I, Laukin V, Martin R, Ussa F, Laukhina E, Rovira C, Veciana J, Pastor JC, Villa R, Aguiló J. Discrete portable measuring device for monitoring noninvasive intraocular pressure with a nano-structured sensing contact lens prototype. International Journal of E-Health and Medical Communications. 2011 (Aceptado).

doy mi consentimiento para que éstas formen parte de la Tesis Doctoral en la modalidad de "compendio de publicaciones" presentada en la Universidad de Valladolid por D/Dña Irene Sánchez Pavón, y titulada *"Lente de contacto con sensor nanoestructurado para la medida y monitorización de la presión intraocular"*, asimismo renuncio a la presentación de las publicaciones como parte de otra tesis doctoral.

Fecha y firma

21 Septiembre 2011

ACEPTACIÓN DE LOS COAUTORES

D/Dña Concepció Rovira Angulo, con DNI/Pasaporte nº 46207573K. como coautor de las publicaciones

Laukhin V, Sánchez I, Moya A, Laukhina E, Martin R, Ussa F, Rovira C, Guimera A, Villa R, Aguiló J, Pastor JC, Veciana J. Non-invasive intraocular pressure monitoring with a contact lens engineered with a nanostructured polymeric sensing film. Sensors and Actuators A 170 (2011) 36– 43.

Sánchez I, Laukhin V, Moya A, Martin R, Ussa F, Laukhina E, Guimera A, Villa R, Rovira C, Aguiló J, Veciana J, Pastor JC. Prototype of a nano-structured sensing contact lens for noninvasive intraocular pressure monitoring. Invest Ophthalmol Vis Sci (Aceptado).

Moya A, Guimerà A, Sánchez I, Laukin V, Martin R, Ussa F, Laukhina E, Rovira C, Veciana J, Pastor JC, Villa R, Aguiló J. Discrete portable measuring device for monitoring noninvasive intraocular pressure with a nano-structured sensing contact lens prototype. International Journal of E-Health and Medical Communications. 2011 (Aceptado).

doy mi consentimiento para que éstas formen parte de la Tesis Doctoral en la modalidad de "compendio de publicaciones" presentada en la Universidad de Valladolid por D/Dña Irene Sánchez Pavón, y titulada *"Lente de contacto con sensor nanoestructurado para la medida y monitorización de la presión intraocular"*, asimismo renuncio a la presentación de las publicaciones como parte de otra tesis doctoral.

Fecha y firma

Bellaterra, 22 de Septiembre de 2011

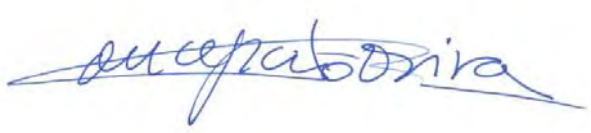

13.- ANEXO III

Sánchez I, Martín R, Ussa F, Fernandez-Bueno I.

The parameters of the porcine eyeball.

Graefes Arch Clin Exp Ophthalmol 2011 249: 475-482.

Graefes Arch Clin Exp Ophthalmol (2011) 249:475–482
DOI 10.1007/s00417-011-1617-9

REVIEW ARTICLE

The parameters of the porcine eyeball

Irene Sanchez · Raul Martin · Fernando Ussa · Ivan Fernandez-Bueno

Received: 15 June 2010 / Revised: 4 January 2011 / Accepted: 5 January 2011 / Published online: 2 February 2011

Abstract
Background The eye of the domestic pig (*Sus scrofa domestica*) is an ex vivo animal model often used in vision sciences research (retina studies, glaucoma, cataracts, etc.). However, only a few papers have compiled pig eye anatomical descriptions. The purpose of this paper is to describe pig and human eye anatomical parameters to help investigators in their choice of animal model depending on their study objective.
Methods A wide search of current medical literature was performed (English language) using PubMed. Anteroposterior axial length and corneal radius, astigmatism, vertical and horizontal diameter, and pachymetry (slit-scan and ultrasound) were measured in five enucleated pig eyes of animals 6 to 8 months old.
Results Horizontal corneal diameter was 14.31±0.25 mm (CI 95% 14.03 mm–14.59 mm), vertical diameter was 12.00±0 mm, anteroposterior length was 23.9±0.08 mm (CI 95% 23.01 mm–29.99 mm), central corneal ultrasound pachymetry was 877.6±13.58 μm (CI 95% 865.70 μm–889.50 μm) and slit-scan pachymetry was 906.2±15.30 μm (CI 95% 892.78 μm–919.61 μm). Automatic keratometry (main meridians) was 41.19±1.76D and 38.83±2.89D (CI 95% 40.53D–41.81D and 37.76D–39.89D respectively) with an astigmatism of 2.36±1.70D (CI 95% 1.72D–3.00D), and manual keratometry was 41.05±0.54D and 39.30±1.15D (CI 95% 40.57D–41.52D and 38.29D–40.31D respectively) with an astigmatism of 1.75±1.31D (CI 95% 0.60D–2.90D).
Conclusion This paper describes the anatomy of the pig eyeball for easy use and interpretation by researchers who are considering their choice of animal model in vision sciences research.

Keywords Porcine cornea · Porcine parameters · Porcine anatomy · Porcine eye · Pig eye · Pig cornea · Pig parameters · Pig anatomy

The authors have no proprietary, financial or commercial interest in any material or method mentioned in this study.

I. Sanchez (✉)
IOBA-Eye Institute and CIBER-BBN, University of Valladolid, Valladolid, Spain
e-mail: isanchezp@ioba.med.uva.es

R. Martin
IOBA-Eye Institute and Department of Physics
TAO – School of Optometry,
University of Valladolid,
Valladolid, Spain

F. Ussa
IOBA-Eye Institute, Ophthalmologist, Glaucoma Unit,
University of Valladolid,
Valladolid, Spain

I. Fernandez-Bueno
IOBA-Eye Institute, University of Valladolid,
Paseo de Belén nº 17 Campus Miguel Delibes,
47011 Valladolid, Spain

Introduction

The pig eye is an ex vivo animal model often used in vision sciences research because its morphology is similar to the human eye [1–6]. The pig eye has been used in neuroretinal studies due to the similarity of the distribution of the retinal layers to that of the human retina [1], and it is also a validated animal model of glaucoma [4]. Moreover, it has been used in cataract surgery research [5], in corneal transplant studies [6, 7], and as a model in aberrometry studies [2, 3].

A few studies compile a complete description of the pig eye [8]; some eye parameters can be found in papers [3, 4] that provide information about the similarities and

differences between pig and human eyes, but only as they pertain to the study. Moreover, there are no papers that collect anatomical characteristics about corneal curvature and refractive power measured by non-invasive techniques (autokeratometer or corneal topography).

The purpose of this paper is to summarise the anatomical parameters of the pig eye, including corneal topography description, to help vision researchers choose an animal model that is appropriate to the objectives of their study.

Materials and methods

This paper presents two principal sections. First, a PubMed search of the English language literature was performed looking for human eye [9, 10] and pig eye parameters. Second, an experimental study to determine the anatomical parameters of the enucleated pig eye was completed.

For the experimental study, five enucleated eyes from five pigs (*Sus scrofa domestica*) were obtained from the local abattoir. Animals were white (not albino) domestic pigs between 6 and 8months of age, and they weighed 120–150 kg. The eyeballs were enucleated around 8:30 a.m. and transported to the laboratory on ice. The measurements were made between 9:00 a.m. and 12:00 a.m. The excess of tissue external to the eyeballs, including muscles, the lacrimal gland, and conjunctiva, was removed with 0.12 mm Castro titanium delicate forceps and Wescott scissors (John Weiss International, Milton Keynes, UK). Pig eyes were always kept in DMEM culture medium (Dulbecco's Modified Eagle's Medium) supplemented with an antibiotic/antimicotic mixture (Gibco, UK). The eyeballs were cannulated for maintenance of the intraocular pressure within normal values (15 mmHg) measured with Perkins tonometry. Anteroposterior eye length, corneal radius, astigmatism, vertical and horizontal diameter, and pachymetry (slit-scan and ultrasound) were measured.

Corneal curvature was measured with a portable autokeratometer (ARK-30 Nidek, Fremont, CA, USA) [11] and with a manual keratometer (OM-4 Topcon, Tokio, Japan). Central corneal thickness was measured with ultrasound pachymetry (Sonogage Corneo-Gage Plus, Renaissance Parkway, Cleveland, OH, USA) calibrated by the manufacturer. Finally, a topographic study of the corneal surface was conducted with an ORBSCAN II (version 3.12: Bausch & Lomb, Rochester, NY, USA) determining central and peripheral corneal thickness, corneal curvature, refractive power, and corneal diameter.

Statistical analysis

The average value with standard deviation (SD) and confidence interval at 95% (CI 95%) of each parameter measured were determined with SPSS 14.0 for Windows.

Results

Literature search results

Sclera

The pig sclera is negatively charged, probably due to the presence of sulphate and uronic groups in glycosaminoglycans at pH 7.4, and the isoelectric point is three, which is the same as that of the human sclera [12]. The scleral spur has a special feature: there is a small, noticeable structure in the nasal quadrant. There are variations in the scleral sulcus depth that depend on the location in the circumference of the limbus. In the temporal quadrant, the scleral spur is characteristic. In the inferior and nasal quadrants, the scleral sulcus is obvious, whereas in the superior quadrant it is not easily visible [13]. There is little nerve innervation in this area [14]. The thickness of the scleral wall ranges from 830 to 1250 μm [12, 15], and the anterior segment is strongly pigmented [16]. The water content is 69.5±1.18% [15]. Histologically, pig sclera is very similar to human sclera, although pig collagen appears more disorganised than human collagen [15].

Cornea

The horizontal corneal diameter of the pig eye is 14.23 mm, and the vertical diameter is 12.09 mm [8]. The ultrasound pachymetry is between 1013±10 μm in an ex vivo model [17] and 666 μm (with a range of 534 μm to 797 μm) in a live animal [18]. The corneal epithelium has a thickness of 80 μm; this thickness is not constant, and can vary by 25 μm. The stromal thickness is 900 μm, and Descemet's membrane with the endothelium has a thickness of approximately 30 μm. Bowman's layer is absent in porcine cornea [17]. The stroma has a large amount of collagen type I [17], with mainly circumferential orientation [19]. Descemet's membrane extends beyond the origin of the cornea, and inserts slightly in the short pectinate ligaments [13].

The water content of the porcine cornea is 71.93±0.47%, and shows a transparency of 54.77±0.47% [20].

No papers were found with a description of pig eye corneal topography curvature obtained with computerised corneal topographies.

Lens

The lens is composed mainly of three types of proteins called crystallins that can be soluble or insoluble. The soluble proteins are α-, β- and γ-crystallins. The α-crystallins make up 35% of the outer lens and 22% of the inner lens (nucleus). The β-crystallins make up 45% of the outer lens and 35% of the inner lens. The γ-crystallins are present in smaller amounts than α-crystallins and β-crystallins, and are found in a greater

proportion in the lens nucleus than in the cortex. The increase of γ-crystallins in the inner lens may contribute to the refractive index gradient [21].

The insoluble proteins of the lens have a higher concentration in the cortex than the nucleus, with an estimated concentration of 25% [21].

The refractive power of the lens is 49.9±1.5 D, with a refractive index of 1.4686 and a negative spherical aberration of −3.6±2.0 D. Its anterior and posterior radii are 7.08±0.35 mm and 5.08±0.14 mm respectively. The lens thickness is 7.4±0.1 mm [3].

The minimum vaulting to introduce an intraocular lens (ICL) in a minipig eye (with 800 μm of corneal thickness [22]) is at least 150 μm, which corresponds to 1/3 to 1/4 of the total thickness of the cornea. The anterior chamber depth is approximately 3.5 mm [23].

Ciliary body

The ciliary body is a structure with abundant vascularisation and innervation. The stroma contains melanocytes with a double-layer epithelium and a pigmented and a non-pigmented layer. In general, the pig eye ciliary body is more pigmented than the human eye ciliary body [16]. In the nasal zone of the ciliary body, there are a few fibres of the ciliary muscle radially oriented. In the temporal zone, closest to the iris, there is a simple organisation of muscle fibres circumferentially distinct from radial fibres. In this zone, fibres are longer and reach the sclera and the scleral spur, although other fibres reach the back of the trabecular meshwork [13]. The cells of the ciliary muscle, myofilaments, do not show disciform or parallel organisation. The density of bands in the cell surface is similar to smooth muscle cells of the blood vessels and the wall of the human bowel. A basal membrane and connective tissue make up an elastic network that surrounds these cells. Cross-sections of the ciliary body show a fine network of radial fibres that extend from the choroid through the ciliary muscle to the trabecular meshwork [14].

McMenamin et al. [13] demonstrated that the muscle fibres are longer in the superior and inferior quadrants, the ligaments are more robust in the nasal and temporal quadrants, and the pigmentation is not homogeneous throughout the whole circumference.

Uveoscleral drainage

The iridocorneal angle appears to be a heterogeneous measure between animals, as shown by Bartholomew [8]. Uveoscleral drainage was measured to evaluate choroid drainage. The intraocular pressure is constant at 10 mmHg, with an average drainage of 2.8±0.9 μl/min. After blocking the conventional pathway of drainage, the drainage declined at an average rate of 1.1±0.5 μl/min. However, blocking the vortex veins does not change the uveoscleral drainage, which is maintained at 1.2±0.8 μl/min [24].

The postoperative inflammatory response of the pig eye is greater than that of the human eye; thus, posterior pole surgery may trigger diffuse choroidal haemorrhage that sometimes may be unstoppable [25]. The choroidal blood flow, with the retinal artery clamped, is 500 μl/min [26].

Lamina cribrosa

The structure of the lamina cribrosa has been studied by second harmonic generation imaging using a scanning laser ophtalmoscope-based microscope. With this technique, the collagen fibres that form the lamina cribrosa and their dehydration have been observed [27].

Retina

Pig retina maintains the structure of ten layers, the same as in the human retina because embryonic development is similar [28]. The outer plexiform layer [29] contains the synapses between the photoreceptors and second-order neurons, bipolar and horizontal cells. The inner plexiform layer is the other synaptic zone and connects third-order neurons, like amacrine and ganglion cells, with the bipolar cells. Müller cells are the main retinal glial cells. Müller cells are the main retinal glial cells. They extend through most of the retina from the outer segments, where their finger-like processes form the outer limiting membrane to their basement membrane, which makes up the inner limiting membrane [29]. The attachment between the retinal pigment epithelium and Bruch's membrane is mediated by the interaction between integrins (the main components of hemidesmosomes) on the retinal pigment epithelium surface and ligands in the extracellular matrix. The hemidesmosomes present in the basal surface of the retinal pigment epithelium maintain cohesion between the epithelium and Bruch's membrane [30].

There is a depressed central area, rich in cones, that is comparable to the human macula [25, 28]. It has the shape of a horizontal band called the foveal streak [31], which is placed over the optic nerve head [16]. The density of cones in this area is between 15,000 and 40,000 cells/mm^2 [16].

The proportion of cones and rods is similar to the human retina, and the paramacular density of cones is also similar [25]. These data are obtained thorough multifocal electroretinography. The fundus reflection is orange to pale grey, with pigmented epithelial cells. The pig eye lacks a tapetum [32]. The retinal circulation is holangiotic [25].

Vitreous

The vitreous is a gel containing collagen and sodium hyaluronate. Sodium hyaluronate has a coil-shaped

molecular structure, and is uniformly distributed in a three-dimensional network of collagen fibres that form a triple helix structure. The volume of the polymer network of the two molecules is only 1–2% of the total volume; the other 98–99% is composed of water. Moreover, the vitreous body represents 80% of the total volume of the eyeball. Its functions are eyeball form maintenance, mechanical stress absorption, maintenance of the homoeostasis of the eye and adjustment of the position of the lens [33]. In addition, the collective diffusion coefficient of the vitreous body is similar to the aqueous humour [29], with a calculated elastic modulus of 57.3±5.5 Pascals [34].

Innervation of the eyeball

The temporal quadrant of the posterior pole is characterised by the entry of the long ciliary nerves [14]. Glutamate is the major neurotransmitter in the neuronal cells of the visual pathway, and the presence of a GoG protein, which is expressed in the metabotropic glutamate receptors of bipolar cells of mammals, is observed [35].

Vascularization of the eyeball

The pig eyeball receives most of its blood supply through the long and short posterior ciliary arteries and the chorioretinal artery. The ciliary processes are fed by the iridociliary artery that forms a ring, the origins of which are the long posterior ciliary arteries [36].

The iris receives its blood supply from the iridociliary arterial circle, the origins of which are the anterior ciliary arteries. Capillaries are oriented radially in the direction of the pupil, and the morphology of the capillaries is characterised by a spiral or zig-zag. The veins also have an undulating morphology and drain into the vortex veins through pars plana veins [36].

Extrinsic ocular motility

The sixth extraocular muscles of the pig are similar to those of the human eye; moreover, the pig eye has a seventh extra ocular muscle that surrounds the optic nerve, and blood vessels called the retractor bulbi muscle. This muscle tends to retract the eyeball into the orbit [25].

Eyelids

The pig eye has a nictitating membrane [25]. The nictitating membrane is located in the medial angle of the two eyelids. The third eyelid mechanically protects the cornea, spreads the tear film and offers local immunological defences provided by the substances produced in lymph nodules. The superficial gland of the third eyelid produces part of the tear film [37]. The movement of the third eyelid is passive and depends on the action of the retractor bulbi muscle: the retraction of the eyeball and third eyelid protrusion towards the temporal angle [37]. The third eyelid cartilage consists of the dorsal and ventral branches and a crossbar resembling an anchor [37]. The deep gland of the third eyelid is also called the Harderian gland. It has a lobular structure, and is situated inside the periorbit on the medial orbit wall. The secretion of this gland is a lubricant that covers the eyeball and has antibacterial and immunological properties [38].

Experimental results

Table 1 summarises the results (average, standard deviation and 95% confidence interval) of the experimental measurements of enucleated pig eye parameters. The differences between porcine anterior segment and human anterior segment are shown in Table 2. Figure 1 shows corneal topography representative of one of the examined pig eyes. Figure 2 shows the topography of a healthy human cornea, to graphically show the differences between pig and human corneas.

Table 1 Data obtained from experimental measurements. Average with standard deviation (SD) and the confidence interval at 95% (CI 95%) was calculated

Parameter measured	Average ± SD	Confidence interval 95%
Ø Horizontal visible iris	14.31±0.25 mm	14.03–14.59 mm
Ø Vertical visible iris	12±0.0 mm	–
Ø Anteroposterior	23.9±0.08 mm	23.01–29.99 mm
Ultrasonic pachymetry	877.6±13.58 μm	865.70–889.50 μm
Slit-scan pachymetry	906.2±15.30 μm	892.78–919.61 μm
K automatic in R1 [a]	41.19±1.76 D	40.53–41.86 D
K automatic in R2 [a]	38.83±2.89 D	37.76–39.89 D
Corneal astigmatism [a]	2.36±1.70 D	1.72–3.00 D
K manual in R1 [b]	41.05±0.54 D	40.57–41.52 D
K manual in R2 [b]	39.30±1.15 D	38.29–40.31 D
Corneal astigmatism [b]	1.75±1.31 D	0.60–2.90 D

Ø=diameter; K=keratometry; R1=steeper main corneal meridian; R2=flatter main corneal meridian; [a] data obtained with ARK−30 automated keratometer; [b] data obtained with OM-4 manual keratometer. Corneal astigmatism was calculated as the difference between the power of the main corneal meridians (R1 and R2)

Table 2 Comparison of average parameters measured in the pig eyeball and estimated average values of the human population according to the literature

Parameter measured	Pig eye	Human eye
Ø Horizontal visible iris	14.31 mm	11.7 mm
Ø Vertical visible iris	12 mm	10.6 mm
Ø Anteroposterior	23.9 mm	24 mm
Ultrasonic pachymetry	877.6 μm	520 μm
Mean corneal radius	8.45 mm	7.80 mm

Discussion

Sclera

Pigmentation of the anterior sclera made regular trans-scleral infrared fundus illumination impossible. This illumination is feasible in human eyes [16].

Some papers show that the human and porcine sclera have comparable permeabilities, and thus pig sclera is an excellent model for studying the pharmacokinetics of trans-scleral drug delivery in vivo [39]. However, Nicoli et al. [15] showed that the different thicknesses of the human and porcine sclera have to be taken into account, even though the permeability of porcine sclera is the same as the human.

Cornea

Porcine corneal thickness is almost twice that of the human cornea, and lacks Bowman's layer [17]. Although Bartholomew [8] showed that pig cornea have Bowman's layer, later histological studies [17] did not find Bowman's layer. The thickness of the cornea as measured with ultrasound pachymetry is 877±14 μm (CI 95% 866–890 μm), which is less than the value obtained by Jay [17] (1013±10 μm) and higher than that of Faber [18] (666 μm). This difference could be due to the different ages of the animals slaughtered or the type of pig used. Additionally, in ex vivo models, corneal pachymetry could increase due to corneal swelling if measurements are taken a long time after animal sacrifice.

There are no previous papers describing the porcine corneal topography, especially the radius of corneal

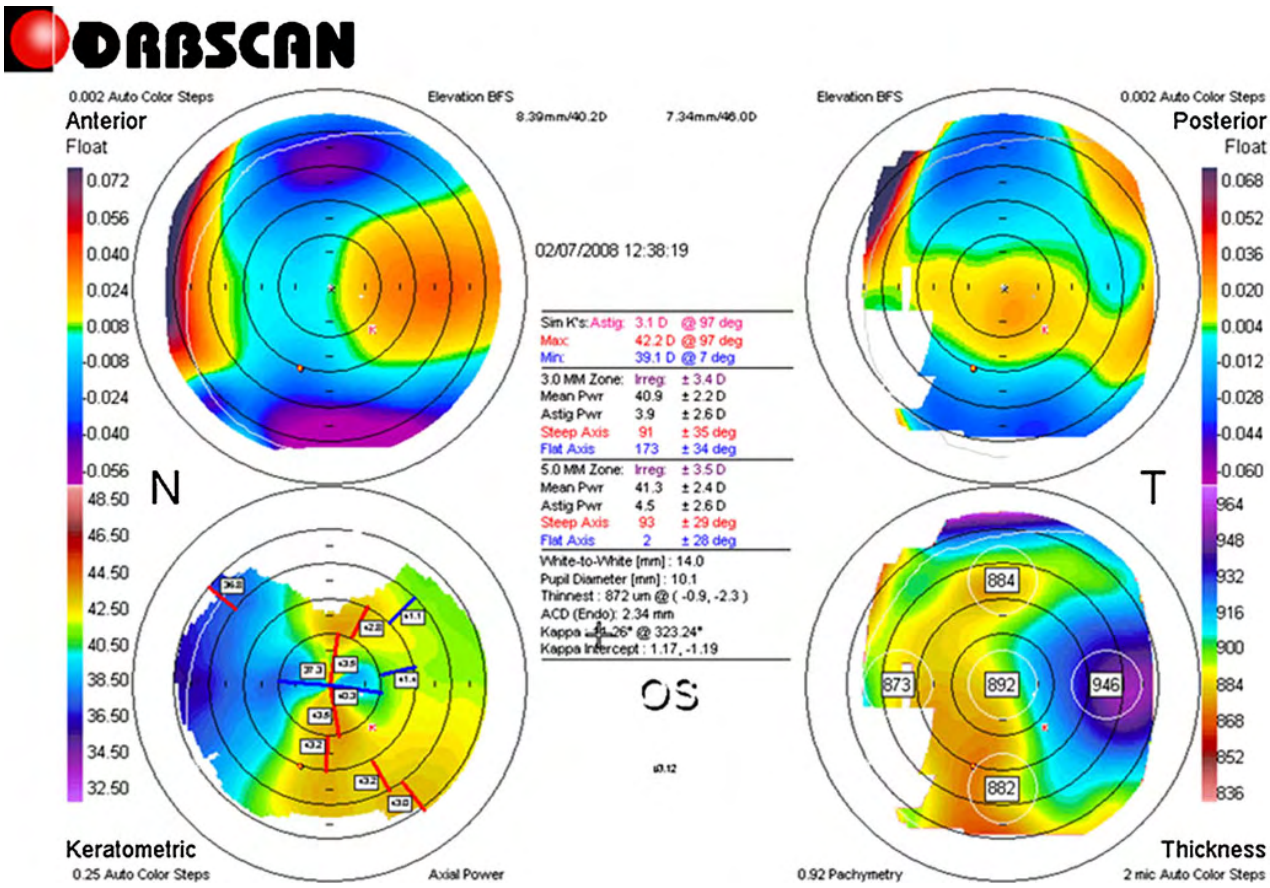

Fig. 1 Slit-scan topography of the pig cornea. *Top*: anterior corneal curvature (right) and posterior corneal curvature (*left*) represented with respect to best-fit sphere calculated by the topography. *Below*: simulated keratometry (*right*) and corneal pachymetry (*left*)

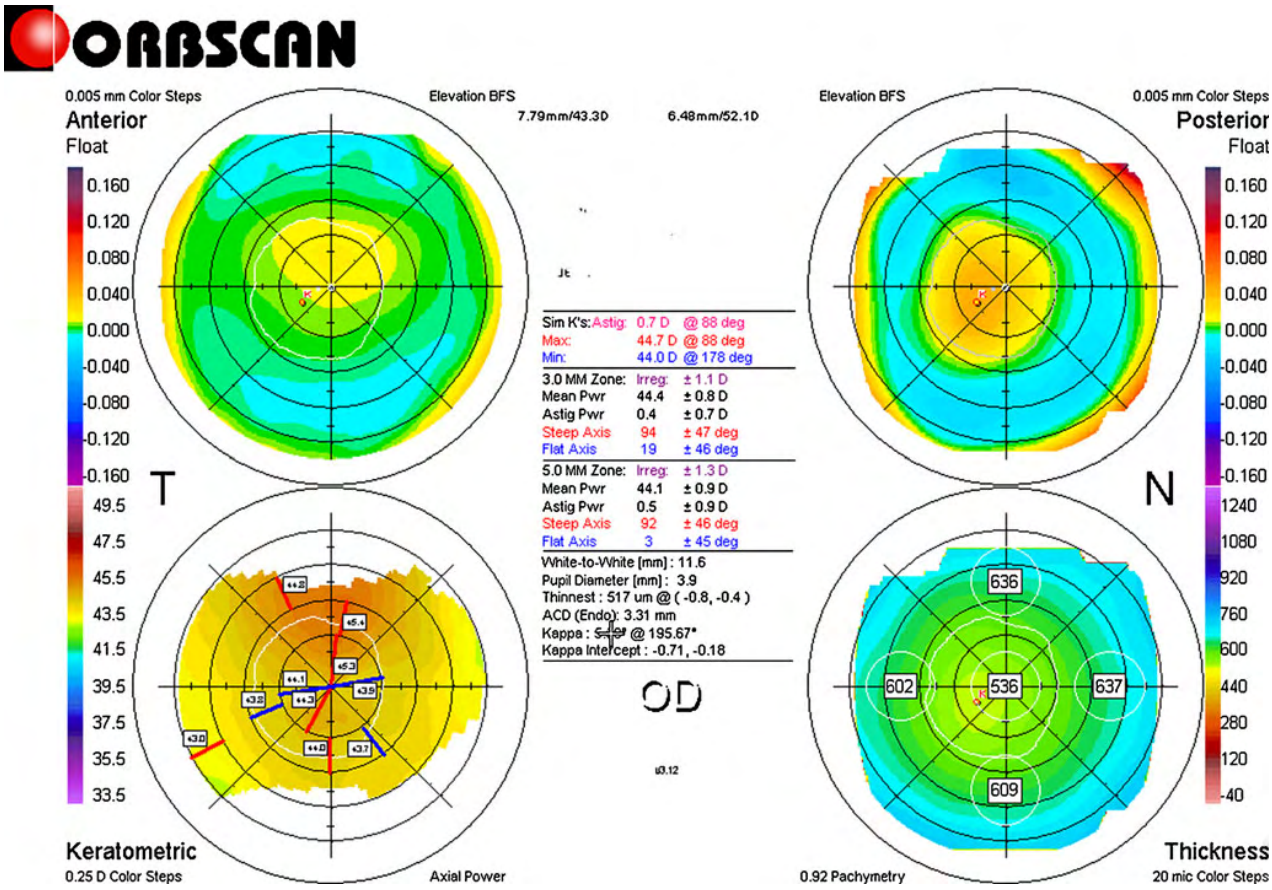

Fig. 2 Slit-scan topography of the human cornea. *Top*: Anterior corneal curvature (*right*) and posterior corneal curvature (*left*) represented with respect to best-fit sphere calculated by the topography. *Below*: simulated keratometry (*right*) and corneal pachymetry (*left*)

curvature, which is easily measurable with actual topography instruments or automatic keratometry. However, our results should be used with caution, because topographical measurements obtained in enucleated eyes and in live studies could be necessary. Pig corneal diameter is larger [18], with a larger corneal radius [9] and greater corneal astigmatism than human cornea. These topographical differences, coupled with corneal thickness differences, would discourage the use of pig eyeball as a model of corneal refractive surgery.

Lens

Some pig lens proteins (α-crystallin and β-crystallin) show the same protein sequence found in human crystallin proteins [21].

The anterior radius of the human lens is 10 mm, and the posterior radius is 6 mm, with a central lens thickness of 4 mm. These radiuses are smaller than those of the porcine eye. Also, central thickness is less than that of the pig eye [3]. For this reason, the use of the pig eye as an animal model in the development of intraocular lenses is difficult [5].

Ciliary body

The pig ciliary muscle is smaller than in the human eye, and has a circumferential area in the temporal quadrant, which appears to be responsible for accommodation [14].

The study of Wagner et al. [24] using enucleated porcine eyes showed that uveoscleral drainage contributes to the total drainage of the aqueous humour and that the choroid does not represent a significant pathway for uveoscleral drainage.

Retina and vitreous

The porcine retina shows great similarity to the human retina, except for its holangiotic vascularisation and macular organisation [25]. The macula has a band form, but photoreceptor cell density is comparable with that of the human macula [16, 25, 28, 29, 31].

The pig central vitreous mechanical properties are very similar to the human vitreous. [34] These similarities allow the pig eye to be used as a model for retinal pathologies. [1]

Extrinsic ocular motility

The seventh extraocular muscle, the retractor bulbi, must especially be taken into account in ocular surgery experimental studies, because the retraction of the eyeball into the orbit may complicate the surgery [25].

Eyelids

The nictitating membrane structure has degenerated to the caruncle and semilunar fold [25].

Axial length

The axial length found in this study is greater than the one obtained by Bartholomew [8]. The difference may be due to the age of the animal, but Bartholomew did not describe the exact age of experimental animals, only using descriptions such as "young adult" [8], whereas our study used 6- to 8-month-old pigs.

Inflammatory reaction of pig eyeball

The pig eye is more reactive than the human eye [7, 25], indicating that further investigation is needed to determine the cause. Warfvinge [40] showed that the immune privilege of the porcine eye allows a lower inflammatory reaction than that of the human eye. It also might be interesting to know why, in general, the pig eye structures seem to be more pigmented than the human eye, and to know the impact of this pigmentation on the use of the pig eye as an animal model in the visual sciences [16].

Conclusions

This paper describes the anatomy of the pig eyeball collected from the findings described in the literature and from our corneal study. It also summarises the differences between human and pig eye for easy use and interpretation by researchers who are choosing an animal model. The main limitations of our experimental study are the limited number of eyes investigated and the fact that the measurements were conducted on dead animals. Therefore, further measurements in other age groups of the same species will benefit the value of the measurements presented.

Acknowledgments The authors thank all slaughterhouse staff at Justino Gutiérrez SL (Laguna de Duero, Valladolid, Spain) for the cooperation in providing samples used in this work. I. Fernandez-Bueno is supported by the "Junta de Castilla y Leon".

References

1. Fernandez-Bueno I, Pastor JC, Gayoso MJ, Alcalde I, Garcia MT (2008) Müller and macrophage-like cell interactions in an organotypic culture of porcine neuroretina. Mol Vis 14:2148–2156
2. Acosta E, Vázquez D, Castillo LR (2009) Analysis of the optical properties of crystalline lenses by point-diffraction interferometry. Ophthalmic Physiol Opt 29:235–246
3. Wong KH, Koopmans SA, Terwee T, Kooijman AC (2007) Changes in spherical aberration after lens refilling with a silicone oil. Invest Ophthalmol Vis Sci 48:1261–1267
4. Ruiz-Ederra J, García M, Hernández M, Urcola H, Hernández-Barbáchano E, Araiz J, Vecino E (2005) The pig eye as a novel model of glaucoma. Exp Eye Res 81:561–569
5. Nishi O, Nishi K, Nishi Y, Chang S (2008) Capsular bag refilling using a new accommodating intraocular lens. J Cataract Refract Surg 34:302–309
6. Kim MK, Oh JY, Ko JH, Lee HJ, Jung JH, Wee WR, Lee JH, Park CG, Kim SJ, Ahn C, Kim SJ, Hwang SY (2009) DNA microarray-based gene expression profiling in porcine keratocytes and corneal endothelial cells and comparative analysis associated with xeno-related rejection. J Korean Med Sci 24:189–196
7. Faber C, Wang M, Scherfig E, Sørensen KE, Prause JU, Ehlers N, Nissen MH (2009) Orthotopic porcine corneal xenotransplantation using a human graft. Acta Ophthalmol 87:917–919
8. Bartholomew LR, Pang DX, Sam DA, Cavender JC (1997) Ultrasound biomicroscopy of globes from young adult pigs. Am J Vet Res 58:942–948
9. Newell FW (1993) Oftalmología fundamentos y conceptos, 7th edn. Mosby, España
10. Forrester J, Dick A, McMenamin P, Lee W (1996) The eye basics sciences in practice. Saunders, London
11. Pesudovs K (2004) Autorefraction as an outcome measure of laser in situ keratomileusis. J Cataract Refract Surg 30:1921–1928
12. Nicoli S, Ferrari G, Quarta M, Macaluso C, Santi P (2009) In vitro transscleral iontophoresis of high molecular weight neutral compounds. Eur J Pharm Sci 36:486–492
13. McMenamin PG, Steptoe RJ (1991) Normal anatomy of the aqueous humour outflow system in the domestic pig eye. J Anat 178:65–77
14. May CA, Skorski LM, Lütjen-Drecoll E (2005) Innervation of the porcine ciliary muscle and outflow region. J Anat 206:231–236
15. Nicoli S, Ferrari G, Quarta M, Macaluso C, Govoni P, Dallatana D, Santi P (2009) Porcine sclera as a model of human sclera for in vitro transport experiments: histology, SEM, and comparative permeability. Mol Vis 15:259–266
16. Voss Kyhn M, Kiilgaard JF, Lopez AG, Scherfig E, Prause JU, la Cour M (2007) The multifocal electroretinogram (mfERG) in the pig. Acta Ophthalmol Scand 85:438–444
17. Jay L, Brocas A, Singh K, Kieffer JC, Brunette I, Ozaki T (2008) Determination of porcine corneal layers with high spatial resolution by simultaneous second and third harmonic generation microscopy. Opt Express 16:16284–16293
18. Faber C, Scherfig E, Prause JU, Søresen KE (2008) Corneal thickness in pigs measured by ultrasound pachymetry in vivo. Scand J Lab Anim Sci 35:39–43c
19. Elsheikh A, Alhasso D (2009) Mechanical anisotropy of porcine cornea and correlation with stromal microstructure. Exp Eye Res 88:1084–1091
20. Xu YG, Xu YS, Huang C, Feng Y, Li Y, Wang W (2008) Development of a rabbit corneal equivalent using an acellular corneal matrix of a porcine substrate. Mol Vis 14:2180–2189
21. Keenan J, Orr DF, Pierscionek BK (2008) Patterns of crystallin distribution in porcine eye lenses. Mol Vis 14:1245–1253

22. Shiratani T, Shimizu K, Fujisawa K, Uga S, Nagano K, Murakami Y (2008) Crystalline lens changes in porcine eyes with implanted phakic IOL (ICL) with a central hole. Graefes Arch Clin Exp Ophthalmol 246:719–728
23. Chong C, Suzuki T, Totsuka K, Morosawa A, Sakai T (2009) Large coherence length swept source for axial length measurement of the eye. Appl Opt 48:144–150
24. Wagner JA, Edwards A, Schuman JS (2004) Characterization of uveoscleral outflow in enucleated porcine eyes perfused under constant pressure. Invest Ophthalmol Vis Sci 45:3203–3206
25. Bertschinger DR, Beknazar E, Simonutti M, Safran AB, Sahel JA, Rosolen SG, Picaud S, Salzmann J (2008) A review of in vivo animal studies in retinal prosthesis research. Graefes Arch Clin Exp Ophthalmol 246:1505–1517
26. Pandav S, Morgan WH, Townsend R, Cringle SJ, Yu DY (2008) Inability of a confocal scanning laser doppler flowmeter to measure choroidal blood flow in the pig eye. Open Ophthalmol J 2:146–152
27. Agopov M, Lomb L, La Schiazza O, Bille JF (2009) Second harmonic generation imaging of the pig lamina cribrosa using a scanning laser ophthalmoscope-based microscope. Lasers Med Sci 24:787–792
28. Gu P, Harwood LJ, Zhang X, Wylie M, Curry WJ, Cogliati T (2007) Isolation of retinal progenitor and stem cells from the porcine eye. Mol Vis 13:1045–1057
29. Beattie JR, Brockbank S, McGarvey JJ, Curry WJ (2007) Raman microscopy of porcine inner retinal layers from the area centralis. Mol Vis 13:1106–1113
30. Fang IM, Yang CH, Yang CM, Chen MS (2009) Overexpression of integrin alpha6 and beta4 enhances adhesion and proliferation of human retinal pigment epithelial cells on layers of porcine Bruch's membrane. Exp Eye Res 88:12–21
31. Kiilgaard JF, Prause JU, Prause M, Scherfig E, Nissen MH, la Cour M (2007) Subretinal posterior pole injury induces selective proliferation of RPE cells in the periphery in in vivo studies in pigs. Invest Ophthalmol Vis Sci 48:355–360
32. Ng YF, Chan HH, Chu PH, To CH, Gilger BC, Petters RM, Wong F (2008) Multifocal electroretinogram in rhodopsin P347L transgenic pigs. Invest Ophthalmol Vis Sci 49:2208–2215
33. Annaka M, Okamoto M, Matsuura T, Hara Y, Sasaki S (2007) Dynamic light scattering study of salt effect on phase behavior of pig vitreous body and its microscopic implication. J Phys Chem B 111:8411–8418
34. Swindle KE, Hamilton PD, Ravi N (2008) In situ formation of hydrogels as vitreous substitutes: viscoelastic comparison to porcine vitreous. J Biomed Mater Res A 87:656–665
35. Peng YW, Hao Y, Petters RM, Wong F (2000) Ectopic synaptogenesis in the mammalian retina caused by rod photoreceptor-specific mutations. Nat Neurosci 3:1121–1127
36. Ninomiya H, Inomata T (2006) Microvascular anatomy of the pig eye: scanning electron microscopy of vascular corrosion casts. J Vet Med Sci 68:1149–1154
37. Klećkowska-Nawrot J, Dziegiel P (2007) Morphology of the third eyelid and superficial gland of the third eyelid on pig fetuses. Anat Histol Embryol 36:428–432
38. Klećkowska-Nawrot J, Dziegiel P (2008) Morphology of deep gland of the third eyelid in pig foetuses. Anat Histol Embryol 37:36–40
39. Olsen TW, Sanderson S, Feng X, Hubbard WC (2002) Porcine sclera: thickness and surface area. Invest Ophthalmol Vis Sci 43:2529–2532
40. Warfvinge K, Kiilgaard JF, Klassen H, Zamiri P, Scherfig E, Streilein W, Prause JU, Young MJ (2006) Retinal progenitor cell xenografts to the pig retina: immunological reactions. Cell Transplant 15:603–612

14.- ANEXO IV

Laukhin V, Sánchez I, Moya A, Laukhina E, Martin R, Ussa F, Rovira C, Guimera A, Villa R, Aguiló J, Pastor JC, Veciana J.

Non-invasive intraocular pressure monitoring with a contact lens engineered with a nanostructured polymeric sensing film.

Sensors and Actuators A. 2011; 170: 36-43.

Sensors and Actuators A 170 (2011) 36–43

Contents lists available at ScienceDirect

Sensors and Actuators A: Physical

journal homepage: www.elsevier.com/locate/sna

Non-invasive intraocular pressure monitoring with a contact lens engineered with a nanostructured polymeric sensing film

Vladimir Laukhin[a,b,*], Irene Sánchez[c,d], Ana Moya[d,e], Elena Laukhina[d,b], Raul Martin[c,d,f], Fernando Ussa[c], Concepció Rovira[b,d], Antón Guimera[d,e], Rosa Villa[d,e], Jordi Aguiló[d,e], José-Carlos Pastor[c], Jaume Veciana[b,d,*]

[a] Institució Catalana de Recerca i Estudis Avançats (ICREA), Catalunya, Spain
[b] Institut de Ciència de Materials de Barcelona (CSIC), Campus Universitari de Bellaterra, Cerdanyola E-08193 Barcelona, Spain
[c] IOBA-Eye Institute, University of Valladolid, Valladolid, Spain
[d] Networking Research Centre on Bioengineering, Biomaterials and Nanomedicine (CIBER-BBN), Zaragoza, Spain
[e] Institut de Microelectrònica de Barcelona (IMB-CNM, CSIC), Barcelona, Spain
[f] Department of Physics TAO – School of Optometry, University of Valladolid, Valladolid, Spain

ARTICLE INFO

Article history:
Received 27 January 2011
Received in revised form 10 May 2011
Accepted 13 May 2011
Available online 12 June 2011

Keywords:
Glaucoma
Pressure sensor
Nanostructured polymer composite
Contact lens
Intraocular pressure
In vitro experiments

ABSTRACT

A new prototype of contact lens sensor (CLS) for monitoring the intraocular pressure (IOP) variations in a non-invasive way has been developed. The CLS has as a key element a thin film, comprised of a new all-organic flexible highly piezo-resistive sensor, that is glued to the central hole of a doughnut-shaped hard contact lens. A few CLSs were fabricated and tested with an eye phantom and with enucleated pig eyes by means of applying pressure with a low pressure transducer and recording the electrical changes in the sensor with a portable recorder. The developed CLSs are biocompatible permitting to transmit the changes in cornea curvature induced by the IOP variations, directly to the flexible conducting polymeric sensor embedded in the CL. The electrical response of the CLS to pressure changes reveals a high linearity as well as a good reproducibility having the proper sensitivity to perform continuous monitoring of IOP.

1. Introduction

1.1. Glaucoma disease

Glaucoma is the second cause of irreversible blindness worldwide [1]. Its prevalence varies between 1 and 3% depending on the population studied and the diagnostic criteria [2,3]. Moreover, glaucomatous optic neuropathy leads to certain characteristic changes in the optic nerve head together with a visual field loss that is usually associated with an increase in the intra ocular pressure (IOP) with values above 21 mmHg [2]. Peeters et al. have quantified the effect of intraocular pressure reduction on the occurrence of glaucoma and have determined that each mmHg extra IOP reduction corresponds to a decrease in the relative risk of glaucoma conversion by 14% [4].

1.2. Glaucoma diagnosis and monitoring

Since one of the most important parameters in glaucoma diagnosis and treatment is the IOP, the primary goal in its treatment is to reduce the value of the IOP to prevent any optic nerve damage [5–7]. Hughes et al. [8] showed that monitoring IOP over 24 h may change the clinic management of 79% of patients with glaucoma.

So far, the only reliable method known to determine the IOP increase at any time of the day is to establish a 24 h tensional curve with the patient in a hospital environment [9]. Attempts to continuously monitor the IOP in a non-invasive way have been done, but mainly due to technical problems and/or lack of long-term stability none of the developed devices has been integrated into clinical practice [10–14]. Only Leonardi et al. have developed a marketable device, based on a hydrophilic CLS [15,16], which measures changes in cornea curvature due to IOP variations by means of a soft contact lens with a platinum-titanium strain gauge. In this device, the IOP

* Corresponding authors at: Institut de Ciència de Materials de Barcelona (CSIC), Campus Universitari de Bellaterra, Cerdanyola E-08193 Barcelona, Spain. Tel.: +34 935801853; fax: +34 935805729.
E-mail addresses: vladimir@icmab.es (V. Laukhin), vecianaj@icmab.es (J. Veciana).

0924-4247/$ – see front matter © 2011 Elsevier B.V. All rights reserved.
doi:10.1016/j.sna.2011.05.021

changes are transmitted to a Pt-based sensor through the deformation of the soft contact lens.

1.3. Design of a new device for continuous IOP monitoring

The discovery of ultra high piezo-resistive properties in flexible conducting all-organic bi-layer (BL) films [17] has enabled the design and fabrication of novel pressure sensing devices [18]. Such BL films consist of a polycarbonate film, which is covered on one of its sides with a very thin layer of nanostructured crystals of an organic molecular conductor; like the bis(ethylenedithio)tetrathiafulvalene (ET) charge-transfer salt β-$(ET)_2I_3$ [17]. The ultra high piezo-resistivity of such BL films resulted from the softness of the nanocrystals of the conducting salt [19], embedded on one side of the polymeric matrix, that are deformed under a small strain changing their conducting properties. This fact explains why the electrical resistance responses to strain of the BL films are three-to-ten times greater than those exhibited by conventional inorganic metals, like the Pt-based gauges, which have significantly harder crystal structures. Other advantages of using BL films as piezo-resistive materials are that they permit fabrication of strain sensitive active elements that are flexible and transparent. In addition, they can be easily glued over a hole of any configuration for fabricating pressure/deformation sensing devices [18]. All such characteristics made it feasible to fabricate a contact lens sensor (CLS) with such BL films for continuous monitoring of IOP variations [20]. In principle, CLSs made with this material would enable the detection of small changes in cornea curvatures, which are correlated to IOP alterations since it is well known that a change in IOP of 1 mmHg causes a deformation in the cornea curvature radius of 3 microns for a cornea with a total radius of 7.80 mm [21]. Such cornea curvature changes would be transmitted directly to the conducting layer of the BL film through the polymeric matrix underneath, which is in direct contact with the cornea. Moreover, with this CLS design it would be also possible not only to select different organic conductors with distinct electromechanical properties, but also to use alternative polymeric matrices with a wide variety of mechanical properties as well as conducting layers with different thickness levels opening the possibility to tune the performance of the CLS.

The purpose of this study was to provide a proof-of-concept demonstrating that a contact lens equipped with a BL film-based sensor has the capability to monitor in non-invasive way the changes in IOP and develop with them devices usable in clinical practice. Experiments have been carried out on an eye phantom as well as on enucleated pig eyes.

2. Experimental

2.1. Preparation of flexible highly piezo-resistive bi-layer film

A flexible highly piezo-resistive BL film, based on a polycarbonate [poly-(bisphenol-A-carbonate)] matrix containing a conducting top-layer of nanocrystals of the organic molecular metal β-$(ET)_2I_3$, as a sensing component, was prepared using the previously reported synthetic method [22,23]. The texture, structure and electromechanical properties of the prepared BL film, which were characterized by different spectroscopic and microscopic techniques as well as by monoaxial strain/resistance measurements, were identical to those reported by Laukhina et al. [18]. Round-shaped membranes with a thickness of 25 μm, a diameter of 5–7 mm and a mass of ca 1 mg were cut from a BL film sample and used for the CLS fabrication.

Table 1
Parameters of the fabricated CLSs designed according to the anatomical characteristics of pig eyes.

CLS	A	B	C[a]	D
Base radius (mm)	8.8	8.80	8.80	8.80
Base radius 1 (mm)	8.40	8.30	8.20	8.10
Base radius 2 (mm)	12.00	12.00	12.00	12.00
Ø Optic zone (mm)	7.50	7.50	7.50	7.50
Ø Base radius 1 (mm)	10.80	10.80	10.80	10.80
Total Ø (mm)	12.50	12.50	12.50	12.50
Power	0.00 D	0.00 D	0.00 D	0.00 D
Material	XO2	XO2	XO2	XO2
Sagital depth (mm)	2.35	2.37	2.39	2.41
Initial resistance (kΩ)	1.83	1.91	1.64	2.08
Sensitivity (Ω/mmHg)[b]	1.4	1.5	0.5	1.5

[a] Protected contact lens with a rigid cap piece (see text).
[b] Average values obtained from measurements performed over three years.

2.2. Biocompatibility testing of bi-layer films

The biocompatibility of the BL films was tested with a pathology study in six guinea pigs. An experienced surgeon made an interscapular incision and placed a small BL film sample under the skin in the left side and a silicone band (used for retinopexia) in the right side of guinea pigs. The wound was sutured with separated stitches using 7.0-Nylon monofilament. None of the animals showed any complication related to the procedure or infection in the wound site. After 20 days, the animals were sacrificed and a tissue sample was taken for a pathological study using the haematoxylin–eosin staining technique to compare the inflammatory reaction induced in adjacent tissues by the BL film versus the inflammation induced by the standard silicone band. All animals were anesthetised and treated according ARVO norms.

2.3. Fabrication of contact lens sensors

Gas permeable hard contact lenses, fabricated by Conoptica SL (Barcelona, Spain) with XO2 material, were used. CLs were designed and fabricated according to the anatomical characteristics of pig eyes, to ensure an adequate adaptation enabling the measurement of IOP changes (Table 1). Such gas permeable hard CLs were chosen because they have excellent oxygen permeability and are not deformed under hydration maintaining the sensing element tightly fixed. For the fabrication of the CLSs four doughnut-shaped hard contact lenses (Fig. 1) with holes (diameter of 3–4 mm) in its centre were used whose characteristics are given in Table 1. Round-membranes, based on the flexible highly piezo-resistive BL films, were cut and glued on the hole rims of the CLs using the polymerizable BF-2 glue. For the electrical connection, two annealed Pt-wires (diameter of 20 μm) were attached to the sensing layer of the BL film with graphite paste and they were further connected to two twisted copper wires (diameter of 50 μm). The electrical connections were configured as shown in Fig. 1 in order to produce

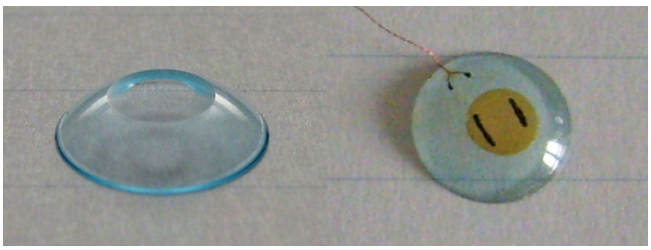

Fig. 1. Left: doughnut shaped hard CL used for fabricating the CLSs. Right: modified CL showing the slightly coloured BL film glued on the CL equipped with wire connections.

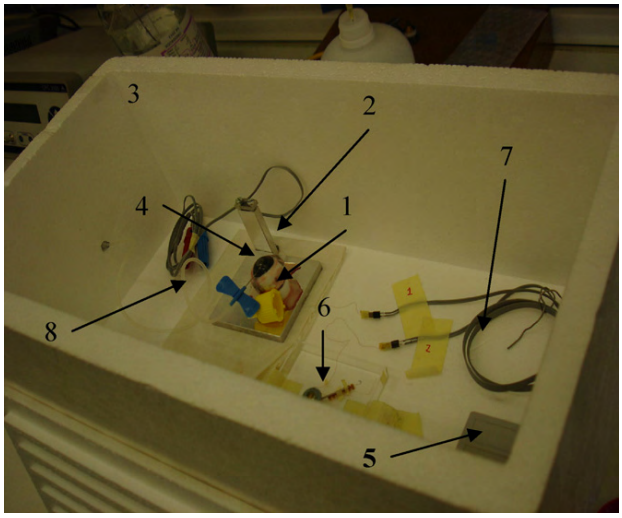

Fig. 2. Experimental setup used for "in vitro" measurements of IOP variations on enucleated pig eye. (1) Enucleated pig eye; (2) special support equipped with electrical connections; (3) thermo-insulating box; (4) the CLS used as the active sensing element; (5) portable recorder unit; (6) the CLS used as a temperature reference; (7) electrical connections; and (8) connection to a low pressure transducer.

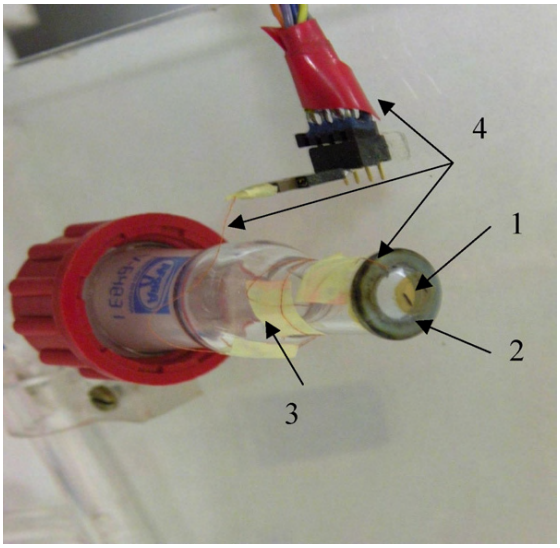

Fig. 3. Image of the eye-phantom developed for measuring electrical response of a CLS to pressure changes. (1) BL-based sensing film of the active CLS connected with two wires; (2) the active CLS; (3) glass adapter connecting the active CLS with the pressure line; and (4) electrical connections to record the electrical responses.

the minimum perturbation to the BL film. One of the fabricated CLSs was covered by an additional rigid "cap" piece, made of the same material as the hard contact lens, resulting in a device in which the external side of the sensing BL film and the delicate electric contacts were protected with a cap piece but the internal side of the BL film was in direct contact with the cornea. It was found that the four fabricated CLSs showed initial resistances in the absence of any deformation in the range of 1.6–2.1 kΩ and that the sensitivity, $\Delta R/\Delta P$, of the three unprotected CLSs was of 1.5 Ω/mmHg while that of the protected one showed a lower sensitivity of 0.5 Ω/mmHg.

2.4. Electronic measurements

A portable unit for long-term monitoring of CLS electrical responses was designed and fabricated according to the nominal resistance values of BL films. The structure of the portable unit was based on a special configuration of a Wheatstone bridge, where the sensor is emplaced in one of its branches (Scheme 1). The upper branches were formed by two variable current sources in order to make the zero adjustment. The other branch had a reference resistance that can be replaced by another BL membrane sensor, with the same characteristics as the sensing one. This reference resistance was located in a part that is not affected by pressure changes, in order to compensate for any temperature change effect. Moreover, to allow high precision measurements and to simplify the data acquisition, the circuit only measured the IOP variations, eliminating the absolute value of IOP, reducing the measurement scale and thus improving the measurement accuracy. This structure shall be integrated and must be ready to send data wirelessly. To enable data modulation, the measurement circuit converts the data into pulses with a system of integration and comparison.

2.5. Experimental set-up and procedure for measurements

To minimize temperature change effects during the measurements, the experiments were performed inside a closed camera made with expanded polyurethane as a thermal insulator (Fig. 2). In order to suppress at the maximum level all possible influences of the temperature variation on the electrical response of a CLS, the measurements were performed using a Wheatstone bridge configuration enabling the compensation of any temperature change effects. CLS D was used as a temperature reference in some experiments.

2.5.1. Set-up for calibration of contact lens sensors

Before proceeding with in vitro experiments, the electrical responses of the fabricated CLSs to pressure changes on an eye-phantom were tested. Pressure was induced by a low pressure transducer (WIKA CPC 2000), enabling to increase, decrease and/or maintain of the pressure, recording the data in a personal computer (PC). The range of pressure changes was from 0 to 22 mmHg. The eye-phantom equipped with the CLS (Fig. 3) was installed inside a thermo-insulated box and it was connected with both the low pressure transducer and the portable recorder unit. In some experiments, a temperature reference CLS was also mounted inside the box and connected to the recorder unit. The electrical responses of the active CLS to pressure changes were monitored by the portable recorder unit connected with a PC via a Bluetooth link.

2.5.2. Experiments with a enucleated pig eyes

The pig eyes were collected in a local slaughterhouse immediately after the sacrifice of the animals whose age ranged between 6 and 8 months. After enucleating, the pig eyes were always kept immersed in DMEM culture medium supplemented with antibiotic/antimicotic mixture (Gibco, UK) and in ice to prevent their degradation. The pig eye was embedded on a special support installed inside a thermo-insulating box, as shown in Fig. 2. A 23G cannula was inserted at 3.5 mm from the sclerocorneal limbus and a Ringer lactate solution was injected through a tube connected to a low pressure transducer (WIKA CPC 2000), as shown in Fig. 4. The pressure working range was from 20 to 50 mmHg, taking into account the data previously measured with a tonometer [24], which corresponds to a pressure range from 7 to 32 mmHg. The active CLS was placed on the ocular surface of the porcine eye, hydrated with distilled water, and connected to the portable recorder unit that was also located inside the thermo-insulating box. The temperature reference CLS was also mounted in the box and connected to the portable recorder unit (see Figs .2 and 4).

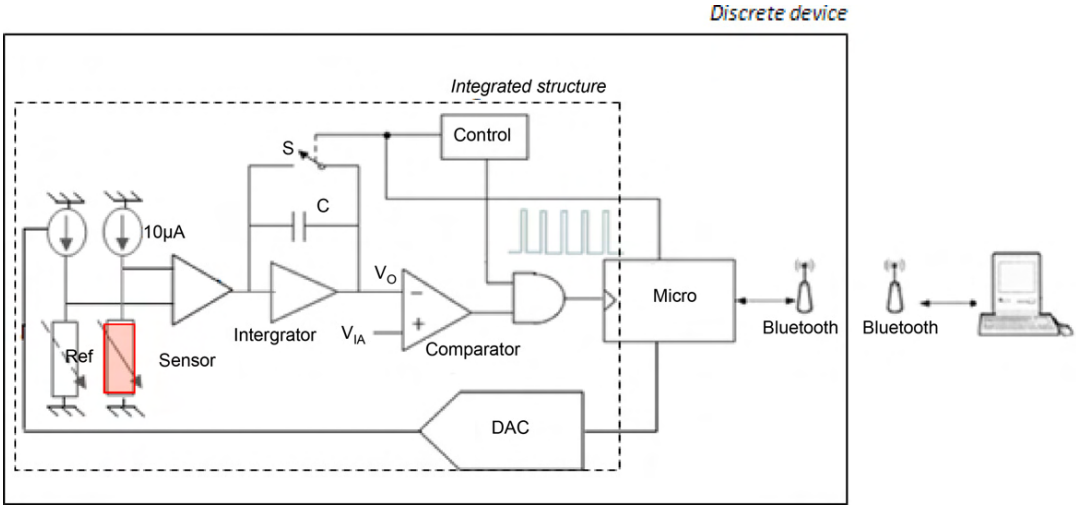

Scheme 1. Electronic configuration of the portable unit used for the measurements.

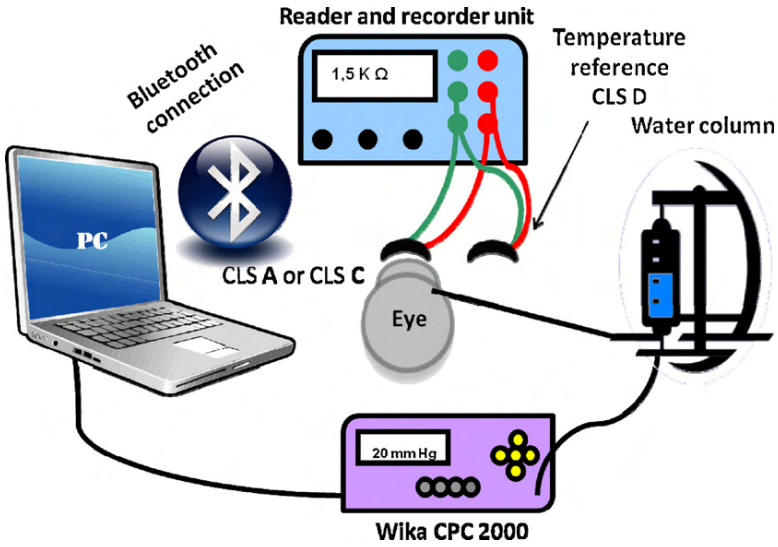

Fig. 4. Setup used for testing the CLS on an enucleated pig eye.

3. Results and discussion

3.1. Calibration of contact lens sensors

Before proceeding to test the developed CLSs with enucleated pig eyes their electrical responses to pressure changes were studied using an eye-phantom (Fig. 3). This configuration permitted to test the responses of CLSs independently of particular peculiarities in the biomechanical properties of the pig eye corneas that may produce misleading results. During these experiments, static gas pressure was applied, using a step-by-step procedure, directly to the CLS from 0 to 20 mmHg for the first two cycles and from 0 to 22 mmHg for the third cycle using pressure changes of 2 mmHg at each step (Fig. 5) and the electrical response of the CLS was recorded continuously with the portable recorder unit.

As shown in Fig. 5, the tested CLS follows nicely the pressure changes produced by the transducer. These measurements also demonstrate that under a constant pressure, such as 10 mmHg, the resistance value of CLS remains almost constant with a slight increase during 20 min, although this resistance drift is significantly lower than the sensor response to a pressure change of 2 mmHg.

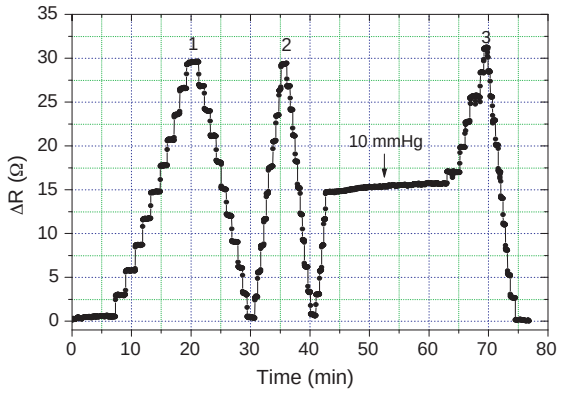

Fig. 5. Electrical response of the CLS B to step-by-step static pressure changes produced by the low pressure transducer. Each step up and down corresponds to a change of 2 mmHg.

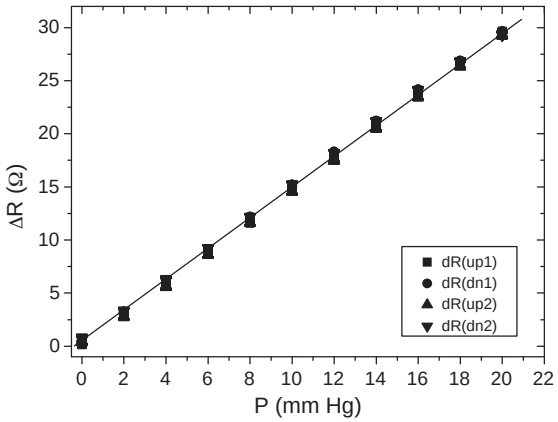

Fig. 6. Electrical response of CLS B to pressure changes using a low pressure transducer. Data were collected from the first and second up–down sweeps shown in Fig. 5.

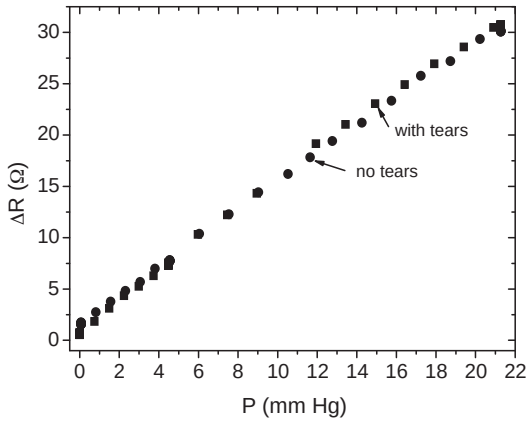

Fig. 8. Electrical responses of CLS B to pressure changes made under artificial tears (squares) and in air (circles).

After this cyclic pressure loading, the resistance of CLS recovers its initial value. Interestingly, the small spikes down appearing at the third load cycle resulted from a pressure leak in the pressure line since they disappeared when the pressure leak was eliminated.

In Fig. 6 the electrical resistance data collected for the first and the second up–down sweeps of Fig. 5 are plotted versus the nominal pressure at which they were collected. This plot shows that the electrical response of the CLS to pressure changes has a high linearity, as well as a good reproducibility, exhibiting a large sensitivity of 1.5 Ω/mmHg. Therefore, the developed CLS used to monitor pressure changes fulfils all requirements to control IOP fluctuations in humans.

3.2. Biocompatibility of the sensing bi-layer films

Since the ultimate goal of this study is to use the CLS to measure IOP variation in humans, it is necessary to know the biocompatibility of the BL film. For this purpose a biocompatibility study was conducted with six guinea pigs. The histological study showed less inflammatory reaction in the BL film site than to the silicone band (Fig. 7) in all samples of tissues. So, this BL film has a higher biocompatibility than a standard silicone band used in conventional eye surgery.

3.3. Effect of physiological media on contact lens sensor responses

The stability of the sensor under the physiological conditions of eyes was also studied using artificial tears. To study the effect of such a medium, the calibrated CLSs B and D (temperature reference) were completely covered with artificial tears and multi-cyclic pressure loading experiments, similar to those made for the calibration of CLS B (Figs. 5 and 6), were carried out. Fig. 8 shows the electrical response of CLS B covered with artificial tears to applied pressure. For comparison purposes, the experimental data collected during the calibration test of CLS B (Fig. 6) are also presented in Fig. 8. As it is clearly seen, the presence of a physiological fluid has no influence on the electrical responses of the CLS to pressure changes.

As a final remark, it should be emphasized that a physiological fluid, like artificial tears, are able to affect the sensing properties of the CLS but only if the liquid are left to be dried. This occurs because the resulting crystallized salts damage the BL film producing micro- and nano-cracks on the surface of the sensing BL film, as shown in Fig. 9. To prevent undesirable salt crystallization on the surface of the BL film, water ablutions after every test have to be done. Indeed, when the CLS was rinsed twice with distilled water, the crystallites of the salt disappeared (Fig. 9). Therefore, rinsing the used CLS with water after measurements permits to recover the functionality of the CLS. This procedure is important for developing a protocol of multiple applications of the CLSs.

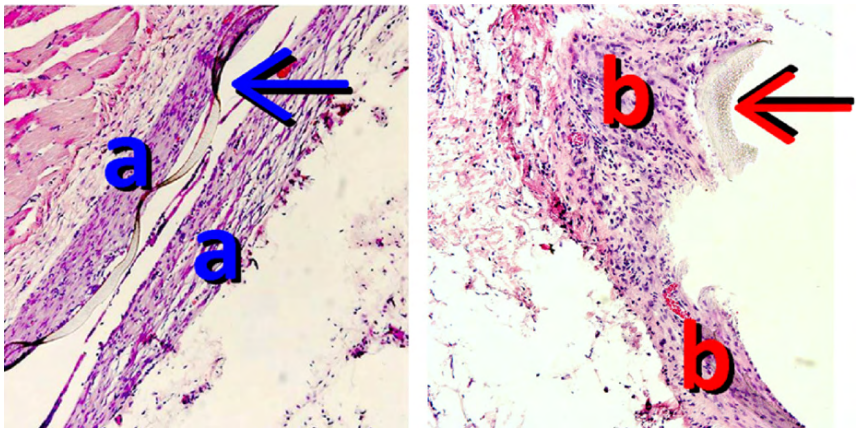

Fig. 7. Haematoxylin–eosin staining of the tissues adjacent to the sensing BL film and to the silicon band. Left: the BL film (arrow) is surrounded by a thin fibrous capsule (a) with occasional lymphocytes. There is no foreign body giant cell reaction or significant inflammatory response (original magnification 10×). Right: the silicone band (arrow) is surrounded by a fibrous capsule and a moderate mixed inflammatory infiltrate composed of lymphocytes with presence of occasional polymorphonuclear leukocytes (b) (original magnification 10×).

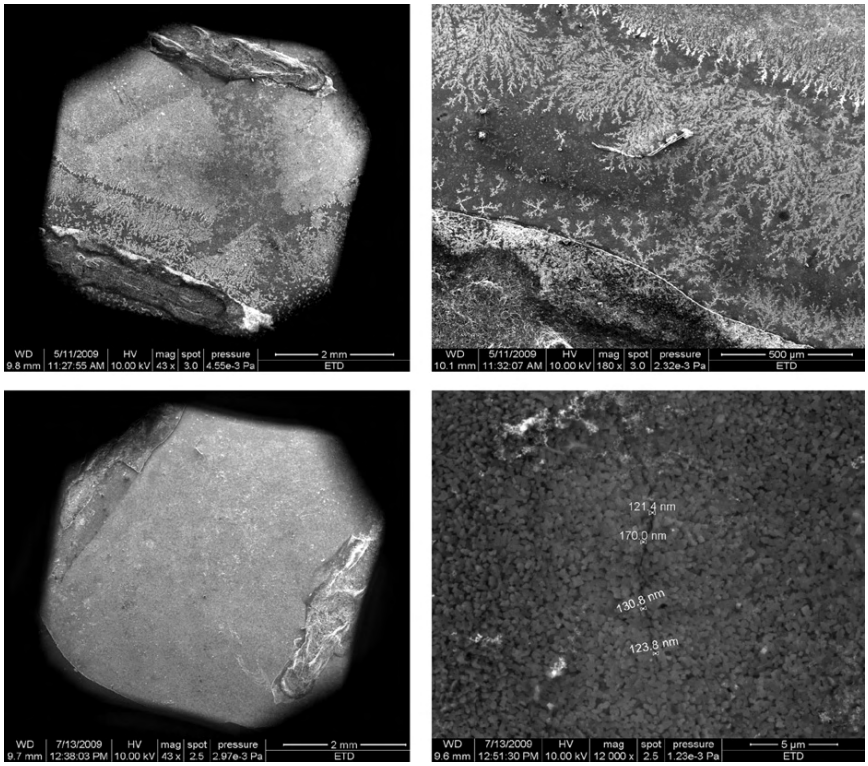

Fig. 9. SEM images at different magnifications collected from a BL film of a CLS. Top: images obtained after drying several times the artificial tears on the membrane. Bottom: images after rinsing twice the membranes shown on top images with distilled water.

3.4. *"In vitro" measurements of IOP variations with contact lens sensors*

The "in vitro" measurements of IOP variations were carried out on 15 ennucleated pig eyes using the fabricated CLSs. The measurements were always conducted within 4 h after the sacrifice of the animal to preserve the elastic properties of the ocular tissues. In these experiments, the CLSs responded well to pressure changes induced in enucleated pig eyes by injecting a Ringer lactate aqueous solution. Because the bio-mechanical properties of the corneas varied significantly from one pig eye to another, a previous calibration of the attained pressure values for each studied eye was performed. For that, two calibration points were measured with a conventional tonometer for each studied eye to get the correspondence between the CLS responses to the actual IOP values. Fig. 10 shows a representative example of the experimental data obtained using the protected CLS.

The static pressure was applied in such experiments to an enucleated pig eye by means of a step-by-step procedure in five different sweeps showing that the CLS responds with a well-defined electrical signal proportional to the pressure changes in the eye. Data were also collected for all the five up–down pressure sweeps and the resistance responses versus the nominal pressures were plotted showing a dependence with a slight deviation from linearity (Fig. 11). Such a slight deviation can be attributed to the biomechanical properties of the pig cornea that transmits the IOP to the sensing element of the CLS in a non-linear fashion. It is worth noticing that the sensitivity of the protected CLS, which has the advantage that facilitates its manipulation, was somewhat smaller (0.5 Ω/mmHg) than that for the non-protected CLSs (1.5 Ω/mmHg). This decrease in sensitivity results from the increasing of the hardness of the frame of the polymeric sensor produced by its protection. Nevertheless, the response of the protected device is good enough to control IOP in the desirable range. Finally, it was also demonstrated that the presence of artificial tears, which was replenished periodically, over the CLS measured on the enucleated pig eye does not have any significant effect on the responses of the CLSs.

For monitoring IOP in humans it shall be necessary to develop improved and more user friendly prototypes of CLSs than those reported here. Indeed, the measurement electronics of the prototypes should have to take care of conditioning the signal from the pressure sensor embedded in the lens, digitalizing it and transmitting data to an external device. This can be done by embedding the electronics in the CLS in order to avoid possible patient discomfort due to the presence of any wires from/to the CLS. In addition, the measured data must be transmitted to a data acquisition system

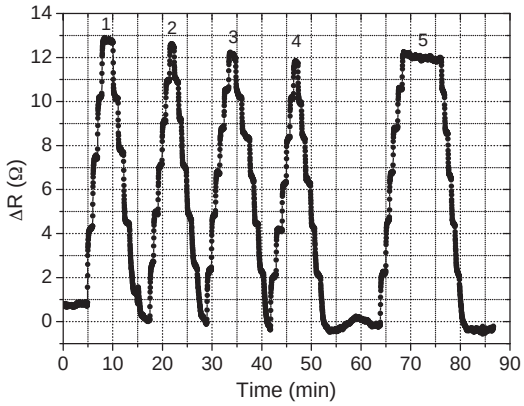

Fig. 10. Electrical response of CLS C to IOP changes made in an ennucleated pig eye. Each step of the first sweep corresponds to a pressure change of 7.5 mmHg whereas for the other four sweeps the changes correspond to 5 mmHg.

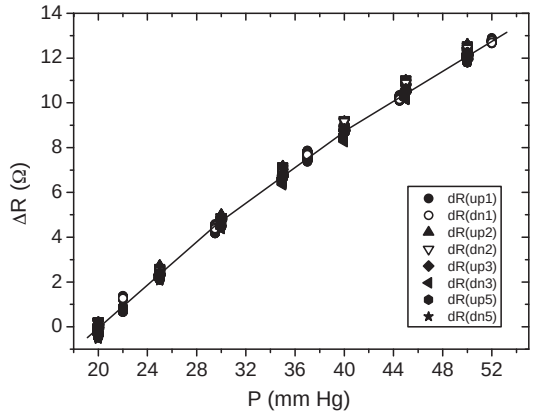

Fig. 11. Electrical response of the CLS C to IOP pressure changes in an enucleated pig eye produced by using a low pressure transducer. Data were collected from the five up–down sweeps shown in Fig. 10.

wirelessly. On the other hand, due to the reduced area available on the CLS, the system cannot be battery powered. This also needs a wireless energy transmission system. The wireless power transmission imply the design of very small and low power measurement electronics that can be only achieved by the development of an Application Specific Integrated Circuit (ASIC) [25]. Presently, we are developing such improved devices as well as performing further work addressed to manufacture short series of CLSs including the gluing of the BL sensing films on the CL and the machining and embedding the contacts and electronic components on the final devices.

4. Conclusions and perspectives

In conclusion, this study validates an alternative approach for continuous monitoring of IOP changes. The developed prototype of CLS permits to transmit the changes in cornea curvature, which are correlated with the IOP, directly to the flexible conducting polymeric sensing bi-layer film embedded in the CL exhibiting an adequate sensitivity to perform continuous monitoring of the IOP changes. The device reported here benefits from the intrinsic advantages of BL films, such as transparency, flexibility, and high sensitivity to deformation, and will permit to develop different CLSs with different performances in order to obtain devices usable in clinical practice.

In the future, this may allow the development of a CLS that will be non-invasive, anaesthesia-free, enabling continuous monitoring of the IOP changes for long periods of time. This sensing device will allow patients to perform their usual activities because it should not interfere with patient vision. Accordingly, such a device is highly promising for the diagnosis and treatment of glaucoma.

Acknowledgements

The research was granted by CIBER-BBN – an initiative funded by the VI National R&D&i Plan 2008–2011, Iniciativa Ingenio 2010, Consolider Program, CIBER Actions and financed by the Instituto de Salud Carlos III with assistance from the European Regional Development Fund-, the Generalitat de Catalunya, under the framework of "Programa Operatiu FEDER de Catalunya" through contract VALTEC09-1-0030 and project SGR2009-516, the European Union Large Project ONE-P (FP7-NMP-2007-212311), the DGI, Spain, projects CTQ2006-06333/BQU and CTQ2010-19501/BQU. Also we would like to thank Conoptica SL for supplying and machining the doughnut-shaped rigid contact lenses and to Prof. Feral Temelli for correcting the manuscript.

References

[1] S. Resnikoff, D. Pascolini, D. Etya'ale, I. Kocur, R. Pararajasegaram, G.P. Pokharel, S.P. Mariotti, Global data on visual impairment in the year 2002, Bull. World Health Organ. 82 (2004) 844–851.
[2] V.C. Sung, J.M. Koppens, S.A. Vernon, P. Pawson, M. Rubinstein, A.J. King, C.L. Tattersall, Longitudinal glaucoma screening for siblings of patients with primary open angle glaucoma: the Nottingham Family Glaucoma Screening Study, Br. J. Ophthalmol. 90 (2006) 59–63.
[3] A. Raychaudhuri, S.K. Lahiri, M. Bandyopadhyay, B.C. Foster, P.J. Reeves, G.J. Johnson, A population based survey of the prevalence and types of glaucoma in rural West Bengal: the West Bengal Glaucoma Study, Br. J. Ophthalmol. 89 (2005) 1559–1564.
[4] A. Peeters, C.A.B. Webers, M.H. Prins, M.P. Zeegers, F. Hendrikse, J.S.A.G. Schouten, Quantifying the effect of intraocular pressure reduction on the occurrence of glaucoma, Acta Ophthalmol. 88 (2010) 5–11.
[5] A.M. Rota-Bartelink, A. Pitt, I. Story, Influence of diurnal variation on the intraocular pressure measurement of treated primary open angle glaucoma during office hours, J. Glaucoma 5 (1996) 410–415.
[6] A.G. Konstas, D.A. Mantziris, W.C. Stewart, Diurnal intraocular pressure in untreated exfoliation and primary open-angle glaucoma, Arch. Ophthalmol. 115 (1997) 182–185.
[7] S. Asrani, R. Zeimer, J. Wilensky, D. Gieser, S. Vitale, K. Lindenmuth, Large diurnal fluctuations in intraocular pressure are an independent risk factor in patients with glaucoma, J. Glaucoma 9 (2000) 134–142.
[8] E. Hughes, P. Spry, J. Diamond, 24-Hour monitoring of intraocular pressure in glaucoma management: a retrospective review, J. Glaucoma 12 (2003) 232–236.
[9] A.G. Konstas, N. Mylopoulos, C.H. Karabatsas, et al., Diurnal intraocular pressure reduction with latanoprost 0.005% compared to timolol maleate 0.5% as monotherapy in subjects with exfoliation glaucoma, Eye 18 (2004) 893–899.
[10] D.M. Maurice, A recording tonometer, Br. J. Ophthalmol. 42 (1958) 321–335.
[11] M.E. Greene, B.G. Gilman, Intraocular pressure measurement with instrumented contact lenses, Invest. Ophthalmol. 13 (1974) 299–302.
[12] M.L. Wolbarsht, J. Wortman, B. Schwartz, D. Cook, A scleral buckle pressure gauge for continuous monitoring of intraocular pressure, Int. Ophthalmol. 3 (1980) 11–17.
[13] R.W. Flower, A.E. Maumenee, E.A. Michelson, Long-term continuous monitoring of intraocular pressure in conscious primates, Ophthalmic Res. 14 (1982) 98–106.
[14] B. Svedbergh, Y. Bäcklund, B. Hök, L. Rosengren, The IOP-IOL. A probe into the eye, Acta Ophthalmol. 70 (1992) 266–268.
[15] M. Leonardi, P. Leuenberger, D. Bertrand, A. Bertsch, P. Renaud, First steps toward noninvasive intraocular pressure monitoring with a sensing contact lens, Invest. Ophthalmol. Vis. Sci. 45 (2004) 3113–3117.
[16] M. Leonardi, E.M. Pitchon, A. Bertsch, P. Renaud, A. Mermoud, Wireless contact lens sensor for intraocular pressure monitoring: assessment on enucleated pig eyes, Acta Ophthalmol. 87 (2009) 433–437.
[17] E. Laukhina, R. Pfattner, L.R. Ferreras, S. Galli, M. Mas-Torrent, N. Masciocchi, V. Laukhin, C. Rovira, J. Veciana, Ultrasensitive piezoresistive all-organic flexible thin films, Adv. Mater. 22 (2010) 977–991.
[18] E. Laukhina, M. Mas-Torrent, C. Rovira, J. Veciana, V. Laukhin, Organic sensor device for e.g. molecular electronics, has layer of organic material having conductive salt or complex including molecule and dopant, and base substrate provided in close contact with layer of organic material, P200602887 (WO2008059095), Spain, 2006.
[19] R. Kondo, M. Higa, S. Kagoshima, H. Hoshino, T. Mori, H. Mori, Electrical and structural properties of θ-type BEDT-TTF organic conductors under uniaxial strain, J. Phys. Soc. Jpn. 75 (2006) 044716–44717.
[20] V. Laukhin, C. Rovira, E. Laukhina, J. Veciana, M. Mas-Torrent, A. Quimera Brunet, J. Aguiló Llobet, R. Villa Sanz, J.C. Pastor, F. Ussa, Truncated contact lens for use in telemetry system, has truncation plane provided parallel to base of lens, and centrally placed polymer nanocomposite material joined to perimeter of truncated zone, Patent: ES2330405-A1; WO2009147277-A1, 2009.
[21] A.K. Lam, W.A. Douthwaite, The effect of an artificially elevated intraocular pressure on the central corneal curvature, Ophthalmic Physiol. Opt. 17 (1997) 18–24.
[22] E. Laukhina, J. Ulanski, A. Khomenko, S. Pesostskii, V. Tkachev, L. Atovmyan, E. Yagubskii, C. Rovira, J. Veciana, J. Vidal-Gancedo, V. Laukhin, Systematic Study of the $(ET)_2I_3$ reticulate doped polycarbonate films: structure, ESR, transport properties and superconductivity, J. Phys. I France 7 (1997) 1665–1675.
[23] E. Laukhina, V. Tkacheva, R. Shibaeva, S. Khasanov, C. Rovira, J. Veciana, J. Vidal-Gancedo, A. Tracz, J.K. Jeszka, A. Sroczynska, R. Wojciechowski, J. Ulanski, V. Laukhin, New conducting molecular metal polycarbonate bilayered composites: $(ET)_2IBr_2$/PC-, $(BET)_2IBr_2$/PC- and $(BET)_2I_3$/PC-films, Synth. Met. 102 (1999) 1785–1786.

[24] M. Shimmyo, A.J. Ross, A. Moy, R. Mostafavi, Intraocular pressure Goldmann applanation tension, corneal thickness, and corneal curvature in Caucasians, Asians, Hispanics, and African Americans, Am. J. Ophthalmol. 136 (2003) 603–613.
[25] R. Durà, F. Mathieu, L. Nicu, F. Pérez-Murano, F. Serra-Graells, A 0.3 mW/Ch 1.25 V piezo-resistance digital ROIC for liquid dispensing MEMS, IEEE Trans. Circuits Syst.-I 56 (2009) 957–965.

Biographies

Vladimir Laukhin graduated as physicist at the Moscow Institute of Physics and Technology in 1969 and earned PhD (Physics) in 1975 at the Institute of Problems of Chemical Physics of Russian Academy of Sciences, where he was working until 2001. Since 2001 he is ICREA Research Professor at *Institut de Ciència de Materials de Barcelona* (CSIC). His research interest has long centred on physics of conducting/superconducting molecular organic materials, with particular emphasis on their electronic and magnetic properties. In the past few years his main efforts have been devoted to a new generation of plastic electronic devices, based on multifunctional organic molecular conductors, to be used for fabrication of very sensitive flexible strain/pressure/temperature sensors and electronic circuits.

Irene Sánchez is a registered Spanish optometrist OD(EC) with a Master degree in visual sciences (M.Sc.). Presently belongs to the Networking Research Centre on Bioengineering, Biomaterials and Nanomedicine (CIBER-BBN), Zaragoza Spain and is working at the Unit of Glaucoma in the IOBA Eye Institute.

Ana Moya received the M.Sc. degree in telecommunications engineering from the Universitat Autònoma de Barcelona, Spain, in 2008. She has been working with the Mico-Nano-Bio Integrated Systems Group in the Institut de Microelectrònica de Barcelona, Centro Nacional de Microelectrónica (IMB-CNM, CSIC), Spain, since 2008, contracted by CIBER-BBN. Specialized in electronic systems, her current researches interested are focused on design and development of electronic systems for biomedical applications.

Elena Laukhina graduated as a chemist in 1975 and obtained her PhD in 1979 from the D. Mendeleyev University of Chemical Technology of Russia, Moscow; in 1979 she moved to the Institute of Chemical Physics of Russian Academy of Science (Chernogolovka) where she was promoted to Senior Researcher in 1999. Since 2007 she is Titular Scientist-Researcher of "El Centro de Investigación Biomédica en Red en Bioingeniería, Biomateriales y Nanomedicina", ICMAB-CSIC, Spain. Her research interest focuses on organic molecular metals and superconductors and developing flexible lightweight materials for electronic application.

Raul Martin is a registered Spanish optometrist OD(EC) with a Master degree in visual sciences (M.Sc.) and he got a PhD degree at the University of Valladolid. Presently he is a teacher of optometry and contact lens in the School of Optometry (University of Valladolid) and is also the optometry head of the IOBA Eye Institute.

Fernando Ussa graduated as Bachelor of Medicine and Surgery in 1991 at the National University of Colombia (Bogotá) and obtained the Degree of specialist in ophthalmology at the Pontifical Xaveriana University of Colombia in 1999. He has been observer fellow in Moorfields Hospital (London, UK) at the glaucoma unit with a clinical attachment at the Southern General Hospital from the University of Glasgow. He got a Master in Glaucoma in 2003 and a Master of Science (M.Sc.) in 2007 from the University of Valladolid. Since 2003 he is the director of the Glaucoma Unit at IOBA, and a honorary instructor of the Department of Surgery of the University of Valladolid. His research area comprehends glaucoma clinical trials, glaucoma genetics and glaucoma devices for diagnosis.

Concepció Rovira Received her PhD degree on Chemistry from the University of Barcelona in 1977. She was a postdoctoral fellow in 1982/1983 at The Johns Hopkins University with Dwaine O. Cowan where she entered in the field organic metals. She was appointed at the CSIC in 1987, and in 1991 she moved to the Institut de Cie'ncia de Materials de Barcelona (CSIC), where was promoted to Full Professor in 2004. Her research interests focus on molecular functional materials and molecular nanoscience and, in particular, in the fields of organic electronics, electron-transfer phenomena, and molecular self-assembly and recognition.

Antón Guimera received the M.Sc. degree in electronic engineering from the Autònoma University of Barcelona in 2006. He joined the Design Department of the National Microelectronics Center (CNM-CSIC) at 2000 as technical engineer. Now, he is working in his PhD based on the study of the corneal barrier function by means of impedance measurements. His research interest fields are the design of electronic systems for biomedical applications and the study of the passive electrical properties of biological tissues.

Rosa Villa Medicine Doctor by the Universitat de Barcelona (1981), and PhD by the Universitat Autonoma de Barcelona (1993). Specialized in nuclear medicine, she had the Spanish National award on Nuclear Medicine in 1985. She joined the Design Department of the National Microelectronics Center (CNM-CSIC) at 1986 where she became researcher at 1992. Now, she belongs to the Biomedical Applications Group Board at the CNM. Her current research interest fields are in the microsystem biomedical applications mainly in the neural stimulation area and in the use of neural networks and fuzzy logic for the definition of clinical prediction areas where she has actively participated in many research projects.

Jordi Aguiló PhD in Physics in 1976, he joined the Computer Science Department, holding a Full Professor position in Computer Technology and Architecture since 1987. In 1985 he became researcher at the Design Department of the Microelectronics National Center (IMBCNM) that lead up to 1997. He is now leading the postgraduate studies at the Microelectronics and Electronic Systems Department at the UAB, coordinating the Biomedical Applications Group from IMB-UAB and the GBIO Group within the CIBER-BBN. His research interest fields are the Micro and Nano System's mainly focusing Biomedical Applications such as Advanced Multi-Micro-Nanosensors, Neural interfaces and Monitoring devices up to Converging Technologies devices and systems.

José-Carlos Pastor Graduated as a MD in 1974 obtained the PhD degree in 1975 by the Navarra's University in Spain. Specialist in Ophthalmology since 1976. In 1979 moved to Santiago de Compostela as Full Professor (Agregado) and Chief of Ophthalmology at the University Hospital. In 1981 moved to Valladolid University as Full Professor (Catedratico) and Chairman of Ophthalmology at the University Hospital. Since 1987–1991 was Vice-Chancelor of Research of the whole University. He founded the IOBA (Eye Institute) of the Valladolid University in 1989. Director of IOBA since 1991. Director of the Spanish Journal of Ophthalmology since 1995–2000. His research interest focuses on glaucoma, retinal detachment, cell therapy and other advanced therapies for retinal diseases, and Intraocular inflammation and scarring.

Jaume Veciana was graduated as a chemist in 1973 and obtained the PhD degree in 1977 from the University of Barcelona (Spain) working in physical organic chemistry. In 1991 he moved to the *Institut de Ciència de Materials de Barcelona* (CSIC) where was promoted to Full Professor in 1996. Since 2004 he is the Director of the *Department of Molecular Nanoscience and Organic Materials* of the same Institute. His research interest focuses on molecular functional materials and molecular nanoscience and in particular in the fields of molecular magnetism, molecular spintronics, and in the processing of molecular compounds as particles and on surfaces for biomedical applications.

15.- ANEXO V

Moya A, Guimerà A, Sánchez I, Laukin V, Martin R, Ussa F, Laukhina E, Rovira C, Veciana J, Pastor JC, Villa R, Aguiló J.

Discrete portable measuring device for monitoring noninvasive intraocular pressure with a nano-structured sensing contact lens prototype.

International Journal of E-Health and Medical Communications. 2011; 2: 1-19.

Discrete Portable Measuring Device for Monitoring Noninvasive Intraocular Pressure with a Nano-Structured Sensing Contact Lens Prototype

Ana Moya, CIBER-BBN and IMB-CNM (CSIC), Spain

Antón Guimerà, CIBER-BBN and IMB-CNM (CSIC), Spain

Irene Sánchez, CIBER-BBN and University of Valladolid, Spain

Vladimir Laukin, ICREA and CSIC, Spain

Raúl Martin, CIBER-BBN and University of Valladolid, Spain

Fernando Ussa, University of Valladolid, Spain

Elena Laukhina, CIBER-BBN and CSIC, Spain

Concepció Rovira, CIBER-BBN and CSIC, Spain

Jaume Veciana, CIBER-BBN and CSIC, Spain

José-Carlos Pastor, University of Valladolid, Spain

Rosa Villa, CIBER-BBN and IMB-CNM (CSIC), Spain

Jordi Aguiló, CIBER-BBN and IMB-CNM (CSIC), Spain

ABSTRACT

A new portable measuring device for monitoring intraocular pressure with a non invasive system using a prototype of contact lens has been developed. The contact lens is based on a new organic flexible highly piezo-resisitive film sensor that is glued to the central hole of a lens. The measuring system is wire connected to the contact lens and incorporates user interface methods and a Bluetooth link for bi-directional wireless data transfer. The key design aspects of such architecture are discussed in this paper. The system is designed with an architecture that can be integrated in the future in order to be placed in the contact lens. The discrete system is used to validate the electronic measurement operation and the contact lens sensor (CLS). The measurement instrument can calibrate the differences of the nominal value of the sensor and measure resistances variations that are related to pressure variations. The measuring system and the contact lens sensor were tested with an eye phantom and with enucleated pig eyes by applying pressure changes between 7 to 32 mmHg recording the electrical changes with the portable device.

Keywords: *Contact Lens, Glaucoma, Handheld Device, Intraocular Pressure, Pressure Sensor*

DOI: 10.4018/jehmc.2011100101

INTRODUCTION

Glaucoma is the second cause of irreversible blindness worldwide (Resnikoff et al., 2004). Its prevalence varies between 1 and 3% depending on population studied and the diagnostic criteria (Raychaudhuri et al., 2005; Sung et al., 2006). Moreover, glaucomatous optic neuropathy leads to certain characteristic changes in the optic nerve head together with a visual field loss that is usually associated with an increase in the intra ocular pressure (IOP) with values superior to basal ones, 21 mmHg (Sung et al., 2006). One of the most important parameters in glaucoma diagnosis is the IOP measurement and for the treatment of this disease the decrease of this IOP value is needed, to prevent the optic nerve damage (Asrani et al., 2000; Konstas, Mantziris, & Stewart, 1997; Rota-Bartelink, Pitt, & Story, 1996). Hughes et al. (2003) showed that punctual IOP measurements are not valid for glaucoma diagnosis demonstrating with a 24 h clinical monitoring that this value changes in an incident rate of 79.3% patients with glaucoma.

At the moment the only reliable method known to determine the IOP tensional curve is to perform continuous punctual measurements during 24 hours (Konstas, Mylopoulos, & Karabatsas, 2004). Due to the complexity of this method, the patient is forced to be admitted in a hospital during a day. Several attempts to enable a non-invasive IOP control with continuous monitoring have been done, however none of the developed devices have been integrated into clinical practice mainly due to technical problems and lack of long-term measurements stability (Flower, Maumenee, & Michelson, 1982; Greene & Gilman, 1974; Maurice, 1958; Svedbergh, Bäcklund, Hök, & Rosengren, 1992; Wolbarsht, Wortman, Schwartz, & Cook, 1980). Leonardi et al. has developed a marketable prototype based on a hydrophilic CLS, (Leonardi, Leuenberger, Bertrand, Bertsch, & Renaud, 2004; Leonardi, Pitchon, Bertsch, Renaud, & Mermoud, 2009) which measures deformations of the eyeball (changes in cornea curvature) due to IOP variations. This device is embedded in a soft contact lens with a platinum-titanium strain gauge. The IOP changes of this device are transmitted to a Pt-based sensor through the deformation of the soft contact lens.

The discovery of ultra high piezo-resistive properties in flexible conducting all-organic bi-layer (BL) films (Laukhina et al., 2010) has enabled the design and fabrication of novel pressure sensor devices (Laukhina, Mas-Torrent, Rovira, Veciana, & Laukhin, 2006). Such BL films consist of a polycarbonate film covered on one of its sides with a thin layer of nanostructured crystals of an organic molecular conductor; like the bis(ethylenedithio)tetrathiafulvalene (ET) charge-transfer salt β-$(ET)_2I_3$. The ultra high piezo-resistivity of such BL films is originated by the softness of the nanocrystals of the conducting salt (Kondo et al., 2006), embedded on the top of the polymeric matrix, that are deformed under small strains changing their conducting properties. Other advantages of using BL films as piezoresistive materials is that they enable to develop strain sensitive active elements that are flexible and transparent and which can be easily glued over a hole of any configuration for fabricating pressure sensing devices. All these characteristics make feasible to develop a contact lens sensor for continuous IOP monitoring with BL. (Laukin, Patent: ES2330405-A1; WO2009147277-A1).

There are some requirements that the final proposed device shall fulfill. The measurement electronics shall be embedded in the contact lens in order to avoid possible patient discomfort due to wire presence, therefore the measured data shall be transmitted wirelessly. Due to the reduced area available on the lens, the system cannot be battery powered. This will also require a wireless energy transmission system. Therefore, the reduced area requirements together with the wireless power transmission imply the design of very small and low power measurement electronics. This can only be achieved by the development of an Application Specific Integrated Circuit (ASIC) with maximum dimensions of 2x2 mm^2 to be

Figure 1. Power and data transmission through an inductive link, from an ASIC emplaced in a contact lens to a pair of glasses

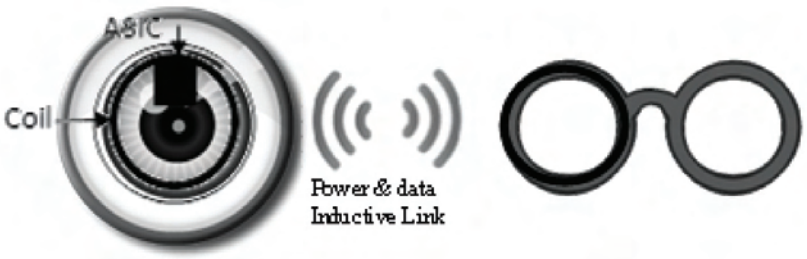

placed on the contact lens. Thanks to the ASIC low powered consumption, it can be powered by an inductive link through two coils as shown in Figure 1. The receiver power coil will be printed in the contact lens and the transmitter power coil will be placed on a pair of glasses. The same link can be used for data transmission.

Here we present a fully embedded handheld device to monitor in a non-invasive way IOP variations in a new concept of contact lens equipped with a BL film-based sensor. This portable device implements the signal conditioning from the pressure sensor embedded in the lens, digitizing and transmitting it to an external device. Therefore, the main objective of this portable device is to study the response of the membrane in front of real stimulus and study the feasibility of the structure that will be integrated. Thus, this discrete device will be used to establish the final system specifications. At the same time, it can also be used to study the effect of different perturbations in the pressure measurements such as the blinking, the tears or temperature changes. Taking into account the power consumption and space limitations of the final design, it is important to determine how these perturbations can be filtered. In this way, the presented device will be useful to determine if it can be filtered by an external post-process or by including a hardware filtering inside the ASIC. It is important to set the specifications of the system before designing the ASIC because of the inability to modify it once done, and its high cost.

METHOD AND PROCEDURE

Contact Lens Sensor

The contact lens was doughnut shaped and in its centre, the flexible piezo-resistive polycarbonate film was incorporated as shown in Figure 2. The parameters of the contact lens were designed according to the anatomical characteristics of the pig eye, in order to ensure an appropriate fitting that enables measurement and register IOP changes. The requirements related with the pressure sensor characteristics shall strongly condition the electronics design, therefore, is needed to know some electrical properties of the membrane shown in Table 1. The device shall be able to detect small variations over big nominal resistance. Moreover, it has a considerable sensibility with the temperature, for this reason, temperature variations must be compensated.

Measurement Method and Design Aspects

Initial Requirements

As it has been mentioned, the main objective of the presented device is to study the capabilities of the presented structure, in order to fix the specifications for a future ASIC development. Thus, the device is based on an easily integrated design using standard CMOS technologies and its implementation must be performed in highly configurable manner in order to study

Figure 2. Left: doughnut shaped rigid CL used for fabricating the CLS. Right: modified CL with BL film glued on the CL equipped with wire connections

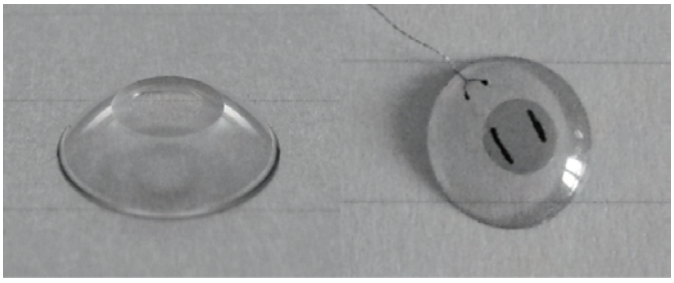

Table 1. Electrical properties of the membrane sensor needed to design the electronic measurement device

Parameter	Value	Unit
Nominal resistance 25ºC	1.5-2.5	kΩ
Pressure sensibility	0.075	%/mmHg
Temperature sensibility	0.3	%/ºC

all its design parameters. The portable device incorporates some accessories to simplify its use to make easily the test of the structure. One of these accessories is a wireless link to communicate with a computer avoiding any discomfort with wires, moreover, portable device must be include a battery and an internal memory to become the device portable and autonomous.

On the other side, there are some requirements related with the pressure sensor characteristics that strongly condition the electronics design. As shown in Table 2 the nominal value of the membrane resistance will be within the 1.5kΩ to 2.5kΩ range and the pressure changes will be very small, 0.075%/mmHg. So, the device shall be able to detect variations around 1.5Ω over a nominal value around 2kΩ, for these reason, the system's structure is based on a special configuration of a Wheatstone Bridge and a system of conversion that will be explained later. Finally, the membrane is also sensible to temperature changes, for this reason, the measurement electronics must be designed with a system that can compensate the temperature effects.

Conditioning and Conversion System

The conditioning and conversion system is formed by two different stages. One for conditioning the sensor signal, and other for conversion the sensor output into a correspondent resistance variation.

The first stage is the conditioning block, formed by a special configuration of a Wheatstone Bridge. As shown in Figure 3 the sensor is placed on one branch and in the other one is placed a reference resistance. The system shall be able to adjust the nominal tolerance, so the upper branches are formed by two variable current sources in order to make this zero adjustment. The output of the Wheatstone Bridge is a differential voltage due to the resistance variation. Using this method the precision of the measure can be increased because only the resistance variation is acquired.

Figure 4 shows the second stage. Differential voltage obtained by the Wheatstone Bridge is amplified by an instrumentation amplifier. It must be provided by a large gain to protect stress signal against circuit noise, together and a good CMRR to attenuate dy-

Table 2. Device specifications

Electrical
Power supply Li-Ion Battery (1170 mAh) Autonomy continuously measuring 26.4 h
Measurement
Storage capacity 39312 measures Resistance calibrated $R_{nominal}$ =2k (1100Ω- 10.9kΩ) Offset of zero adjustment 2.39Ω
Communication Bluetooth or RS232 **Dimensions** 70x55x17 mm **Weight** 10 g

Figure 3. Simplified schematic of measurement system for acquisition and conditioning sensor output signal

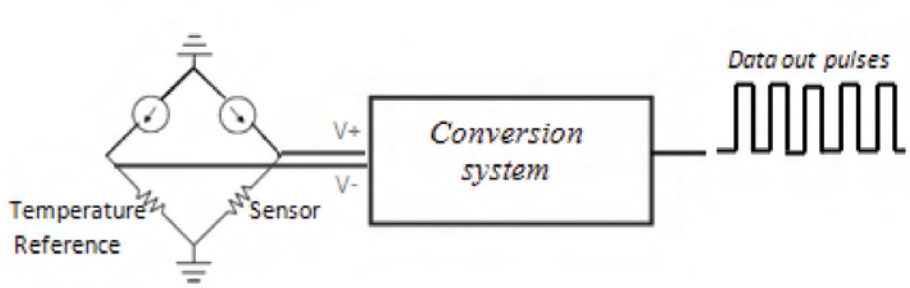

namic disturbing signals. The voltage signal provided by the amplification is transformed in a current signal by using a resistance (R_{int}). The equation to obtain de effective current is given by equation 1.

$$I_{eff} = \frac{G \cdot (V^{+} - V^{-}) + V_{ref}}{R_{int}} \quad (1)$$

Where I_{eff} is the effective current, G is the Gain of the operational controlled by an external resistance, V^{+} and V^{-} are the output voltages of the Wheatstone Bridge, V_{ref} is a reference voltage of the amplifier.

This structure shall be integrated and must be ready to send data in a wireless way. To enable data modulation, the measurement circuit converts the resistance variation into a pulses stream by using a Pulse Density Modulation method. So, to implement the digital quantization a predictive architecture is chosen, inspired in spike-counting A/D techniques applied in neural networks (Asai, Kanazawa, & Amemiya, 2003; Indiveri, Chicca, & Douglas, 2006) and digital images (Chi et al., 2007; Lichtsteiner, Posch, & Delbruck, 2008). Moreover, is a suitable design to make in integrable technology (Durà, Mathieu, Nicu, Pérez-Murano, & Serra-Graells, 2009). Its principle of operation is this: during initialization, both the analog integrator and the digital counter are reset; once in conversion, the current I_{eff} is integrated into an integration voltage (V_{int}); when V_{int} reaches the comparator threshold $V_{ref} \pm V_{th} = \pm V_{comp}$ (depending on the polarity of the I_{eff}), the window comparator generates the corresponding pulse. A third comparator determines if the pulse comes from one comparator or other. Pulses are introduced to a counter, that count or discount depending on the value of the comparator with hysteresis output. At the end of the acquisition time (T_{window}), the integrating A/D conversion is completed and the counter has the value of

Figure 4. Schematic of the amplification, integration and comparison stages. They convert the voltage drop of the Weatshtone Bridge, into a proportional number of pulses

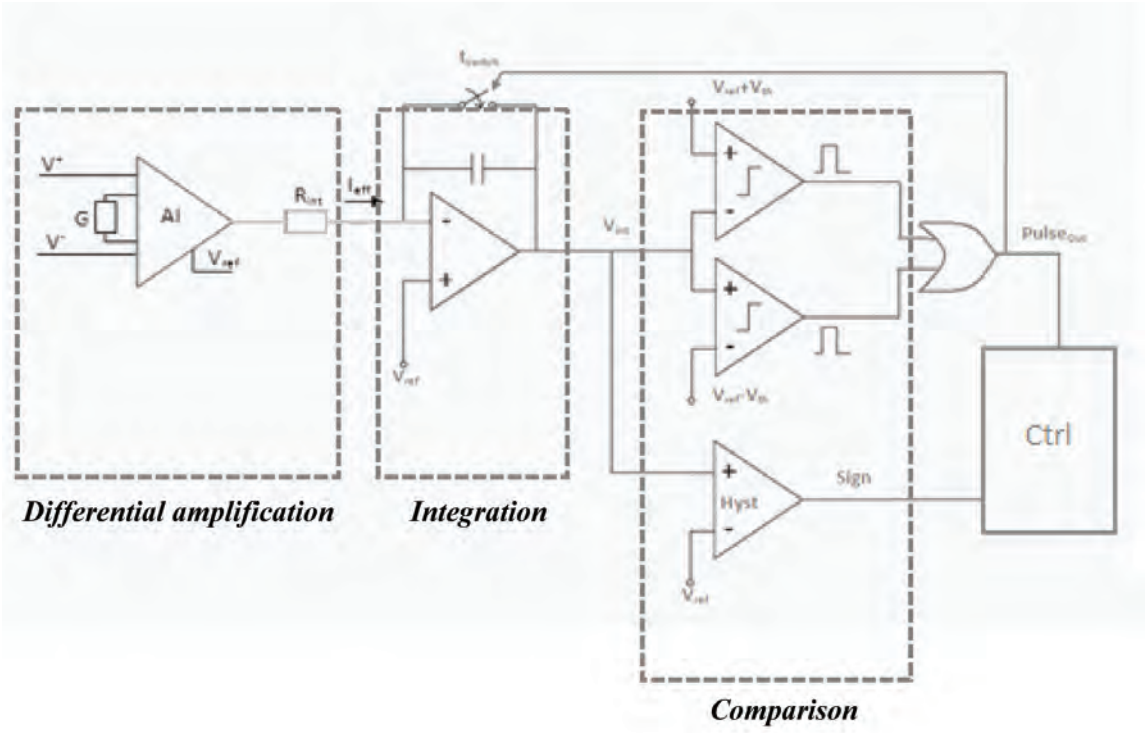

number of pulses. This value is equivalent to the variation of resistance of sensor. Figure 5 shows the $V_{int,}$ that correspond a ramp with positive or negative slope and the comparator output pulses.

Due to the switching device, the reset time cannot be null, as shown in Figure 6. Hence, some time is lost at each pulse generation in order to reset the analog integrator. Therefore, no integration in the integration capacity (C_{int}) is possible during this event time, so the resulting pulse frequency is decreased compared to the ideal case. This effect is more important when de pulse period is small and comparable to the reset time causing saturation of the response. Figure 7 shows the error caused by the switching device. In the practice the measurement range goes between 7 to 32 mmHg, if the sensor has a sensibility of 2-3Ω/mmHg for a lens with nominal resistance of 1.5-2.5kΩ, the

Figure 5. Integrator output, V_{int} and comparator output, $Pulse_{Out}$, for a positive (left) and negative (right) slope

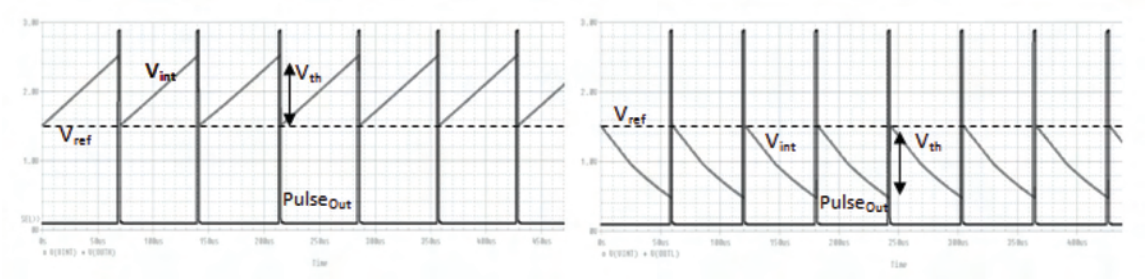

Figure 6. Event duration, t_{reset}, during the switching device, that cause an error in the $Pulse_{Out}$ count

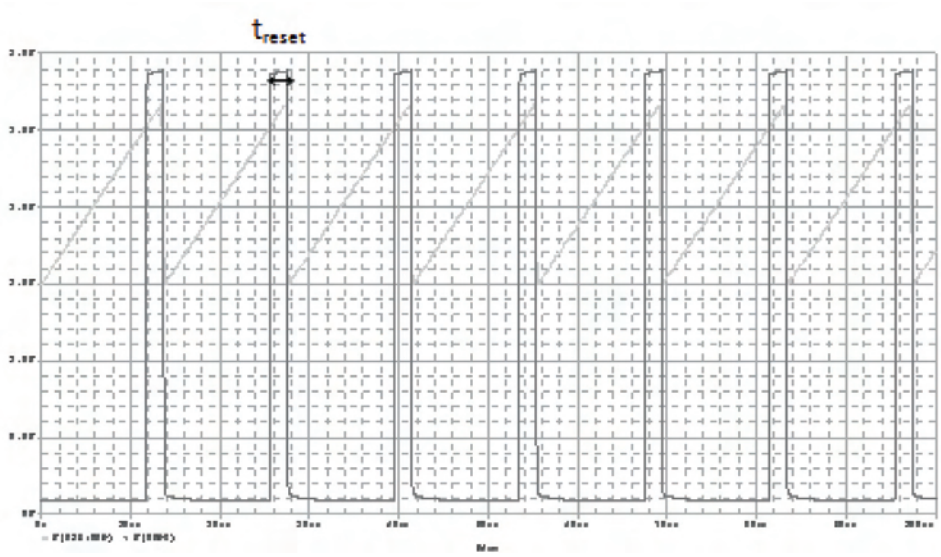

electronic device has to measure changes from 2 to 75Ω. This range causes a maximum error of 0.12Ω that corresponds to a 0.16% of variation from the nominal value. Hence, reset time is important to take into consideration to calculate the relation between pulses and resistance change. Introducing Reset Time (T_{reset}) value in equation 2 switching time error is eliminated. The equation to determine the variation of resistance of all stages is

$$\Delta R = \frac{Pulse_{out} \cdot R_{int} \cdot C_{int} \cdot (V_{comp} - V_{ref})}{(T_{reset} N_{pulse} - T_{window}) \cdot G \cdot I_{ref}} \quad (2)$$

where, $Pulse_{Out}$ is the number of pulses, R_{int} the resistance to transform the output amplifier voltage into a current signal, C_{int} the capacitor of integration, V_{ref} the reference voltage of the comparators, V_{comp} the tension to comparate, T_{reset} the time of the switching device, T_{window} the time to take one count, G the gain of the amplification and I_{ref} the reference current of the current source.

The other important parameter is the Window time, which corresponds to the time for taking one measurement. When this time is bigger, the resolution increases as seen in Figure 8.

Zero Adjustment System

Before starting the measurement, is necessary to adjust the nominal membrane resistance tolerance. The objective of the zero adjustment is to achieve a null output; therefore the measures performed after this process represents the pressure variation respect this time point. This process is performed by changing the current generated by the configurable current sources placed in the upper side of the Wheatstone Bridge, as shown in Figure 3. The schematic of the robust discrete current source is shown in Figure 9, that is controlled by an input voltage (V_{in}). First, is measured the voltage between the two branches of the bridge due to the differences between reference resistance and sensor resistance. If this difference isn't zero, the injected current is changed until the null output is reached. To modify the injected current, different voltages are applied to the input. These voltages are provided by a digital analog converter (DAC) of a microcontroller.

There are some restrictions for performing the compensation. These restrictions are given by the design of the current source and the resolution of the V_{in}. V_{in} values vary from 0.5 to 3V, which are the accepted input values of the operational. Its resolution is given by the

Figure 7. Error caused by the time of the switch that can cause the saturation of the curve. This error has been compesated by introducting the switching time in the ecuation to calculate the resistance variation

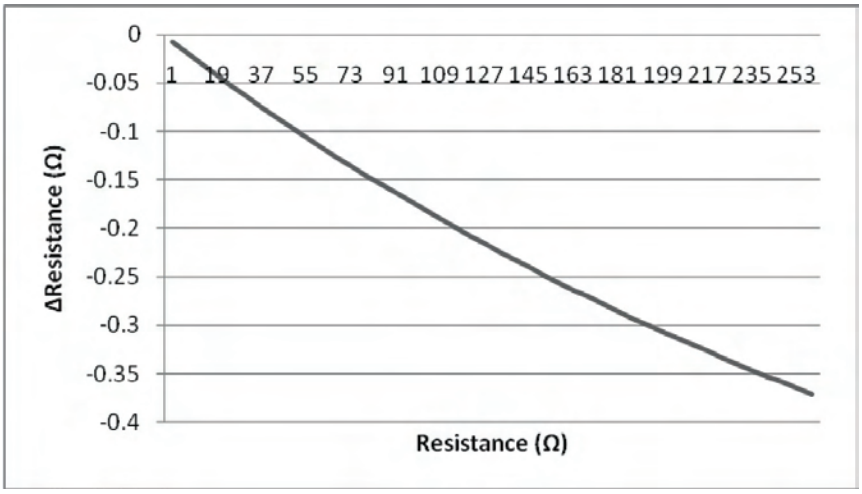

Figure 8. Resolution of the system due to the differences in the Window Time of measurement

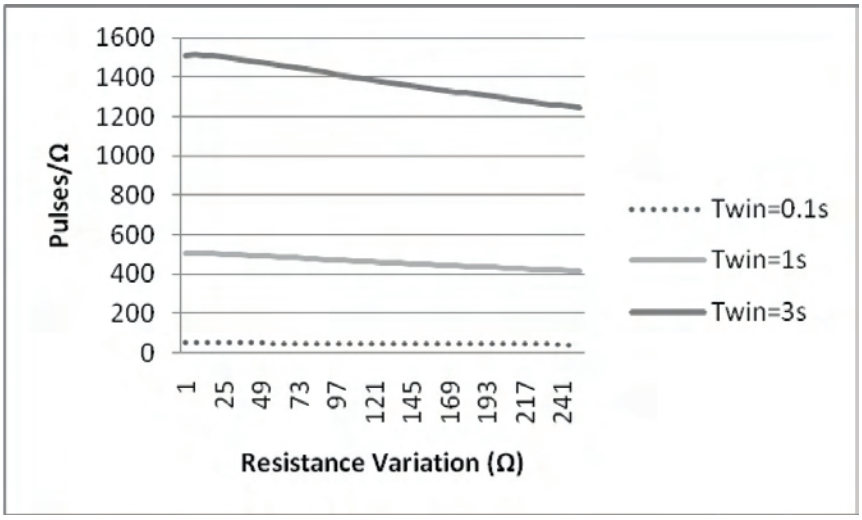

DAC. The resolution of the used DAC, with 12 bits, is given by the following equation

$$V_{resolution} = \frac{V_{max} - V_{min}}{2^{bits} - 1} \quad (3)$$

where V_{max} is the maximum input voltage of the current source and V_{min} the minimum, resulting a resolution of 0.61 mV. With this resolution, the offset of the zero (the minimum change calibrated on the nominal resistance sensor) can be evaluated by the following equation

$$R_{offset} = \frac{R_{ref}}{I_{ref}}(\Delta I_{min}) = \frac{R_{ref}}{I_{ref}}\left(\frac{V_{resolution}}{R_{source}}\right) \quad (4)$$

where R_{ref} is 2kΩ, I_{ref} is 10μA and a R_{source} is 51kΩ, the evaluated offset is 2.39 Ω, that cor-

Figure 9. Schematic of the robust current source, used to compensate the Wheatstone Bridge

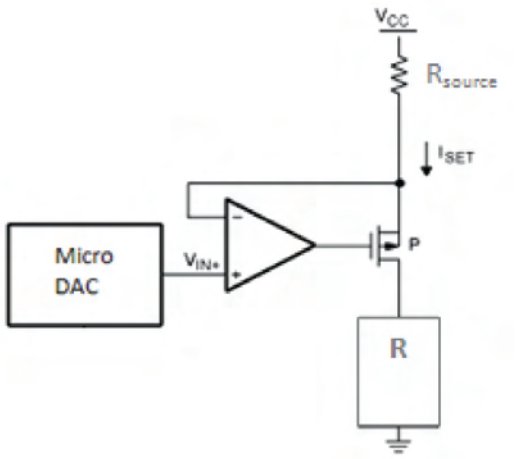

respond a 0.12% of variation from the nominal value.

The calibrated range of the sensor nominal resistance depends on the fixed reference resistance, the value of the fixed current source and the range of the variable current source. With a resistance source of 51kΩ, is obtained a range of current values from 5.8μA to 55μA.

$$I_{var} = \frac{Vcc - Vin}{R_{source}} \quad (5)$$

With a reference resistance of 2kΩ and a fixed current of 10μA, the maximum range that can compensate the system goes from 1100Ω to 10.9kΩ. This range is sufficient for this application where the sensor nominal values vary from 1.5kΩ to 2.5kΩ.

$$R_{sensor} = \frac{I_{var_{max,min}}}{I_{ref}} \cdot R_{ref} \quad (6)$$

The precision of the system depends on the stability of the current sources, the precision of the reference voltages and the capacity of the integrator and the oscillator frequency to count pulses. It's important to leave well characterized the discrete system before being integrated due the expensive it is to take an integrated. In the discrete system can modify the design and change components but in the ingrate system this is not possible.

Temperature Compensation

As seen in Contact Lens Sensor section, the membrane doesn't discriminate if the resistance changes are produced by pressure or temperature. For this reason, the electronic measurement is designed with a system that can compensate the temperature effects. This is achieved with the Wheatstone Bridge. One branch of the bridge has the membrane sensor, and the other one is connected a reference resistor. In our design, it is possible to change this reference resistor by another membrane with the same electrical characteristics than the sensor, but placed, in a part of the lens that is not affected by pressure changes, only by temperature changes. If these two membranes have the same nominal value, the dependence of temperature will be cancelled. But if their nominal value is different, the dependence of temperature will not be fully cancelled. Figure 10 shows the error due to the differences in the nominal resistance between the two branches of the Wheatstone Bridge. It is interesting to note that the matching between these nominal values is very important in order to achieve good temperature compensation.

Figure 10. Error due to the differences in the nominal resistance between the two branches of the Wheatstone Bridge, with a typical sensibility value of 0.3%/ºC

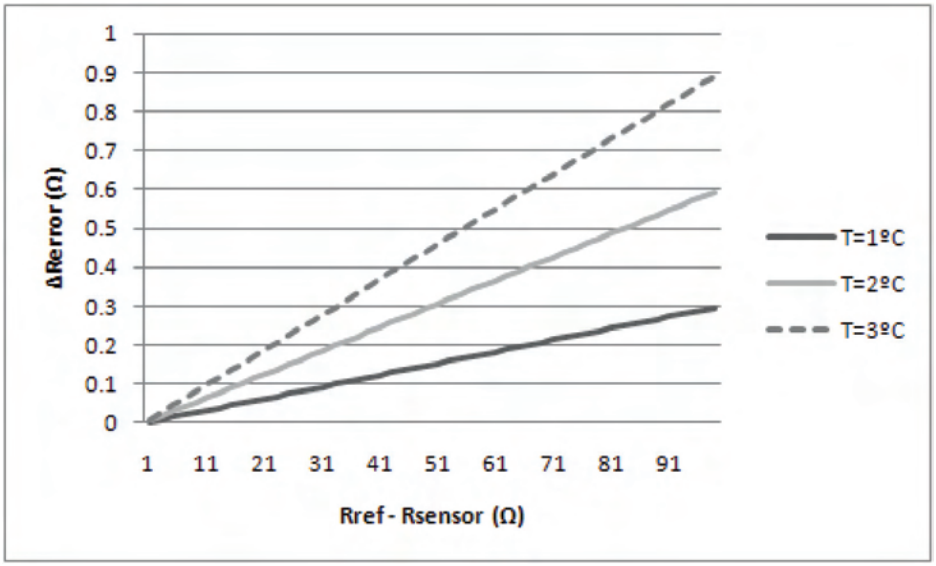

Implemented Device

Using the described system architecture as the basis of its measurement circuit, a hand-held device with some accessories was developed to simplify its use. This hand-held device allows testing the structure that will be implemented in the ASIC. In Figure 12 a photo of the measurement device is shown. The final size and weight of it is 70x55x17mm and 10g.

The device is wire connected to the sensing contact lens, taking continuous measurements of IOP variations. The device is comfortable enough for the patient to allow testing for several hours. It is also connected to a computer by a Bluetooth link to allow free movement for the patient, since there will be no wires attached

Figure 12. Implemented portable device

from the device to the computer. It is battery powered and includes an internal memory, so it can operate autonomously saving data for hours.

In Figure 11 the hardware architecture of the handheld device is schematically shown. The device is based on a high performance 32 bit ARM7TDMI microcontroller.

The presented hand-held device is composed by the following blocs:

- *Microcontroller:* It controls all the internal (timers, ADC, UART) and external (Bluetooth module) peripherals. It also computes the variation of resistance value from the counter which determines the pulse density in a specific window time, to obtain the variation of resistance and, consequently, the IOP variations.
- *Conditioning and conversion:* Structure that will be implemented in the final ASIC detailed in the previous sections.
- *Power supply:* Different voltage levels required for the circuitry (3.3V, 3V, 0.5V, 1.5V and 2.5V) are coming from the battery. Some regulators and voltage divisors are needed.
- *Bluetooth communication module:* it consists on a commercial Bluetooth to RS-232 interface that allows the communication between the microcontroller and the PC.

RESULTS AND DISCUSSION

The test and characterization of the presented device have been divided in different stages. Firstly, it is tested by using dummy resistances with the same characteristics as the CLS. Secondly it is tested by using the CLS adapted to an eye phantom and finally, it is tested by using an enucleated pig eye.

For simulate the electrical response the membrane sensor with a high precision we have implemented a discrete dummy of it. This dummy has been divided in two parts. On one hand, we have used a 2kΩ resistance and for simulate the nominal resistance of the CLS. On the other hand, we have used a potentiometer to simulate the variations produced by the pressure. This used potentiometer has resistance of 50Ω in 25 turns. Thus, each turn is equivalent to 2Ω. This technique permits to implement low value variations over a high nominal value. Using this setup several tests have been carried out. In Figure 13 it is shown the response of the device to little variations of the measured resistance. Each step is equivalent to one turn of the potentiometer. As can be note the mea-

Figure 11. Hardware block diagram

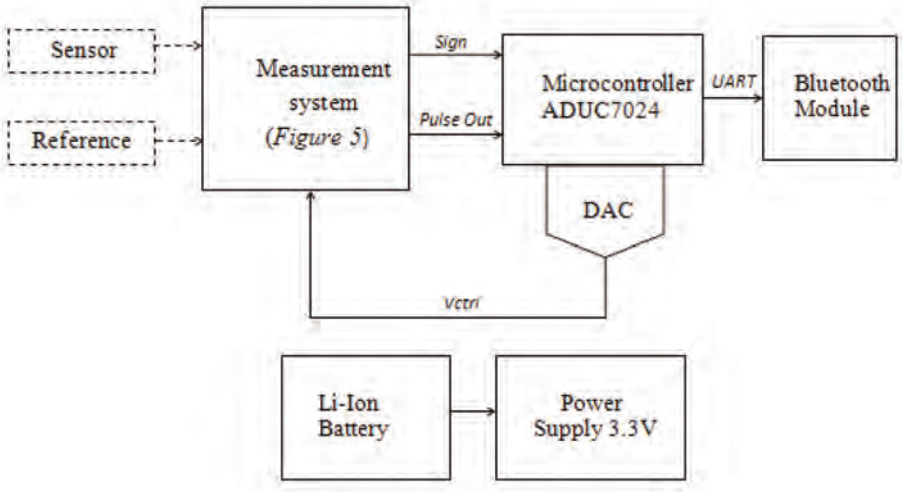

sured resistance follows with high precision the applied variations. On the other hand, to study the stability of the measurement system along the time, we have made a long time test. It consists in measuring one resistance during 24 hours as shown in Figure 14. As can be note the stability of the measure is very high, the maximum registered variation is low than 0.5Ω. This error can be associated to a flicker noise of the system.

Once validated the measurement system with dummy resistances, a test using the CLS adapted on an eye phantom have been carried out. During these experiments, the static gas pressure was applied using a step-by-step procedure directly to the CLS with an IOP simulator (WIKA CPC, 2000). In the experiments with eye phantom the pressure has been changed from 0 to 22 mmHg in steps of 2 mmHg. Then, the electrical response of the CLS was recorded continuously with the hand-held device. As shown in Figure 15, the tested CLS follows nicely the pressure changes produced by the transducer. These measurements also demonstrate that resistance of CLS recovers its initial value. In Figure 16, the electrical resistance data collected for the two up-down sweeps off Figure 15 are plotted versus the nominal pres-

Figure 13. Response of the device to little variations of the measured resistance. Each step is equivalent to one turn of the potentiometer

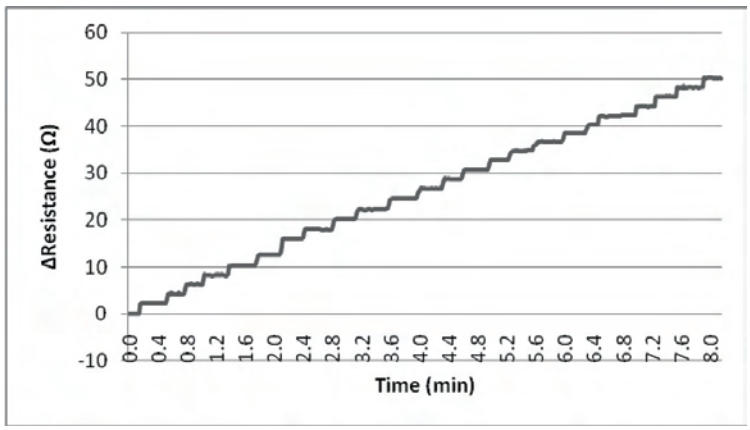

Figure 14. Resistance measurement during 26 hours with the dummy resistance

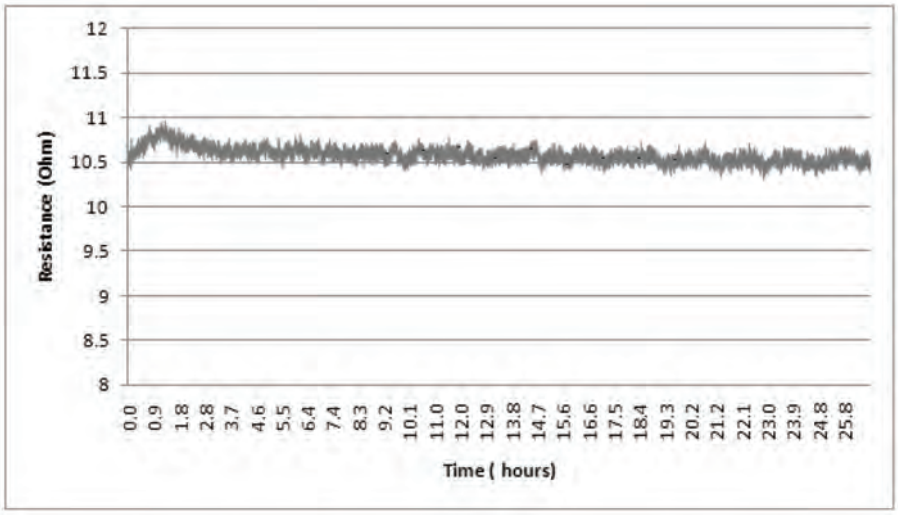

Figure 15. Electrical response of the CLS in an eye phantom, to step-by-step static pressure changes applied with the IOP simulator (WIKA CPC, 2000)

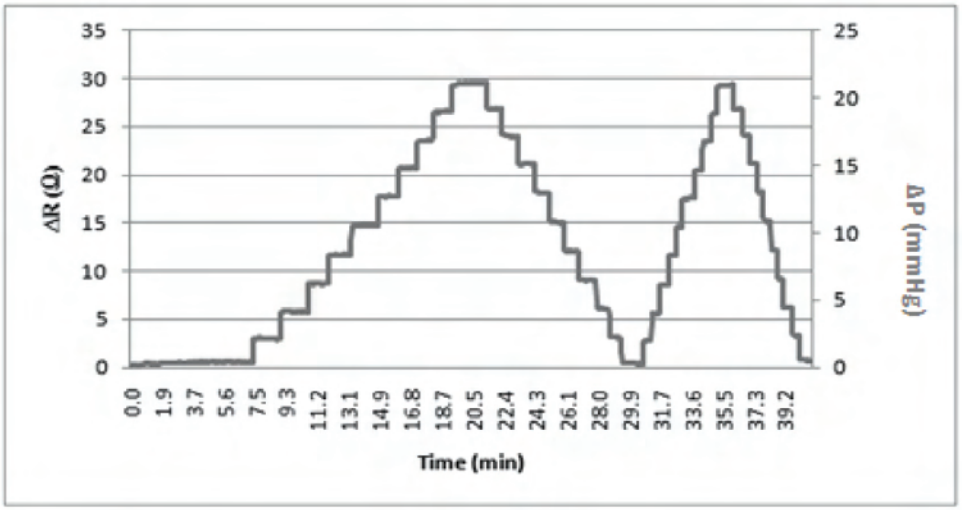

Figure 16. Resistance variation of the CLS versus the applied pressure variation using a low-pressure transducer. Data has been collected from the two up-down sweeps of Figure 15

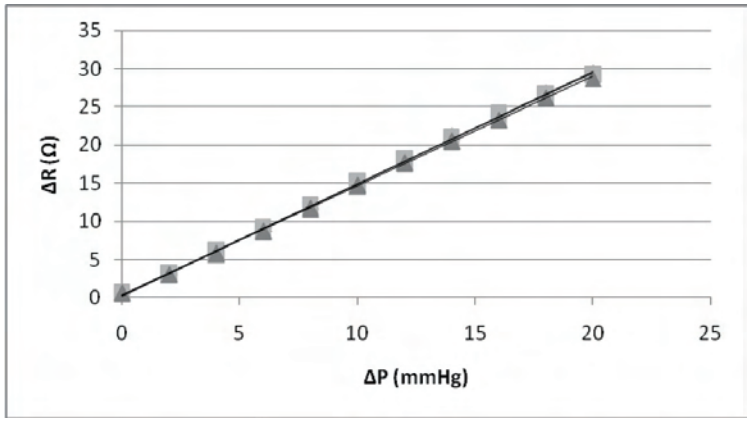

Figure 17. Setup used for testing the CLS on an enucleated pig eye

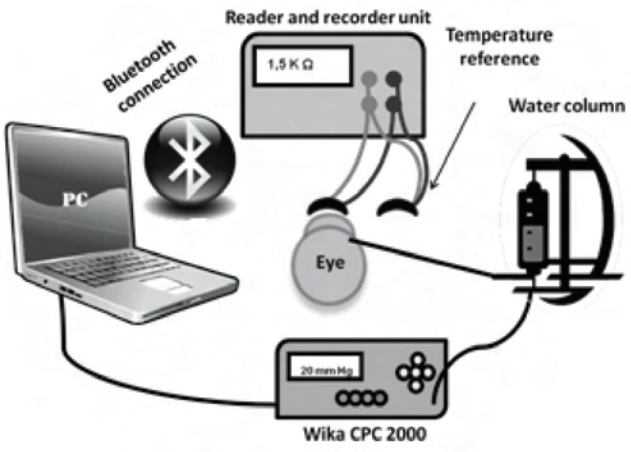

sure at which they were collected. This plot shows that the electrical response of the CLS to pressure changes has a high linearity, as well as a good reproducibility, exhibiting a large sensitivity of 1.5 Ω/mmHg. Therefore, the developed CLS and the approach used to monitor pressure changes fulfill all requirements to control IOP fluctuations in humans. The resolution and repeatability can be evaluated by representing the registered resistance variation versus the applied pressure variation, as can be observed in Figure 16. It is important to note the highly repeatability of the system.

Finally, the device has been tested by using enucleated pig eyes. During these tests, the IOP has been changed from 20 to 50 mmHg by using a same pressure transducer as can be observed in Figure 17. Then the IOP has been measured by using the CLS. The static pressure was applied in such experiments to an enucleated pig eye by a step-by-step procedure in five different sweeps showing that the CLS responds with a well-defined electrical signal to pressure changes in the eye as we can observe in Figure 18. In Figure 19, the electrical resistance data collected for the five up-down sweeps off are plotted versus the nominal pressure at which they were collected. This plot shows that the electrical response of the CLS to pressure changes has a good reproducibility also with pig eyes.

CONCLUSION

It has been developed and evaluated a portable measurement device adapted to measure intraocular pressure changes with a non-invasive system, using a prototype of contact lens.

The portable device has been design with a structure that will be integrated in the near future in an ASIC, and it has incorporated some accessories like wireless link and a battery to simplify its use and to make easily the test of the structure. It has been made several experiments in vitro to evaluate the response of the membrane sensor in front of real stimulus and to study the feasibility of the structure that will be integrated. It's important to establish the final specifications of the ASIC before its design due to the inability to modify it once done and its high cost. The system has an adequate resolution to detect variations of 1.5Ω over 2000Ω. It's necessary to do more tests to end the study of the effect of different perturbations such as the blinking or tear.

On the other hand, it has been validated the method for continuous monitoring of IOP in an in-vitro model of porcine eyeball. The electrical

Figure 18. Electrical response of CLS to IOP pressure changes made on an enucleated pig eye

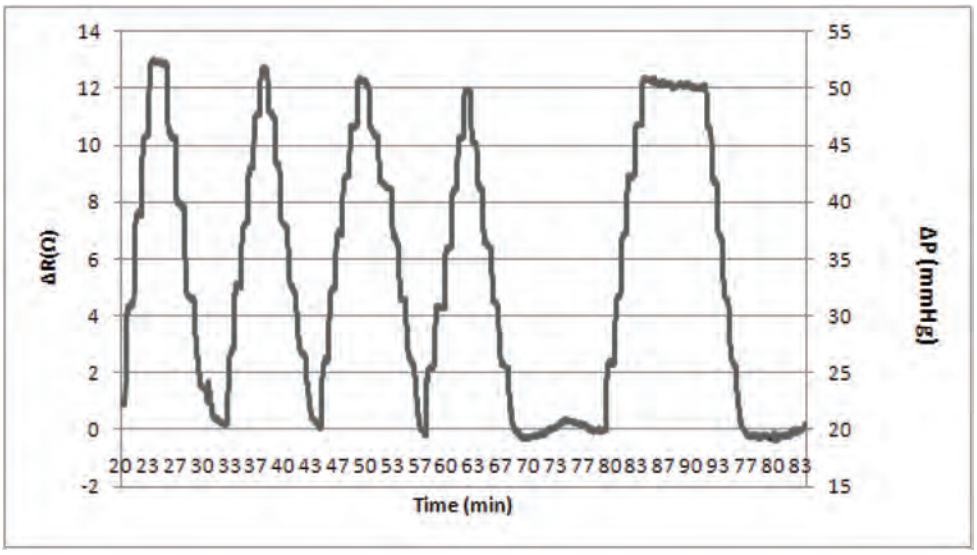

Figure 19. Resistance variation of the CLS versus the applied pressure variation on an enucleated pig eye modelled using a low-pressure transducer. Data has been collected from the two up-down sweeps of Figure 18

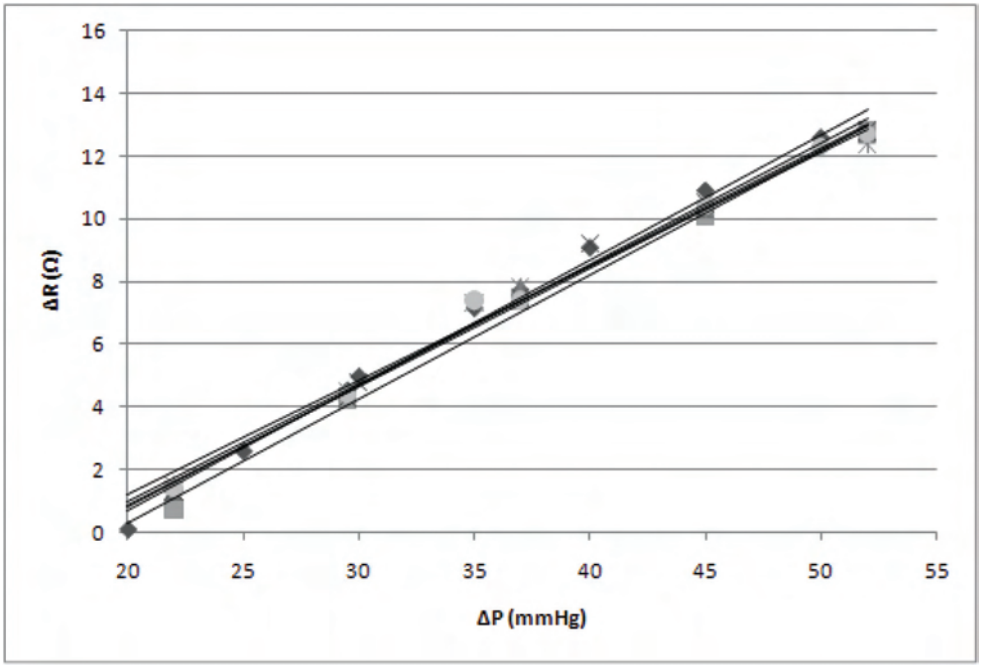

response of the CLS to pressure changes reveals a high linearity as well as a good reproducibility having the proper sensitivity to perform continuous IOP monitoring. The developed prototype of CLS permits to transmit the changes in cornea curvature, which are correlated with the IOP exhibiting an adequate sensitivity to perform continuous monitoring of IOP. In the future this may allow the development of a sensing CL that will be minimally invasive, anesthesia-free, enabling continuous monitoring of IOP for long periods of time. This sensing device will allow to the patient to perform their usual activities because it should not interfere with patient vision. The device may also be useful for diagnosis and treatment of glaucoma.

ACKNOWLEDGMENT

This research was supported by Intramural Project. Networking Research Centre on Bioengineering, Biomaterials and Nanomedicine (CIBER-BBN).

REFERENCES

Asai, T., Kanazawa, Y., & Amemiya, Y. (2003). A subthreshold MOS neuron circuit based on the volterra system. *IEEE Transactions on Neural Networks*, *14*, 130–1312. doi:10.1109/TNN.2003.816357

Asrani, S., Zeimer, R., Wilensky, J., Gieser, D., Vitale, S., & Lindenmuth, K. (2000). Large diurnal fluctuations in intraocular pressure are an independent risk factor in patients with glaucoma. *Journal of Glaucoma*, *9*, 134–142.

Chi, Y. M., Mallik, U., Clapp, M. A., Choi, E., Cauwenberghs, G., & Etienne-Cummings, R. (2007). CMOS camera with in-pixel temporal change detection and ADC. *IEEE Journal of Solid-state Circuits*, *42*, 2187–2196. doi:10.1109/JSSC.2007.905295

Durà, R., Mathieu, F., Nicu, L., Pérez-Murano, F., & Serra-Graells, F. (2009). A 0.3mW/Ch 1.25V Piezo−Resistance Digital ROIC for liquid dispensing MEMS. *IEEE Transactions on Circuits and Systems-I*, *56*, 957–965. doi:10.1109/TCSI.2009.2015210

Flower, R. W., Maumenee, A. E., & Michelson, E. A. (1982). Long-term continuous monitoring of intraocular pressure in conscious primates. *Ophthalmic Research*, *14*(2), 98–106. doi:10.1159/000265179

Greene, M. E., & Gilman, B. G. (1974). Intraocular pressure measurement with instrumented contact lenses. *Investigative Ophthalmology*, *13*(4), 299–302.

Indiveri, G., Chicca, E., & Douglas, R. (2006). A VLSI array of low-power spiking neurons and bistable synapses with spike-timing dependent plasticity. *IEEE Transactions on Neural Networks*, *17*, 211–221. doi:10.1109/TNN.2005.860850

Kondo, R., Higa, M., Kagoshima, S., Hoshino, H., Mori, T., & Mori, H. (2006). Electrical and structural properties of θ-type BEDT-TTF organic conductors under uniaxial strain. *Journal of the Physical Society of Japan*, 75.

Konstas, A. G., Mantziris, D. A., & Stewart, W. C. (1997). Diurnal intraocular pressure in untreated exfoliation and primary open-angle glaucoma. *Archives of Ophthalmology*, *115*, 182–185.

Konstas, A. G., Mylopoulos, N., & Karabatsas, C. H. (2004). Diurnal intraocular pressure reduction with latanoprost 0.005% compared to timolol maleate 0.5% as monotherapy in subjects with exfoliation glaucoma. *Eye (London, England)*, *18*, 893–899. doi:10.1038/sj.eye.6701345

Laukhin, V., Rovira, C., Laukhina, E., Veciana, J., Mas-Torrent, M., Guimerà Brunet, A., et al. (2010). *Argentina Patent No. ES2330405-A1; WO2009147277-A1: Truncated contact lens for use in telemetry system, has truncation plane provided parallel to base of lens, and centrally placed polymer nanocomposite material joined to perimeter of truncated zone.* Buenos Aries, Argentina: The Argentina Trademark System.

Laukhina, E., Mas-Torrent, M., Rovira, C., Veciana, J., & Laukhin, V. (2006). *Argentina Patent No. P200602887 (WO2008059095): Organic sensor device for e.g., molecular electronics, has layer of organic material having conductive salt or complex including molecule and dopant, and base substrate provided in close contact with layer of organic material*. Buenos Aries, Argentina: The Argentina Trademark System.

Laukhina, E., Pfattner, R., Ferreras, L. R., Galli, S., Mas-Torrent, M., & Masciocchi, N. (2010). Ultrasensitive piezoresistive all-organic flexible thin films. *Advanced Materials (Deerfield Beach, Fla.)*, *22*, 977–091.

Leonardi, M., Leuenberger, P., Bertrand, D., Bertsch, A., & Renaud, P. (2004). First steps toward noninvasive intraocular pressure monitoring with a sensing contact lens. *Investigative Ophthalmology & Visual Science*, *45*(9), 3113–3117. doi:10.1167/iovs.04-0015

Leonardi, M., Pitchon, E. M., Bertsch, A., Renaud, P., & Mermoud, A. (2009). Wireless contact lens sensor for intraocular pressure monitoring: Assessment on enucleated pig eyes. *Acta Ophthalmologica*, *87*(4), 433–437. doi:10.1111/j.1755-3768.2008.01404.x

Lichtsteiner, P., Posch, C., & Delbruck, T. (2008). A 128x180 120 dB 15 μs latency asynchronous temporal contrast vision sensor. *IEEE Journal of Solid-state Circuits*, *43*, 566–576. doi:10.1109/JSSC.2007.914337

Maurice, D. M. (1958). A recording tonometer. *The British Journal of Ophthalmology*, *42*(6), 321–335. doi:10.1136/bjo.42.6.321

Raychaudhuri, A., Lahiri, S. K., Bandyopadhyay, M., Foster, P. J., Reeves, B. C., & Johnson, G. J. (2005). A population based survey of the prevalence and types of glaucoma in rural West Bengal: The West Bengal Glaucoma Study. *The British Journal of Ophthalmology*, *89*, 1559–1564. doi:10.1136/bjo.2005.074948

Resnikoff, S., Pascolini, D., Etya'ale, D., Kocur, I., Pararajasegaram, R., Pokharel, G. P., & Mariotti, S. P. (2004). Global data on visual impairment in the year 2002. *Bulletin of the World Health Organization*, *82*, 844–851.

Rota-Bartelink, A. M., Pitt, A., & Story, I. (1996). Influence of diurnal variation on the intraocular pressure measurement of treated primary open angle glaucoma during office hours. *Journal of Glaucoma*, *5*, 410–415. doi:10.1097/00061198-199612000-00009

Sung, V. C., Koppens, J. M., Vernon, S. A., Pawson, P., Rubinstein, M., King, A. J., & Tattersall, C. L. (2006). Longitudinal glaucoma screening for siblings of patients with primary open angle glaucoma: The Nottingham Family Glaucoma Screening Study. *The British Journal of Ophthalmology*, *90*, 59–63. doi:10.1136/bjo.2005.072751

Svedbergh, B., Bäcklund, Y., Hök, B., & Rosengren, L. (1992). The IOP-IOL: A probe into the eye. *Acta Ophthalmologica*, *70*(2), 266–268. doi:10.1111/j.1755-3768.1992.tb04135.x

Wolbarsht, M. L., Wortman, J., Schwartz, B., & Cook, D. (1980). A scleral buckle pressure gauge for continuous monitoring of intraocular pressure. *International Ophthalmology*, *3*(1), 11–17. doi:10.1007/BF00136208

Ana Moya received the M.Sc. degree in telecommunications engineering from the Universitat Autònoma de Barcelona, Spain, in 2008. She has been working with the Mico Nano Bio Integrated Systems Group in the Institut de Microelectrònica de Barcelona, Centro Nacional de Microelectrónica, (IMB CNM, CSIC), Spain, since 2008, contracted by CIBER BBN. Specialized in electronic systems, her current researches interested are focused on design and development of electronic systems for biomedical applications.

Antón Guimerà received the MSc degree in electronic engineering from the Autonoma University of Barcelona in 2006. He joined the Design Department of the National Microelectronics Center (CNM CSIC) at 2000 as technical engineer. Now, he is working in his PhD based on the study of the corneal barrier function by means of impedance measurements. His Research interest fields are the design of electronic systems for biomedical applications and the study of the passive electrical properties of biological tissues.

Irene Sánchez is a registered Spanish optometrist OD(EC) with a Master degree in visual sciences (MSc). Presently belongs to the Networking Research Centre on Bioengineering, Biomaterials and Nanomedicine (CIBER BBN), Zaragoza Spain and is working at the Unit of Glaucoma in the IOBA Eye Institute.

Vladimir Laukhin graduated as physicist at the Moscow Institute of Physics and Technology in 1969 and earned PhD (Physics) in 1975 at the Institute of Problems of Chemical Physics of Russian Academy of Sciences, where he was working until 2001. Since 2001 he is ICREA Research Professor at Institut de Ciència de Materials de Barcelona (CSIC). His research interest has long centred on physics of conducting/superconducting molecular organic materials, with particular emphasis on their electronic and magnetic properties. In the past few years his main efforts have been devoted to a new generation of plastic electronic devices, based on multifunctional organic molecular conductors, to be used for fabrication of very sensitive flexible strain/pressure/temperature sensors and electronic circuits.

Raul Martin is a registered Spanish optometrist OD(EC) with a Master degree in visual sciences (MSc) and he got a PhD degree at the University of Valladolid. Presently he is a teacher of optometry and contact lens in the School of Optometry (University of Valladolid) and is also the optometry head of the IOBA Eye Institute.

Fernando Ussa graduated as a medical doctor in 1991 from the University of Colombia (Bogotá) and obtained the Ophthalmology Specialty in 1999 from the La Samaritana University Hospital (Colombia). He has been observer fellow in Moorfields Hospital (London, UK) and got a Master in Glaucoma in 2003 and a Master of Science (MsC) in 2007 from the University of Valladolid. Since 2003 he is the Glaucoma Unit director at IOBA (University Institute of Applied Ophthalmobiology), University of Valladolid. His research area comprehends glaucoma clinical trials, glaucoma genetics and glaucoma devices for diagnosis.

Elena Laukhina graduated as a chemist in 1975 and obtained her PhD in 1979 from the D. Mendeleyev University of Chemical Technology of Russia, Moscow; in 1979 she moved to the Institute of Chemical Physics of Russian Academy of Science (Chernogolovka) where she was promoted to Senior Researcher in 1999. Since 2007 she is Titular Scientist Researcher of "El Centro de Investigación Biomédica en Red en Bioingeniería, Biomateriales y Nanomedicina", ICMAB CSIC, (Spain). Her research interest focuses on organic molecular metals and superconductors and developing flexible lightweight materials for electronic application.

Concepció Rovira received her PhD degree on Chemistry from the University of Barcelona in 1977. She was a postdoctoral fellow in 1982/1983 at The Johns Hopkins University with Dwaine O.Cowan where she entered in the field organic metals. She was appointed at the CSIC in 1987, and in 1991 she moved to the Institut de Cie`ncia de Materials de Barcelona (CSIC), where was promoted to Full Professor in 2004. Her research interests focus on molecular functional materials and molecular nanoscience and, in particular, in the fields of organic electronics, electron transfer phenomena, and molecular self assembly and recognition.

Jaume Veciana graduated as a chemist in 1973 and obtained the PhD degree in 1977 from the University of Barcelona (Spain) in 1977 working in physical organic chemistry. In 1991 he moved to the Institut de Ciència de Materials de Barcelona (CSIC) where was promoted to Full Professor in 1996. Since 2004 he is the Director of the Department of Molecular Nanoscience and Organic Materials of the same Institute. His research interest focuses on molecular functional materials and molecular nanoscience and in particular in the fields of molecular magnetism, molecular spintronics, and in the processing of molecular compounds as particles and on surfaces for biomedical applications.

José Carlos Pastor graduated as a MD in 1974 obtained the PhD degree in 1975 by the Navarra's University in Spain. Specialist in Ophthalmology since 1976. In 1979 moved to Santiago de Compostela as Full Professor (Agregado) and Chief of Ophthalmology at the University Hospital. In 1981 moved to Valladolid University as Full Professor (Catedratico) and Chairman of Ophthalmology at the University Hospital. Since 1987 to 1991 was Vice Chancelor of Research of the whole University. He founded the IOBA (Eye Institute) of the Valladolid University in 1989. Director of IOBA since 1991. Director of the Spanish Journal of Ophthalmology since 1995 to 2000. His research interest focuses on glaucoma, retinal detachment, cell therapy and other advanced therapies for retinal diseases, and Intraocular inflammation and scarring.

Rosa Villa, Medicine Doctor by the Universitat de Barcelona (1981), and Ph.D. by the Universitat Autonoma de Barcelona (1993). Specialized in nuclear medicine, she had the Spanish National award on Nuclear Medicine in 1985. She joined the Design Department of the National Microelectronics Center (CNM CSIC) at 1986 where she became researcher at 1992. Now, she belongs to the Biomedical Applications Group Board at the CNM. Her current research interest fields are in the microsystem biomedical applications mainly in the neural stimulation area and in the use of neural networks and fuzzy logic for the definition of clinical prediction areas where she has actively participated in many research projects.

Jordi Aguiló, PhD in Physics in 1976, he joined the Computer Science Department, holding a Full Professor position in Computer Technology and Architecture since 1987. In 1985 he became researcher at the Design Department of the Microelectronics National Center (IMBCNM) that lead up to 1997. He is now leading the postgraduate studies at the Microelectronics and Electronic Systems Department at the UAB, coordinating the Biomedical Applications Group from IMB UAB and the GBIO Group within the CIBER BBN. His research interest fields are the Micro and Nano System's mainly focusing Biomedical Applications such as Advanced Multi Micro Nanosensors, Neural interfaces and Monitoring devices up to Converging Technologies devices and systems.

16.- ANEXO VI

Sánchez I, Laukhin V, Moya A, Martin R, Ussa F, Laukhina E, Guimera A, Villa R, Rovira C, Aguiló J, Veciana J, Pastor JC.

Prototype of a nano-structured sensing contact lens for noninvasive intraocular pressure monitoring.

Invest Ophthalmol Vis Sci Oct 21;52(11):8310-5.

Prototype of a Nanostructured Sensing Contact Lens for Noninvasive Intraocular Pressure Monitoring

Irene Sánchez,[1,2] *Vladimir Laukhin,*[2,3,4] *Ana Moya,*[5] *Raul Martin,*[1,2,6] *Fernando Ussa,*[1,2] *Elena Laukhina,*[2,4] *Anton Guimera,*[2,5] *Rosa Villa,*[2,5] *Concepcio Rovira,*[2,4] *Jordi Aguiló,*[2,5] *Jaume Veciana,*[2,4] *and Jose C. Pastor*[1,2]

Purpose. To present the application of a new sensor based on a flexible, highly piezoresistive, nanocomposite, all-organic bilayer (BL) adapted to a contact lens (CL) for non-invasive monitoring intraocular pressure (IOP).

Methods. A prototype of a sensing CL, adapted to a pig eyeball, was tested on different enucleated pig eyes. A rigid, gas-permeable CL was designed as a doughnut shape with a 3-mm hole, where the BL film–based sensor was incorporated. The sensor was a polycarbonate film coated with a polycrystalline layer of the highly piezoresistive molecular conductor β-$(ET)_2I_3$, which can detect deformations caused by pressure changes of 1 mm Hg. The pig eyeballs were subjected to controlled-pressure variations (low-pressure transducer) to register the electrical resistance response of the CL sensor to pressure changes. Similarly, a CL sensor was designed according to the anatomic characteristics of the eye of a volunteer on the research team.

Results. A good correlation (r^2 = 0.99) was demonstrated between the sensing CL electrical response, and IOP (mm Hg) changes in pig eyes, with a sensitivity of 0.4 Ω/mm Hg. A human eye test also showed the high potential of this new sensor (IOP variations caused by eye massage, blinking, and eye movements were registered).

Conclusions. A new nanostructured sensing CL for continuous monitoring of IOP was validated in an in vitro model (porcine eyeball) and in a human eye. This prototype has adequate sensitivity to continuously monitor IOP. This device will be useful for glaucoma diagnosis and treatment. (*Invest Ophthalmol Vis Sci.* 2011;52:8310–8315) DOI:10.1167/iovs.10-7064

Glaucoma is the second leading cause of irreversible blindness worldwide.[1] Its prevalence varies between 1% and 3%, depending on the population studied and the diagnostic criteria.[2,3] Moreover, glaucomatous optic neuropathy leads to certain characteristic changes in the optic nerve head and visual field loss and is usually associated with increased intraocular pressure (IOP), with values higher than 21 mm Hg.[2]

However, one of the most important parameters in glaucoma diagnosis and treatment is IOP measurement because the primary treatment goal is to reduce IOP to prevent optic nerve damage. IOP fluctuates during the day, with a maximum value at daybreak and a minimum at the end of the afternoon.[4] This fluctuation is partially related to circadian rhythms,[4] but IOP can also be influenced by other factors, such as accommodation,[5] action of the extraocular muscles (convergence),[6] blood pressure,[7] atmospheric pressure,[8] blinking,[6] and others (e.g., body position, Valsalva maneuvers).[6,9–11] The only reliable method to determine whether IOP increases at any time of the day is to construct a 24-hour tensional curve with the patient in a hospital environment.[4] Thus, the measurement and monitoring of IOP is a widely studied aspect in the literature. Hughes[12] showed that monitoring IOP for 24 hours may change the clinical management of a high percentage, >70%, of patients with glaucoma.

Attempts to continuously monitor IOP have been made, but none of the devices developed has been integrated into clinical practice mainly because of technical problems, lack of long-term stability, and other issues.[13–17] Some devices to monitor IOP are based on the principle that a change in IOP of 1 mm Hg causes a change in corneal curvature of 3 μm for a corneal radius of 7.80 mm.[10,18]

The purpose of this study was to present a proof of concept of the application of a new sensor based on a conducting, all-organic, nanocomposite bilayer (BL) adapted in a contact lens (CL) for noninvasive monitoring of IOP.

Materials and Methods

Contact Lens Sensor

A rigid, gas-permeable CL material (Boston XO2; Conoptica SL, Barcelona, Spain) was designed according to the anatomic characteristics of the pig eye to ensure an adequate flat fitting that enabled us to measure and register any changes in the apex corneal curvature induced by IOP alterations. The CL was designed according to the pig eye corneal radius and corneal topography (Orbscan II, version 3.12; Bausch & Lomb, Rochester, NY).[19] The CL was doughnut-shaped (central hole diameter 3.0 mm). A round membrane based on a piezoresistive BL film was glued over the hole. Two delicate Pt-based wires, each with a diameter of 20 μm, were attached to the sensing layer of the BL

From the [1]IOBA-Eye Institute and the [6]Department of Physics TAO—School of Optometry, University of Valladolid, Valladolid, Spain; [2]Networking Research Centre on Bioengineering, Biomaterials and Nanomedicine (CIBER-BBN), Zaragoza, Spain; [3]Institucio Catalana de Recerca i Estudis Avançats (ICREA), Barcelona, Spain; [4]Institut de Ciencia de Materials de Barcelona (ICMAB-CSIC), Barcelona, Spain; and [5]Centre National of Microelectronics (CNM-CSIC), Barcelona, Spain.

Supported by CIBER-BBN, an initiative funded by the VI National R+D+i Plan 2008-2011, Iniciativa Ingenio 2010, Consolider Program, CIBER Actions; by the Instituto de Salud Carlos III with assistance from the European Regional Development Fund, Generalitat de Catalunya, under the framework of Programa Operatiu FEDER de Catalunya, contract VALTEC09-1-0030; and by project SGR2009-516, the European Union Large Project One-P (FP7-NMP-2007-212311), the DGI, Spain, projects CTQ2006-06333/BQU and CTQ2010-19501/BQU.

Submitted for publication January 15, 2011; revised May 5 and August 1, 2011; accepted September 12, 2011.

Disclosure: **I. Sánchez**, None; **V. Laukhin**, P; **A. Moya**, None; **R. Martin**, None; **F. Ussa**, None; **E. Laukhina**, P; **A. Guimera**, None; **R. Villa**, None; **C. Rovira**, P; **J. Aguiló**, None; **J. Veciana**, P; **J.C. Pastor**, None

Corresponding author: Irene Sánchez, Campus Miguel Delibes Paseo de Belen 17, IOBA-Eye Institute, University of Valladolid, Valladolid, Spain 47011; isanchezp@ioba.med.uva.es.

film-based membrane with graphite paste and were connected with two copper wires, each with a diameter of 50 μm. The prototype is shown in Figure 1. The electrical connection was configured in such a way as to minimize sensor deformation. The developed electrical connection enabled the sensing lens to access the recording apparatus, a discrete device specifically designed for this study. This device was connected with a wireless device (Bluetooth, Kirkland, WA) to a personal computer to continuously register the measurements of the CL sensor.

A flexible, highly piezoresistive BL film, with the molecular metal β-$(ET)_2I_3$ (bis-[ethylenedithio]tetrathiafulvalene) as a sensing component, was prepared using a previously reported synthetic method.[20–22] The texture, structure, and electromechanical properties of the prepared BL film, which were characterized by different spectroscopic and microscopic techniques and by resistance-pressure measurements, were identical with those reported; in the laboratory, the BL film was able to detect deformations caused by a pressure change of 1 mm Hg, which fulfills the requirements of glaucoma control device.[23,24] Nearly circular membranes were cut from the prepared BL film sample and were used as a sensing element to register changes in IOP. To avoid damaging the sensing BL film-based membrane, it was covered by an additional "cap" piece made of the same material as the rigid contact lens.

In Vitro Experimental Procedure

Thirty enucleated pig eyes were used. The eyeballs were collected in the local slaughterhouse immediately after the animals were euthanatized, for which the age ranged between 6 and 8 months. After enucleation, pig eyes were kept in ice and immersed in Dulbecco's modified Eagle's medium supplemented with antibiotic/antimycotic mixture (Gibco, Paisley, UK). Measurements were conducted within 4 hours to preserve the elastic properties of the ocular tissues.

The pig eyeballs were subjected to controlled-pressure variations to register and compare them with the variations in resistance taken by the sensor CL (Fig. 2). A 23-gauge cannula was inserted in the vitreous chamber, 3.5 mm from the sclerocorneal limbus, and Ringer's lactate solution was injected through a closed system using a glass bottle as a water column controlled by a low-pressure transducer (CPC 2000; WIKA Alexander Wiegand GmbH & Co., Klingenberg, Germany). The transducer permitted the increase, decrease, and maintenance of IOP in a range of 20 to 55 mm Hg.[25]

The sensing CL demonstrated good hydrostability; therefore, it was placed on the ocular surface on the porcine eye and hydrated with distilled water without any precaution. The sensing lens was connected to the discrete device made for this project, which registered the changes in electrical resistance captured by the sensor CL as a result of changes induced in IOP.

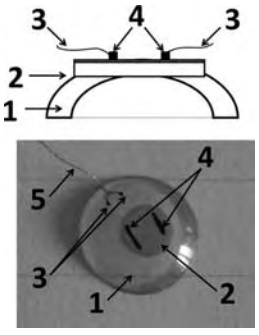

FIGURE 1. Schematic view (*top*) and image (*bottom*) of the IOP sensing lens composed of a doughnut-like contact lens (1), the highly piezoresistive BL film-based membrane (2), and electrical connections with a linear configuration of the contacts. Two 20-μm-thick Pt wires (3) are attached to the conducting layer of the membrane using graphite paste (4). The Pt wires are attached to 50-μm-thick Cu wires (5), which are connected to the collecting data device.

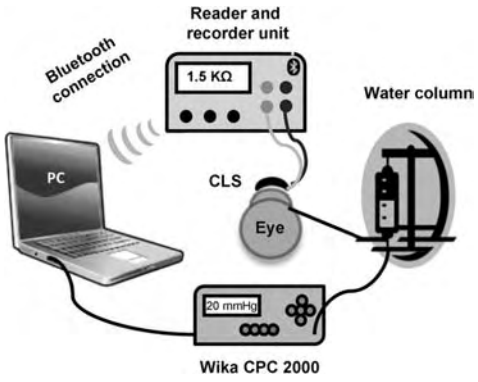

FIGURE 2. Schematic representation of in vitro experimental design.

Output signals of the low-pressure transducer (mm Hg) and the sensing CL electrical resistance changes (Ω) were automatically stored on the same computer, registering every 5 seconds. The graph of the IOP changes was compared to the electrical changes recorded by the sensing CL. To minimize the temperature effect, all pressure tests on cannulated pig eyes were carried out at a stabilized temperature, using another sensing lens that revealed the same temperature resistance coefficient as the temperature reference. The correlation between the change in IOP induced by low-pressure transducer and the CL sensor measurements was calculated with the r^2 coefficient.

In Vivo Experimental Procedure

A CL sensor was designed and flat fitted to the eye of a volunteer on the research team. This CL was made according to the subject's corneal topography (Orbscan II, version 3.12; Bausch & Lomb). Flat fitting was used to guarantee that the sensor film would detect corneal curvature changes related to IOP changes. The CL was worn for 2 hours to register the influence of blinking and eye movements on the sensor's electrical response.

The ocular surface of the volunteer was anesthetized with oxybuprocaine hydrochloride and tetracaine hydrochloride, and a therapeutic CL (Purevision; Bausch & Lomb) was fitted to protect the cornea. The CL sensor was piggyback fitted onto this.

A discrete device for conditioning and digitizing the data has been designed. The device was powered by a battery and had an internal memory to operate while it autonomously saved data for 24 hours. The CL sensor was wire connected to the discrete device accessory to continuously register the measurements of the CL sensor caused by blinking, eye movements, and IOP fluctuations. This device was wirelessly (Bluetooth)–connected to a personal computer to allow the patient to move without restriction while measurements were performed.

The Human Sciences Ethical Committee of the University of Valladolid, Spain, approved this protocol. The subject was treated in accordance with the Declaration of Helsinki.

RESULTS

In Vitro Experimental Results

The pig eyeballs were stimulated by applying controlled changes of increasing and decreasing IOP so that the sensing CL registered periods of electrical resistance values with an excellent time agreement. Figure 3 shows the recorded IOP changes induced by the low-pressure transducer and the output signal (ΔR) of the sensing CL. We collected data for all five up-down (Fig. 3) pressure steps and plotted the resistance changes (ΔR) to determine the sensitivity of the CL sensor (Fig. 4). The graph shows a linear correlation between IOP and sensor

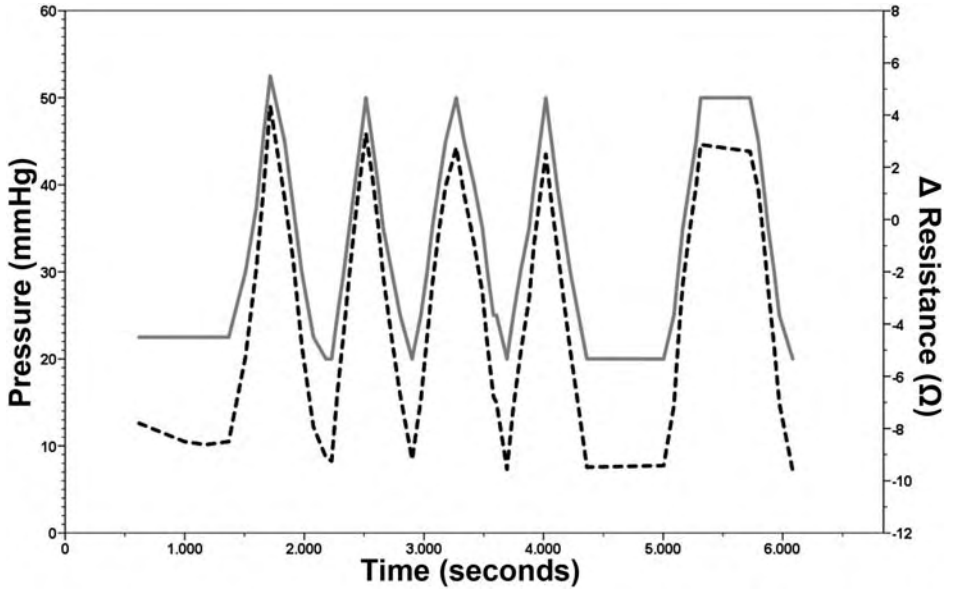

FIGURE 3. Representation of IOP variations and CL sensor outputs over time in a single study eye. *Gray solid line*: pressure changes (mm Hg); *black dotted line*: electrical resistance (Ω) variations. Pressure changes (up and down) and resistance changes showed similar trends. When pressure was constant (20 mm Hg or 50 mm Hg), resistance was also constant.

resistance response ($r^2 = 0.99$), with a sensitivity of 0.4 Ω/mm Hg.

In Vivo Experimental Results

No relevant clinical biomicroscopic signs (grade >2; Efron grading scales) of CL complications (corneal staining, limbal injection, or other) were found. Figure 5 shows the 2-hour plot of the output signal of the CL sensor while it was fitted to the volunteer's eye. Variations in electric resistance were caused by massage of the eye, strong blinking, and eye movements.

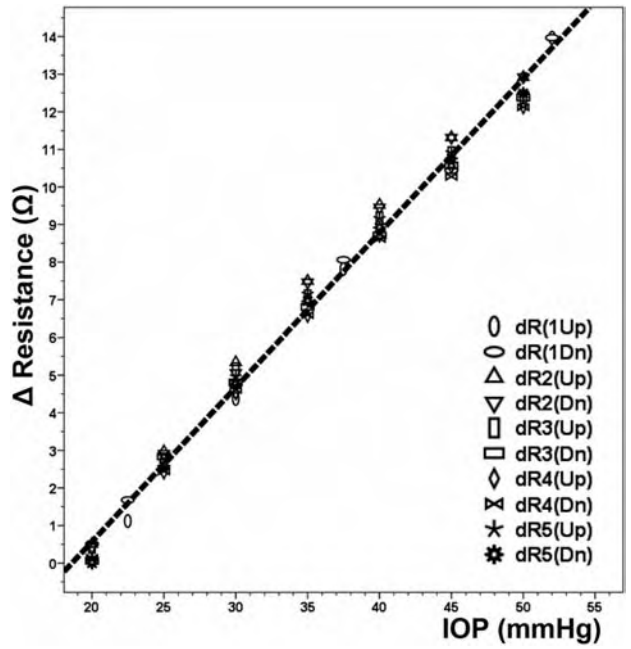

FIGURE 4. Calibration of the CL sensor. Changes in the electrical response of the lens to IOP variations on a pig eye induced using a low-pressure transducer are plotted. Data were collected from the five up-down steps shown in Figure 3. A high linear correlation between IOP and sensor resistance changes was found ($r^2 = 0.99$), with a sensitivity of 0.4 Ω/mm Hg.

These results show the high potential of this new sensor to monitor IOP for extended periods of time.

DISCUSSION

Accurate IOP monitoring is important for glaucoma patients because increased IOP causes retinal ganglion cells to die, leading to irreversible blindness.[26–28] For this reason, much research has focused on developing methods and devices to monitor IOP. The first attempt was made by Maurice,[13] but Greene and Gilman[14] published the first noninvasive IOP-monitoring system using a CL device in rabbits. In addition, Wolbarsht[15] designed a pressure transducer on a band that recorded IOP, Flower[16] tested an IOP-measuring system in adult rhesus macaque (*Macaca mulatta*) monkeys, and Svedbergh[17] created an intraocular lens to measure IOP. Leonardi[11,18] has developed a marketable prototype of a hydrophilic sensor CL to indirectly measure IOP. This prototype measures deformations of the eyeball (changes in corneal curvature) caused by IOP variations and uses a soft CL with a platinum-titanium strain gauge, or it uses an invasive method such as the sensor for monitoring IOP.[29,30] Recently, Mansouri and Shaarawy[31] reported the clinical use of a wireless ocular telemetry sensor described by Leonardi[18] with device intolerance and technical device malfunction in 13% of the patients tested. In addition, Twa et al.[32] have proposed a novel contact lens–embedded pressure sensor, but this sensor cannot permit prolonged use beyond 30 minutes or the wireless connection necessary for IOP monitoring.

CL Sensor

Some of the devices proposed to monitor IOP are based on the principle that a change in IOP of 1 mm Hg causes a change in the corneal curvature of 3 μm, given a corneal radius of 7.80 mm.[10,18,31] By engineering composite materials at the submicrometer or nanometer scale, it is possible to obtain flexible and highly conductive BL films that contain organic molecular conductors such as a coating metallic or semiconductor-like layer.[20–22,33] These BL films combine properties that are difficult to reconcile (e.g., flexibility, transparency, electrical conductivity, long-term stability, and light weight). One such BL film is a polycarbonate film coated with a metallic polycrystal-

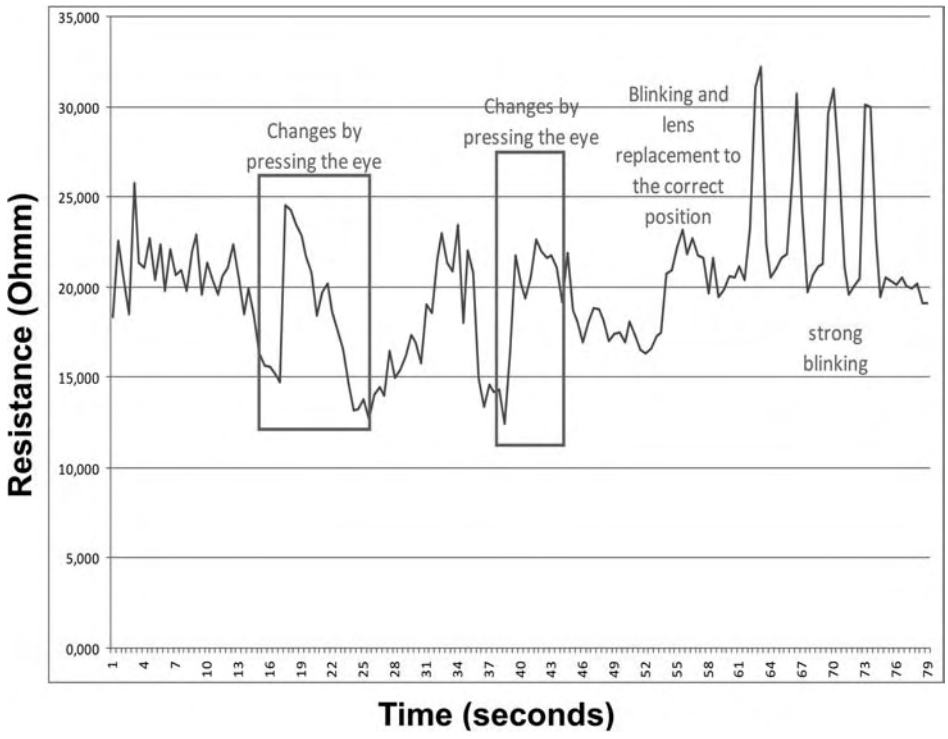

FIGURE 5. Results of an in vivo experiment. *Gray line*: changes in the resistance of the CL caused by increases in IOP produced by gentle pressing of the eye and strong blinking.

line layer based on the organic molecular metal β-$(ET)_2I_3$. This electroconductive BL film can sense resistance to strain with extremely high sensitivity; the film is able to sense a relative strain of $\approx 10^{-3}\%$.[23,24] The electrical resistance responses of the BL films to strain are 3 to 10 times greater than those exhibited by inorganic metal-based gauges. The BL film can be used as a pressure-sensing membrane in pressure sensors with a sensitivity of 1.4 Ω/mm Hg,[23,24] which is higher than the sensitivity of other IOP contact lens sensors.[18,31]

Another advantage of this piezoresistive material is its transparency: BL films show transparency up to 70% to 80%[33] of the visible spectrum (550–900 nm). Therefore, the BL film–based sensor must function reliably when size, performance, robustness, light weight, and transparency are important. The BL film embedded as a membrane in a CL can be applied as a highly sensitive pressure sensor that fulfills the requirements of a noninvasive IOP-monitoring device. We found that the developed CL sensor has good sensitivity (0.4 Ω/mm Hg) that be used in noninvasive IOP monitoring as well-defined electrical signals. The electrical resistance response of one of the prototypes of sensing lenses, reported by Leonardi et al.,[37] was only 0.4 Ω for maximum pressure fluctuation.

Electronic Measurements

In developing an IOP-monitoring system, electronic measurements are responsible for conditioning the signal from the pressure sensor embedded in the lens, digitizing it, and transmitting it to an external device. In the final prototype, the electronic measuring system should be embedded in the CL to avoid possible patient discomfort caused by any wires to and from the sensor lens. The measured data must then be wirelessly transmitted to a data acquisition system. However, because of the reduced area available on the lens, the system cannot be battery powered, which would also require a wireless energy transmission system. Wireless power transmission implies the design of very small and low-power electronic measuring devices, which can only be achieved through the development of an application-specific integrated circuit (ASIC).[34]

In future, the integrated electronic measurement system will be improved and further developed to avoid the use of wires. The purpose of this device was to establish the membrane characteristics and study the feasibility of the circuitry to successfully develop the ASIC. Therefore, all tests with the discrete device had to be performed to establish the system specifications. At the same time, it could be used to study the effects of blinking, tears, and temperature to determine whether they could be filtered by either software or hardware.

To satisfy all requirements, the system's structure was based on a special configuration of a Wheatstone bridge.[35] It was formed by four branches, and the sensor was placed in one of them. This configuration permitted only the measurement of IOP variations, eliminating the absolute value and reducing the measurement scale and thereby simplifying data acquisition and permitting increased resolution of the measurements.

This structure was integrated and sent data wirelessly. To enable data modulation, the measurement circuit converted the data into pulses using a pulse density modulation system.[34]

Current discrete devices that are wired to the sensing CL can be used to take measurements for a few hours, but they may not be comfortable enough to be used for a long time. For this reason, our system should work wirelessly, allowing patients to perform normal activities while recording the fluctuations of their IOP throughout the day. Therefore, an integrated device, or ASIC, embedded in the CL and powered by an inductive link will be developed. The antenna of the inductive link will be also embedded in the lens to receive energy from an external device and to transmit the measured data from the sensor.

Clinical Implications

Continuous monitoring of IOP could be of paramount importance in patients with suspected glaucoma, such as the patient with normal IOP values but a pattern of visual field loss and

optic nerve head changes suggestive of normal tension glaucoma. Continuous monitoring could also be used in glaucoma patients to check the IOP values and modify patient management.[12] Thus far, the only clinically proven method known to determine whether IOP increases at any time of the day is to conduct a 24-hour tensional curve with the patient in a hospital environment.[4]

A CL sensor able to record the IOP changes could be a useful, noninvasive, easy-to-handle, and inexpensive tool that would find clinical application in glaucoma diagnosis. This study presents proof of concept of a new method for continuous monitoring of IOP, based on a sensing CL, in an in vitro model of porcine eyeball and in a human eye to validate this measurement principle. In humans, eye movements and blinking are filtered from the signal so that they do not interfere with the monitoring of IOP. They are easily distinguishable because they are observed as a disturbance in the sharp and short signal. It should be noted that fluctuations in corneal thickness and hydration could induce an anterior flattening of the corneal curvature that could affect IOP measurements.[36] The effect of diurnal variation of the cornea must be assessed in further investigations.

This new CL sensor is not free of limitations, similar to previous CL sensors described in the literature.[18,31,32,37] Sensor transparency must be improved to avoid visual disturbances to the patient. Individual patient-tailored calibration could be necessary because corneal curvature change caused by IOP change depends on the basal corneal radius. The IOP value depends on corneal thickness. In addition, like current CL sensors, our sensor measures IOP change,[18,31,37] but this is not the IOP magnitude itself. Finally, a filtration procedure must be designed to differentiate the signal caused by IOP fluctuation of the noise related to such activities as blinking and eye movement. These issues must be resolved before commercial and clinical use of this new prototype, but the results of this study show that this prototype has adequate sensitivity to continuously monitor IOP, which could be very useful for diagnosing and treating glaucoma. In future, this may allow a CL sensor to be developed that would be minimally invasive and would continuously monitor IOP for 24-hour periods, allowing the patient to maintain a normal lifestyle while using the CL sensor, with minimal interference with vision and with highly accurate measurement of IOP variations.

Acknowledgments

The authors thank Conoptica Company for supplying and manufacturing the doughnut-shaped contact lenses.

References

1. Resnikoff S, Pascolini D, Etya'ale D, et al. Global data on visual impairment in the year 2002. *Bull World Health Organ*. 2004;82:844–851.
2. Sung VC, Koppens JM, Vernon SA, et al. Longitudinal glaucoma screening for siblings of patients with primary open angle glaucoma: the Nottingham Family Glaucoma Screening Study. *Br J Ophthalmol.* 2006;90:59–63.
3. Raychaudhuri A, Lahiri SK, Bandyopadhyay M, Foster PJ, Reeves BC, Johnson GJ. A population based survey of the prevalence and types of glaucoma in rural West Bengal: the West Bengal Glaucoma Study. *Br J Ophthalmol.* 2005;89:1559–1564.
4. Konstas AG, Mylopoulos N, Karabatsas CH, et al. Diurnal intraocular pressure reduction with latanoprost 0.005% compared to timolol maleate 0.5% as monotherapy in subjects with exfoliation glaucoma. *Eye.* 2004;18:893–899.
5. Read SA, Collins MJ, Becker H, et al. Changes in intraocular pressure and ocular pulse amplitude with accommodation. *Br J Ophthalmol.* 2010;94:332–335.
6. Doshi S, Harvey W. Assessment of ocular pressure. In: Doshi S, Harvey W, eds. *Eye Essentials: Assessment and Investigative Techniques*. Philadelphia: Elsiever; 2005:97–117.
7. Joe SG, Choi J, Sung KR, Park SB, Kook MS. Twenty-four hour blood pressure pattern in patients with normal tension glaucoma in the habitual position. *Korean J Ophthalmol.* 2009;23:32–39.
8. Van de Veire S, Germonpre P, Renier C, Stalmans I, Zeyen T. Influences of atmospheric pressure and temperature on intraocular pressure. *Invest Ophthalmol Vis Sci.* 2008;49:5392–5396.
9. Khan JC, Hughes EH, Tom BD, Diamond JP. Pulsatile ocular blood flow: the effect of the Valsalva manoeuvre in open angle and normal tension glaucoma: a case report and prospective study. *Br J Ophthalmol.* 2002;86:1089–1092.
10. Lam AK, Douthwaite WA. The effect of an artificially elevated intraocular pressure on the central corneal curvature. *Ophthalmic Physiol Opt.* 1997;17:18–24.
11. Leonardi M, Leuenberger P, Bertrand D, Bertsch A, Renaud P. First steps toward noninvasive intraocular pressure monitoring with a sensing contact lens. *Invest Ophthalmol Vis Sci.* 2004;45:3113–3117.
12. Hughes E, Spry P, Diamond J. 24-Hour monitoring of intraocular pressure in glaucoma management: a retrospective review. *J Glaucoma.* 2003;12:232–236.
13. Maurice DM. A recording tonometer. *Br J Ophthalmol.* 1958;42:321–335.
14. Greene ME, Gilman BG. Intraocular pressure measurement with instrumented contact lenses. *Invest Ophthalmol.* 1974;13:299–302.
15. Wolbarsht ML, Wortman J, Schwartz B, Cook D. A scleral buckle pressure gauge for continuous monitoring of intraocular pressure. *Int Ophthalmol.* 1980;3:11–17.
16. Flower RW, Maumenee AE, Michelson EA. Long-term continuous monitoring of intraocular pressure in conscious primates. *Ophthalmic Res.* 1982;14:98–106.
17. Svedbergh B, Bäcklund Y, Hök B, Rosengren L. The IOP-IOL: a probe into the eye. *Acta Ophthalmol (Copenh).* 1992;70:266–268.
18. Leonardi M, Pitchon EM, Bertsch A, Renaud P, Mermoud A. Wireless contact lens sensor for intraocular pressure monitoring: assessment on enucleated pig eyes. *Acta Ophthalmol.* 2009;87:433–437.
19. Sanchez I, Martin R, Ussa F, Fernandez-Bueno I. The parameters of the porcine eyeball. *Graefes Arch Clin Exp Ophthalmol.* 2011;249:475–482.
20. Laukhina E, Ulanski J, Khomenko A, et al. Systematic study of the (ET)2I3 reticulate doped polycarbonate films: structure, ESR, transport properties and superconductivity. *J Phys I France.* 1997;7:1665–1675.
21. Ulanski J, Kryszewski M. Reticulate composites. In: Bloor D, Brook RJ, Fleming MC, Mahajan S, Cahn RW. *The Encyclopedia of Advanced Materials.* Oxford: Pergamon Press; 1994:2301–2304.
22. Laukhina E, Tkacheva V, Chuev I, et al. New flexible low-density metallic materials containing the (BEDT-TTF)2(IxBr1-x)3 molecular metals as active components. *Phys Chem B.* 2001;105:11089–11097.
23. Laukhina E, Mas-Torrent M, Rovira C, Veciana J, Laukhin V. Organic sensor device and its applications. European patent P200602887 (WO2008059095). November 14, 2006.
24. Laukhina E, Pfattner R, Ferreras LR, et al. Ultrasensitive piezoresistive all-organic flexible thin films. *Adv Mater.* 2010;22:977–981.
25. Shimmyo M, Ross AJ, Moy A, Mostafavi R. Intraocular pressure, Goldmann applanation tension, corneal thickness, and corneal curvature in Caucasians, Asians, Hispanics, and African Americans. *Am J Ophthalmol.* 2003;136:603–613.
26. Li S, Wang X, Li S, Wu G, Wang N. Evaluation of optic nerve head and retinal nerve fiber layer in early and advance glaucoma using frequency-domain optical coherence tomography. *Graefes Arch Clin Exp Ophthalmol.* 2010;248:429–434.
27. Harwerth RS, Vilupuru AS, Rangaswamy NV, Smith EL 3rd. The relationship between nerve fiber layer and perimetry measurements. *Invest Ophthalmol Vis Sci.* 2007;48:763–773.

28. Shin IH, Kang SY, Hong S, et al. Comparison of OCT and HRT findings among normal, normal tension glaucoma, and high tension glaucoma. *Korean J Ophthalmol.* 2008;22:236–241.
29. Pan T, Brown JD, Ziaie B. An artificial nano-drainage implant (ANDI) for glaucoma treatment. *Conf Proc IEEE Eng Med Biol Soc.* 2006;1:3174–3177.
30. Stay MS, Pan T, Brown JD, Ziaie B, Barocas VH. Thin-film coupled fluid-solid analysis of flow through the Ahmed glaucoma drainage device. *J Biomech Eng.* 2005;127:776–781.
31. Mansouri K, Shaarawy T. Continuous intraocular pressure monitoring with a wireless ocular telemetry sensor: initial clinical experience in patients with open angle glaucoma. *Br J Ophthalmol.* 2011;95:627–629.
32. Twa MD, Roberts CJ, Karol HJ, et al. Evaluation of a contact lens-embedded sensor for intraocular pressure measurement. *J Glaucoma.* 2010;19:382–390.
33. Laukhina E, Rovira C, Ulanskii J. Organic metals as active components in surface conducting semi-transparent films. *Synth Met.* 2001;121:1407–1408.
34. Durà R, Mathieu F, Nicu L, Pérez-Murano F, Serra-Graells F. A 0.3mW/Ch 1.25V piezo-resistance digital ROIC for liquid dispensing MEMS. *IEEE Trans Circuits Syst I.* 2009;56:957-965.
35. Puente de Wheatstone PAR. *Medidas por Comparación: Sensores y Acondicionadores de Señal*. 4th ed. Marcobo, Spain: Boixareu Editores; 2003:114–117.
36. Read SA, Collins MJ. Diurnal variation of corneal shape and thickness. *Optom Vis Sci.* 2009;86:170–180.
37. Leonardi M, Leunberger P, Bertrand D, Renaud P. A soft contact lens with a MEMS strain gauge embedded for intraocular pressure monitoring. *IEEE Transducers Solid-State Sensors: Actuators and Microsystems.* 2003;2:1043–1046.

17.- ANEXO VII

Sánchez I, Martín R, Ussa F.

Measurement of intraocular pressure in a porcine ex vivo model eye.

Optometry and Vision Science (enviado)

Optometry and Vision Science

Measurement of intraocular pressure in a porcine ex vivo model eye

--Manuscript Draft--

Manuscript Number:	
Full Title:	Measurement of intraocular pressure in a porcine ex vivo model eye
Article Type:	Technical Report
Keywords:	ex vivo animal model; pig eye animal model; glaucoma model; hypertension model, IOP model.
Corresponding Author:	Irene Sanchez, OD Networking Research Centre on Bioengineering, Biomaterials and Nanomedicine (CIBER-BBN), Zaragoza, Spain. Valladolid, Valladolid SPAIN
Corresponding Author Secondary Information:	
Corresponding Author's Institution:	Networking Research Centre on Bioengineering, Biomaterials and Nanomedicine (CIBER-BBN), Zaragoza, Spain.
Corresponding Author's Secondary Institution:	
First Author:	Irene Sanchez, OD
First Author Secondary Information:	
Order of Authors:	Irene Sanchez, OD
	Raul Martin, Phd
	Fernando Ussa, MD
Order of Authors Secondary Information:	
Abstract:	Purpose: To compare the pressure inside and outside the pig eye in relation to the location of cannulation for the injection of liquid into the anterior or vitreous chamber. Material and method: Eleven enucleated pig eyes were used. 46 measurements of IOP were taken with a Perkins tonometer when the eye was cannulated in the anterior chamber. 49 measurements were taken when the eye was cannulated in the vitreous chamber. The eyeball was connected to a low-pressure transducer to control, maintain and modify the pressure in the eyeball. Results: No significant difference (p=0.138, ANOVA) was found between the Perkins pressure measurements from cannulations in the anterior and vitreous chambers. A linear relationship between transducer and Perkins measurements was found when the eye was cannulated in the anterior chamber (IOP=-7.749+0.763transducer;R2=0.940,p<0.001) and when it was cannulated in the vitreous chamber (IOP=-7.476+0.730transducer,R2=0.885,p<0.001). No difference was found between the Perkins/transducer pressure ratios (p=0.500 ANOVA) from cannulations in anterior and vitreous chambers. There were no differences in the measurements among eyes that could affect pressure outcomes. A direct relationship between the insufflate pressure inside the eyeball and the Perkins pressure was found. Conclusion: The pressure measured by Perkins applanation tonometry in an ex vivo porcine eye model is not correlated with the area of cannulation, keeping constant pressure with a low-pressure transducer. A linear equation was generated that correlates the pressure gauge with IOP Perkins, which would apply to future studies that use the pig eye as an exvivo animal model of hypertension in glaucoma.

Title Page

Title: Measurement of intraocular pressure in a porcine ex vivo model eye.

Author: Irene Sanchez [1,2] OD.

Co-authors: Raul Martin [2,3] *PhD*, Fernando Ussa [2] *MD*

[1] Networking Research Centre on Bioengineering, Biomaterials and Nanomedicine (CIBER-BBN), Zaragoza, Spain.

[2] IOBA-Eye Institute, University of Valladolid. Valladolid, Spain.

[3] Department of Physics TAO – School of Optometry, University of Valladolid. Valladolid, Spain.

Location: IOBA-Eye Institute, University of Valladolid, Valladolid, Spain.

Reprint requests to Irene Sanchez OD, IOBA Eye Institute. Paseo de Belén nº 17 Campus Miguel Delibes. 47011 Valladolid, Spain. Tel: (+34) 983 423559, Fax: (+34) 983 423274 Email: isanchezp@ioba.med.uva.es.

Number of words: 2344

Figures: 3

Tables: 1

The authors have no proprietary, financial or commercial interest in any material or method mentioned in this study.

American Journal Experts reviewed the English grammar of this manuscript.

Date of submission: 06.03.2012

ABSTRACT

Purpose: To compare the pressure inside and outside the pig eye in relation to the location of cannulation for the injection of liquid into the anterior or vitreous chamber.

Material and method: Eleven enucleated pig eyes were used. 46 measurements of IOP were taken with a Perkins tonometer when the eye was cannulated in the anterior chamber. 49 measurements were taken when the eye was cannulated in the vitreous chamber. The eyeball was connected to a low-pressure transducer to control, maintain and modify the pressure in the eyeball.

Results: No significant difference (p=0.138, ANOVA) was found between the Perkins pressure measurements from cannulations in the anterior and vitreous chambers. A linear relationship between transducer and Perkins measurements was found when the eye was cannulated in the anterior chamber (IOP=-7.749+0.763transducer;R^2=0.940,p<0.001) and when it was cannulated in the vitreous chamber (IOP=-7.476+0.730transducer,R^2=0.885,p<0.001). No difference was found between the Perkins/transducer pressure ratios (p=0.500 ANOVA) from cannulations in anterior and vitreous chambers. There were no differences in the measurements among eyes that could affect pressure outcomes. A direct relationship between the insufflate pressure inside the eyeball and the Perkins pressure was found.

Conclusion: The pressure measured by Perkins applanation tonometry in an ex vivo porcine eye model is not correlated with the area of cannulation, keeping constant pressure with a low-pressure transducer. A linear equation was generated that correlates the pressure gauge with IOP Perkins, which

would apply to future studies that use the pig eye as an exvivo animal model of hypertension in glaucoma.

Keywords: ex vivo animal model; pig eye animal model; glaucoma model; hypertension model, IOP model.

1. INTRODUCTION

Glaucoma is a pathology with a neurodegenerative etiology. It is irreversible and is the second leading cause of blindness worldwide[1]. The prevalence is between 1% and 3%, depending on the study population[2,3], and around 50% of glaucoma patients remain undiagnosed[4]. Glaucoma is characterized by a loss of ganglion cells in the retina. This loss is mainly caused by increases in the intraocular pressure (IOP). The maintenance of IOP above 21 mm Hg causes a thinning of the lamina cribosa[5], an area through which the ganglion cells of the retina must pass. The death of nerve cells results in permanent defects in the visual field[2,6,7].

The porcine eye is a commonly used glaucoma animal model because its size is similar to the human eye, and it has been used as an ocular hypertension model or glaucoma model[8-18]. There are different methods for generating an ocular hypertension model: cauterizing episcleral veins[8,9], blocking the iridocorneal angle to prevent aqueous flow through the trabecular meshwork[10], injecting fluids into the eye in live animals[9,11] and developing ex vivo models[12,13,19].

These animal models are used for pharmacokinetic and pharmacodynamic studies testing new treatments for reducing IOP in glaucoma[14,15,20], developing laser treatments with similar function to the iridotomy[17], monitoring the loss of ganglion cells[8,10] and introducing lesions in the lamina cribosa[11,12]. In ex vivo

models of ocular hypertension with injection of liquid, the best method for liquid infusion and their effects on IOP measurements are not clear. Some studies have performed cannulation in the anterior chamber[16,18], others in the vitreous chamber[21] and some through the optic nerve[22]. However, there are no studies comparing the changes in IOP from infusions in different areas of the eye. Usually, Goldman tonometry is not used on animals because it requires a slit lamp to conduct the measurements. For this reason, Perkins applanation tonometry or other tonometers, such as a Tonopen[23,24], are used frequently.

The purpose of this study is to compare two different methods of increasing IOP in a porcine eye ex vivo model, anterior chamber infusion versus vitreous chamber infusion, to determine whether these induce different IOPs and how they affect the experimental model.

2. MATERIAL AND METHODS

Eleven enucleated pig eyes (*Sus scrofa domestica*) were obtained from the local abattoir. Animals were white (not albino) domestic pigs between six and eight months of age, and they weighed 120 to 150 kg. The eyes were enucleated around 8:30 AM, just after slaughter. The measurements were made between 9:00 AM and 12:00 AM. Excess tissue surrounding the eyeball was removed with Moorfield conjunctival forceps and Wescott tenotomy wide-handle scissors (John Weiss international, Milton Keynes, UK) to facilitate the experimental measurements.

An experienced surgeon did not perform enucleation. For this reason, eyes with signs of any trauma, including loss of form, visible retinal detachment, lens dislocation and other, which were verified via direct ophthalmoscopy before performing the experimental measurements, were not used for this study.

2.1. Anterior chamber infusion

Forty-six Perkins measurements were taken from six porcine eyes that were cannulated with a 23-G cannula, in the anterior chamber at 2 mm before the esclerocorneal limbus parallel to the iris, taking care to not touch it or the corneal endothelium.

2.2. Vitreous chamber infusion

Forty-nine Perkins measurements were taken from five porcine eyes that were cannulated in the vitreous chamber at 3.5 mm from the sclerocorneal limbus with a 20-G cannula normally used in standard vitrectomy surgery.

2.3. Anatomical study

The corneal radius and corneal thickness were measured in five porcine eyes by manual keratometry (OM-4 Topcon, Japan) and ultrasound pachymetry (Sonogage Inc., Cleveland, Ohio; calibrated by the manufacturer).

2.4. Experimental design

The eyeball was connected to a low-pressure transducer (CPC 2000, WIKA Alexander Wiegand GmbH & Co, Klingenberg, Germany) to monitor and modify the eyeball pressure. This device emits air to a conduit that communicates with

a glass bottle of Ringer's lactate solution. The pressure in the glass bottle flushes the liquid by another conduit that reaches to the eyeball. The height of the serum level should be the same as the point of cannulation of the eyeball (Figure 1). The pressure is scheduled in the low-pressure transducer, and the whole circuit has the same pressure if differences of heights are avoided. The liquid remained free of air and vice versa.

2.5. IOP measurement

To measure IOP, a Perkins tonometer (Clement Clarke International, Edinburgh, England) calibrated by the manufacturer was used. The measurement was performed by instilling a drop of fluorescein (sodium fluorescein strips, Bausch & Lomb, dissolved in 0.9% saline solution) as a standard procedure in an eye examination.

2.6. Statistical analysis

Statistical analysis was performed using the SPSS 15.0 (SPSS Chicago, Illinois, USA) statistical package for Windows.

The normality of the data was tested by Kolmogorov-Smirnov test. Multivariate analysis of variance (ANOVA with a Bonferroni correction for multiple comparisons) was used to detect differences between IOP measurements. The ratio of the pressure induced by the low-pressure transducer to the Perkins value was determined to detect differences between cannulations performed in the anterior chamber and in the vitreous chamber. A p value of less than 0.05 was considered statistically significant.

The IOP induced with the transducer (WIKA CPC 2000), when the eye was cannulated at the anterior or posterior chamber, was compared with Perkins tonometer measurements. Linear regression was used to quantify the correlation between both measurements, which was represented by the correlation coefficient (R^2). A p value of less than 0.05 was considered statistically significant.

3. RESULTS

3.1. Working range for the measurement of IOP

The corneal pachymetry was 877.60±13.58 µm, (95% CI 865.70 to 889.50 µm), and the corneal radii were 8.69±0.56 mm (95% CI 8.94 to 8.48 mm) in the flatter meridian and 8.19±0.35 mm (95% CI 8.33 to 8.06 mm) in the steeper meridian. Because the corneal thickness of the pig eye is different from the human eye, we defined a working range of pressure from 20 to 70 mm Hg with the WIKA low-pressure transducer. However, Perkins measurements showed lower pressure outcomes, ranging from 5 to 45 mm Hg.

3.2. Differences between anterior chamber versus vitreous chamber cannulation

No significant difference (p=0.138, ANOVA) was found between the Perkins' pressure measurements when the cannulation was in the anterior chamber and when it was in the vitreous chamber.

When the cannulation was in the anterior chamber, the pressure induced by the transducer was linearly related to the Perkins measurement (R^2=0.940, p<0.001). An equation that relates the transducer pressure to Perkins measurement was obtained (Figure 2): Perkins IOP= -7.749 + 0.763 WIKA transducer pressure.

When the cannulation was in the vitreous chamber, the pressure induced by the transducer was linearly related to the Perkins measurement (R^2=0.885, p<0.001). An equation that relates the transducer pressure to Perkins measurement was obtained (Figure 3): Perkins IOP= -7.476 + 0.730 WIKA transducer pressure.

No difference was found between the ratios of Perkins to WIKA pressure (p=0.500 ANOVA) from cannulations in the anterior chamber and in the vitreous chamber.

3.3. Effect of the eye globe on IOP measurement

A multiple comparison ANOVA with Bonferroni correction was conducted to test the effect of the eye globe on the IOP measurement. A significance level close to 1 (p>0.939) was found when comparing Perkins measurements or the Perkins/transducer ratios between the IOP measurements from cannulations in the anterior and vitreous chambers. Therefore, there were no differences in the measurements among the different eyes (pairwise comparison).

The pressure induced by the transducer was linearly related to the measurement of Perkins IOP. An equation was obtained for each eye that related the two pressures through a linear regression model with R^2 close to 1 ($p<0.001$) (Table 1).

4. DISCUSSION

The pig eye is a common model of ocular hypertension[8-12,17]. However, there is no consensus on the best way to induce IOP. Many different techniques have been reported[8-12,19], but no studies have evaluated the possible confounding effects of the method used to induce the pressure. This study helps clarify this issue and proposes a method to induce IOP that is not affected by the area of the eye in which the infusion takes place.

To calculate the range of work, a high-pressure gauge is needed to start measuring IOP with Perkins tonometry in the normal range. This is because the enucleated eye is in the phthisis, which is characterized by a lack of production of aqueous humor (the emptying of uveal vessels and choroidal flow), which is of great importance to maintain the basal pressure of the eyeball. For these reasons, it was necessary to increase the pressure inside the eyeball to recover its natural tone.

We found a direct relationship between the insufflated pressure inside the eyeball and the measurement from the outside, which could be described mathematically by the equation of a line, regardless of the point of cannulation.

This result indicates that the pig eyeball meets Hooke's law for elastic bodies, in accord with previously findings[25].

No statistically significant differences were found in the pressure measured by Perkins applanation tonometry between the two areas in which the cannulation for the infusion of fluid in the pig ex vivo model eye was performed. Leaking of fluid can lead to erroneous measurements[25]. To avoid this problem, the best option could be to use a pressure system that maintains the pressure within the eyeball even if fluid is lost. Classical studies recommended gluing the cannulation point with cyanoacrylate or using some kind of dye in the liquid so that leaks can be easily perceived[25]. Also, a high-density liquid such as silicone oil has been used to obstruct the drainage pathway of aqueous humor[9,25]. In this study, the use of a low-pressure transducer ensured that the pressure within the eyeball was kept constant in the range defined, without being influenced by leakage of intraocular fluid.

It is important to reliably know the relationship of the gauge pressure inside the eyeball with the IOP[12], as in many experimental studies with animal models that used tonometry IOP control with Tonopen[10]. This tonometer is easy to use for non-specialists in the technique of tonometry, but comparative studies with applanation tonometry values show that IOP can be underestimated, especially at pressures higher than 21 mm Hg[23,24].

Another study limitation was due to the design of the tonometers. IOP measurement with the Perkins tonometer is based in the Imbert-Fick law, which

sets the IOP is the ratio between the tonometer weight and flattened area, assuming that the eye behaves like an infinitely thin, dry, elastic and spherical membrane. The cone-prism has a diameter of 7 mm, and in the process of measuring it, the corneal area is flattened and has a diameter of 3.06 mm, corresponding to the point of equality between the pressure exerted with the tonometer and IOP[26]. The Perkins tonometer is calibrated for a corneal thickness of 550 µm and corneal radius of 7.80 mm, but keratometry of the porcine cornea is flatter than human cornea, as the former has an average radius of 8.45 mm and is thicker than human cornea. For this reason, the tonometer flattened a larger diameter of 3.06 mm using a greater force with the calibrated tonometry (corneal thickness of 550 µm), which caused the difference between it and the Perkins measurements of IOP. This error will be similar for all measurements because all eyes have similar corneal thickness and radius. For this reason, this lack of Perkins measurement probably has a limited repercussion on this study's conclusions because the objective of this study was to determine whether Perkins measurement depends of the method of inducing the IOP (anterior versus vitreous chamber infusion). Also, we found the equivalence between the pressure inside the eyeball and the IOP measured by Perkins applanation tonometry that could be useful to ex vivo models, but more research is necessary to validate this equivalence in an in vivo pig model of hypertension.

In conclusion, the pressure measured by Perkins applanation tonometry in an ex vivo porcine eye model is not correlated with the region of cannulation (either anterior or vitreous chamber), keeping constant pressure with a low-pressure

transducer. An equation was determined that correlates the pressure gauge with Perkins IOP, which would enable its use in studies that use the pig eye as an ex vivo animal model of hypertension in glaucoma, facilitating the interpretation of manometric measurements.

Acknowledgements: The authors thank all slaughterhouse staff Justino Gutiérrez SL (Laguna de Duero, Valladolid, Spain) for the cooperation in providing samples used in this work. The research was granted by CIBER-BBN grant.

REFERENCES

1. Resnikoff S, Pascolini D, Etya'ale D, et al. Global data on visual impairment in the year 2002. Bull World Health Organ. 2004;82:844–851.

2. Sung VC, Koppens JM, Vernon SA, et al. Longitudinal glaucoma screening for siblings of patients with primary open angle glaucoma: the Nottingham Family Glaucoma Screening Study. Br J Ophthalmol. 2006;90:59–63.

3. Raychaudhuri A, Lahiri SK, Bandyopadhyay M, et al. A population based survey of the prevalence and types of glaucoma in rural West Bengal: the West Bengal Glaucoma Study. Br J Ophthalmol. 2005;89:1559–1564.

4. Sharts-Hopko NC, Glynn-Milley C. Primary open-angle glaucoma. Am J Nurs. 2009;109:40–47.

5. Ren R, Wang N, Li B, et al. Lamina cribrosa and peripapillary sclera histomorphometry in normal and advanced glaucomatous Chinese eyes with various axial length. Invest Ophthalmol Vis Sci. 2009;50:2175–2184.

6. Goldbaum MH, Jang GJ, Bowd C, et al. Patterns of glaucomatous visual field loss in sita fields automatically identified using independent component analysis. Trans Am Ophthalmol Soc. 2009;107:136–144.

7. Harwerth RS, Vilupuru AS, Rangaswamy NV, et al. The relationship between nerve fiber layer and perimetry measurements. Invest Ophthalmol Vis Sci. 2007;48:763–773.

8. Suarez T, Vecino E. Expression of endothelial leukocyte adhesion molecule 1 in the aqueous outflow pathway of porcine eyes with induced glaucoma. Mol Vis. 2006;12:1467–1472.

9. Ruiz-Ederra J, García M, Martín F, et al. Comparison of three methods of inducing chronic elevation of intraocular pressure in the pig (experimental glaucoma). Arch Soc Esp Oftalmol. 2005;80:571–579.

10. Rosolen SG, Rigaudière F, Le Gargasson JF. A new model of induced ocular hyperpressure using the minipig. J Fr Ophtalmol. 2003;26:259–67.

11. Balaratnasingam C, Morgan WH, Bass L, et al. Axonal transport and cytoskeletal changes in the laminar regions after elevated intraocular pressure. Invest Ophthalmol Vis Sci. 2007;48:3632–3644.

12. Thornton IL, Dupps WJ, Roy AS, et al. Biomechanical effects of intraocular pressure elevation on optic nerve/lamina cribrosa before and after peripapillary scleral collagen cross-linking. Invest Ophthalmol Vis Sci. 2009;50:1227–1233.

13. Zhang M, Rao PV. Blebbistatin, a novel inhibitor of myosin II ATPase activity, increases aqueous humor outflow facility in perfused enucleated porcine eyes. Invest Ophthalmol Vis Sci. 2005;46:4130–4138.

14. Hasegawa Y, Nishimura J, Niiro N, et al. Prostaglandin F2alpha, but not latanoprost, increases the Ca2+ sensitivity of the pig iris sphincter muscle. Invest Ophthalmol Vis Sci. 2006;47:4865–4871.

15. Hosseini M, Rose AY, Song K, et al. IL-1 and TNF induction of matrix metalloproteinase-3 by c-Jun N-terminal kinase in trabecular meshwork. Invest Ophthalmol Vis Sci. 2006;47:1469–76.

16. Vaajanen A, Vapaatalo H, Oksala O. A modified in vitro method for aqueous humor outflow studies in enucleated porcine eyes. J Ocul Pharmacol Ther. 2007;23:124–131.

17. Liu Y, Nakamura H, Witt TE, et al. Femtosecond laser photodisruption of porcine anterior chamber angle: an ex vivo study. Ophthalmic Surg Lasers Imaging. 2008;39:485–490.

18. Shaarawy T, Wu R, Mermoud A, et al. Influence of non-penetrating glaucoma surgery on aqueous outflow facility in isolated porcine eyes. Br J Ophthalmol. 2004;88:950–952.

19. Morgan WH, Cringle SJ, Kang MH, et al. Optimizing the calibration and interpretation of dynamic ocular force measurements. Graefes Arch Clin Exp Ophthalmol. 2010;248:401–407.

20. Song J, Deng PF, Stinnett SS, et al. Effects of cholesterol-lowering statins on the aqueous humor outflow pathway. Invest Ophthalmol Vis Sci. 2005;46:2424–2432.

21. Hallberg P, Lindén C, Bäcklund T, et al. Symmetric sensor for applanation resonance tomometry of the eye. Med Biol Eng Comput. 2006;44:54–60.

22. Von Freyberg A, Sorg M, Fuhrmann M, et al. Acoustic tonometry: feasibility study of a new principle of intraocular pressure measurement. J Glaucoma. 2009;18:316–320.

23. Kalesnykas G, Uusitalo H. Comparison of simultaneous readings of intraocular pressure in rabbits using Perkins handheld, Tono-Pen XL, and TonoVet tonometers. Graefes Arch Clin Exp Ophthalmol. 2007;245:761–762.

24. Andrada Marquez MT, Fesser Oroz I, Antón López A. Comparative study of two portable tonometers: Tono-Pen XL and Perkins. Arch Soc Esp Oftalmol. 2003;78:189–96.

25. Maquet Dussart JA. La rigidez ocular. Estudio clínico experimental. Doctoral Thesis. University of Valladolid, Medicine School. 1985.

26. Ma J. Cone prism: principles of optical design and linear measurement of the applanation diameter or area of the cornea. Appl Opt. 1999;38:2086–2091.

FIGURES AND TABLES

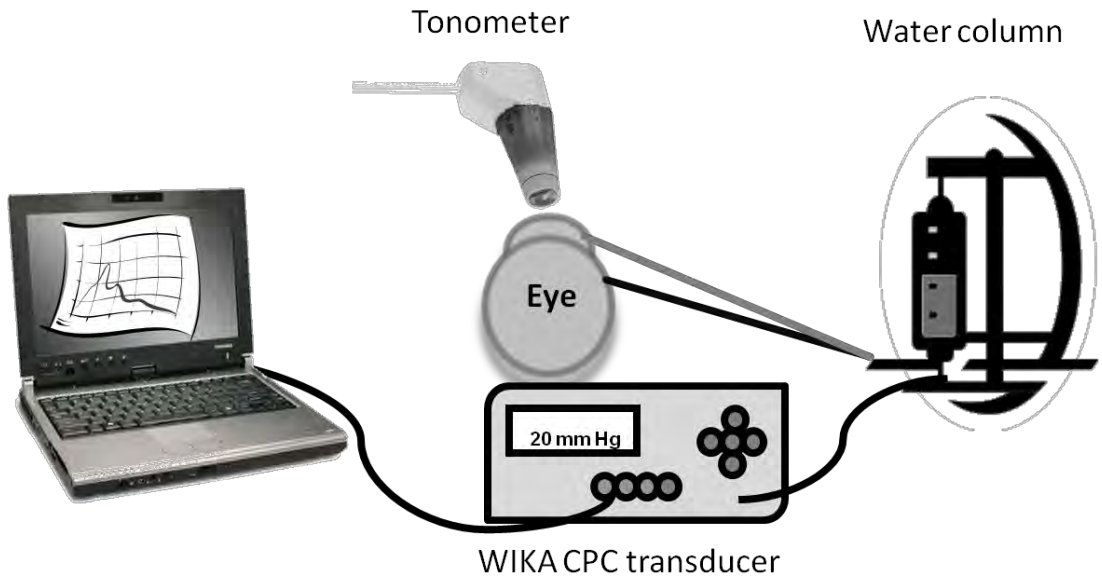

Figure 1. Schematic representation of the experimental design.

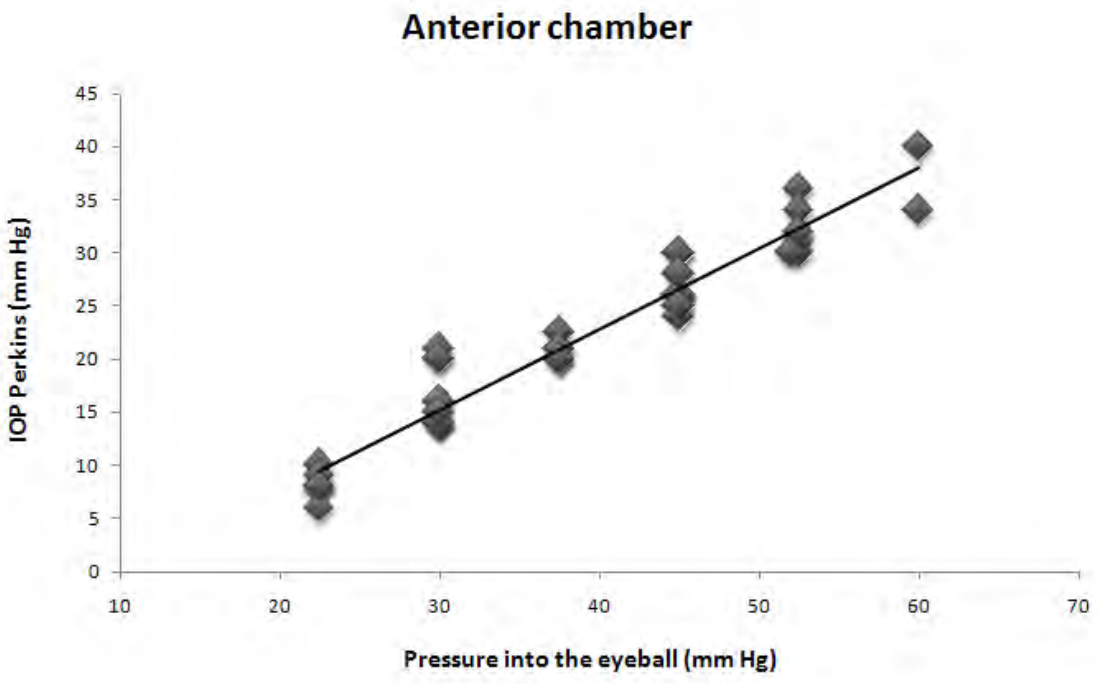

Figure 2. Graphical representation of the equation relating the pressure generated inside the eye though the infusion of fluid and IOP, taken by Perkins tonometry in eyes cannulated in the anterior chamber.

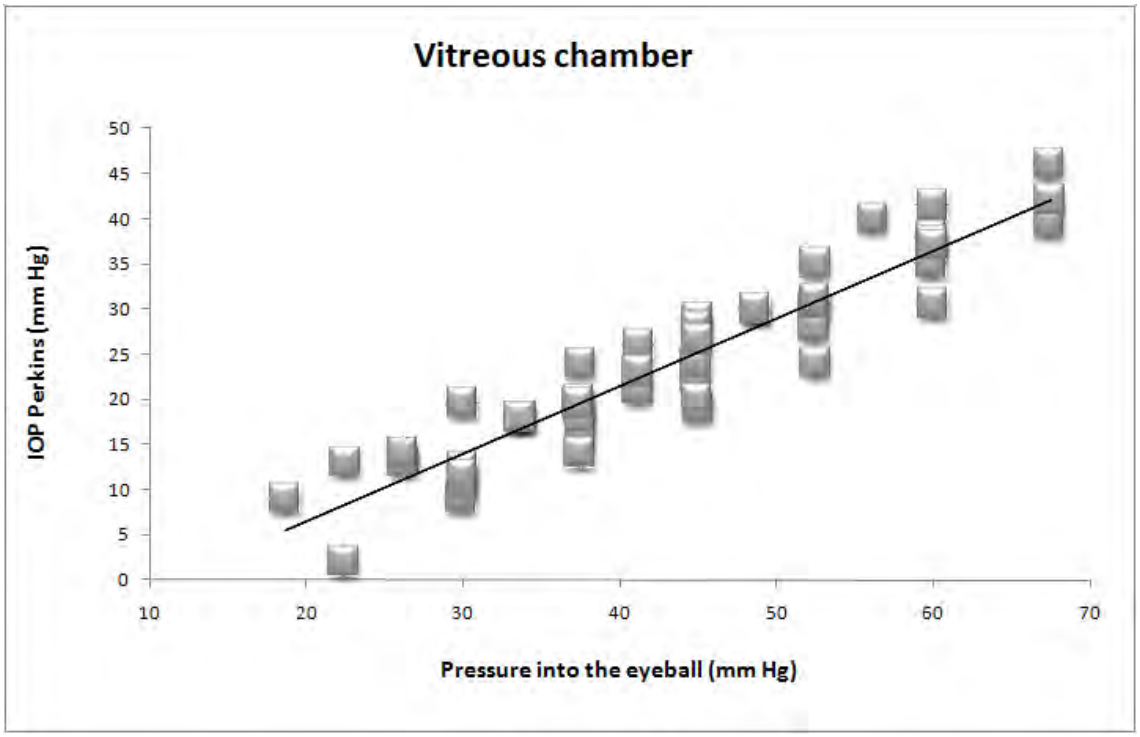

Figure 3. Graphical representation of the equation relating the pressure generated inside the eye though the infusion of fluid and IOP, taken by Perkins tonometry in eyes cannulated in the vitreous chamber.

Eye	Equation	R^2
Vitreous chamber		
# 1	P = -4,607 + 0.689 T	0.954 (p<0.01)
# 2	P = -5.497 + 0.762 T	0.949 (p<0.01)
# 3	P = -12.568 + 0.760 T	0.938 (p<0.01)
# 4	P = -14.701 + 0.899 T	0.960 (p<0.01)
# 5	P = -15.151 + 0.863 T	0.966 (p<0.01)
# 6	P = -5.545 + 0.678 T	0.993 (p<0.01)
Anterior chamber		
# 7	P = -10.750 + 0.842 T	0.963 (p<0.01)
# 8	P = -4.845 + 0.744 T	0.897 (p<0.01)
# 9	P = -7.076 + 0.731 T	0.897 (p<0.01)
# 10	P = -9.286 + 0.800 T	0.988 (p<0.01)
# 11	P = -9.714 + 0.800 T	0.988 (p<0.01)

Table 1. Equation relating the pressure inside the eyeball with the Perkins IOP measurements for each measurement. Eyes 1 through 5 were cannulated in the vitreous chamber and eyes 6 through 11 in anterior chamber. P = Perkins pressure; T = transducer pressure.

Table

Eye	**Equation**	**R^2**
Vitreous chamber		
# 1	P = -4,607 + 0.689 T	0.954 (p<0.01)
# 2	P = -5.497 + 0.762 T	0.949 (p<0.01)
# 3	P = -12.568 + 0.760 T	0.938 (p<0.01)
# 4	P = -14.701 + 0.899 T	0.960 (p<0.01)
# 5	P = -15.151 + 0.863 T	0.966 (p<0.01)
# 6	P = -5.545 + 0.678 T	0.993 (p<0.01)
Anterior chamber		
# 7	P = -10.750 + 0.842 T	0.963 (p<0.01)
# 8	P = -4.845 + 0.744 T	0.897 (p<0.01)
# 9	P = -7.076 + 0.731 T	0.897 (p<0.01)
# 10	P = -9.286 + 0.800 T	0.988 (p<0.01)
# 11	P = -9.714 + 0.800 T	0.988 (p<0.01)